

Assessment of Aquifer-Stream Connectivity Related to Groundwater Abstraction in the Lower Fraser Valley

Phase 1 Field Investigation

Glenn Hall, Diana M. Allen, Mike Simpson, Habtamu Tolera, Bryan Jackson, Mary Ann Middleton, and Michele Lepitre



The **Water Science Series** are scientific technical reports relating to the understanding and management of B.C.'s water resources. The series communicates scientific knowledge gained through water science programs across B.C. government, as well as scientific partners working in collaboration with provincial staff. For additional information visit: <http://www2.gov.bc.ca/gov/content/environment/air-land-water/water/water-science-data/water-science-series>.

ISBN: 978-0-7726-7165-3

Citation:

Hall, G. Allen, D.M., Simpson, M., Tolera, H., Jackson, B., Middleton, M.A., Lepitre, M. 2017. Assessment of hydraulic connectivity related to groundwater extraction on selected sensitive steams: Phase 1 Field Investigation. Water Science Series, WSS2017-02. Prov. B.C., Victoria B.C.

Author's Affiliation:

Glenn Hall, B.Sc. Honours student
Department of Earth Sciences
Simon Fraser University

Diana M. Allen, P.Geo.
Department of Earth Sciences
Simon Fraser University

Mike Simpson, P.Geo.
Groundwater Section, Resource Authorizations
South Coast Natural Resource Region
Ministry of Forests, Lands, Natural Resource Operations
and Rural Development

Habtamu Tolera, P.Geo.
Groundwater Section, Resource Authorizations
South Coast Natural Resource Region
Ministry of Forests, Lands, Natural Resource Operations
and Rural Development

Bryan Jackson
Groundwater Section, Resource Authorizations
South Coast Natural Resource Region
Ministry of Forests, Lands, Natural Resource Operations
and Rural Development

Mary Ann Middleton
Department of Earth Sciences
Simon Fraser University

Michele Lepitre, P.Geo.
Groundwater Section, Resource Authorizations
South Coast Natural Resource Region
Ministry of Forests, Lands, Natural Resource Operations
and Rural Development

© Copyright 2017

Cover Photograph: Photograph of instream piezometers installed in Union Creek, Langley, B.C. by Glenn Hall

Acknowledgements

The authors gratefully acknowledge the following organizations and individuals who contributed to this study. Ministry of Forests, Lands, Natural Resource Operations and Rural Development (Bryan Robinson) for his assistance with site selection and well installation; Ministry of Environment & Climate Change Strategy (Robin Pike and Jon Goetz) for installing the hydrometric stations; Ministry of Forests, Lands, Natural Resource Operations and Rural Development staff (Lise Galand, Frew Azene, Shirley Wang, Lizanne Steunenber, Emily Elsliger and Tessa Villeneuve) for assisting with the pumping test and making streamflow measurements. We also thank Klaus Rathfelder (ENV) for reviewing this report. We are grateful to the Township of Langley for providing and facilitating the use of the public park as the research study site. This work was supported by the Ministry of Environment & Climate Change Strategy, Groundwater Science Program.

Disclaimer: The use of any trade, firm, or corporation names in this publication is for the information and convenience of the reader. Such use does not constitute an official endorsement or approval by the Government of British Columbia of any product or service to the exclusion of any others that may also be suitable. Contents of this report are presented for discussion purposes only. Funding assistance does not imply endorsement of any statements or information contained herein by the Government of British Columbia.

EXECUTIVE SUMMARY

Abstraction of groundwater from a pumping well located beside a stream can result in sourcing of the pumped water directly from the stream and consequent depletion of stream discharge. The ability to accurately estimate stream depletion due to pumping is necessary for water rights management. This requires an understanding of the hydraulic connectivity between the aquifer and the stream. In British Columbia, evaluation of hydraulic connectivity is required for water licensing decisions under the *Water Sustainability Act*. Sensitive streams, as designated under the Water Sustainability Regulation under the *Water Sustainability Act*, are particularly at risk if hydraulically connected to an aquifer from which groundwater is abstracted.

The purpose of this study was to build an understanding of the interaction between groundwater and sensitive streams for the purpose of identifying streams that are more vulnerable to groundwater abstraction. The project was carried out collaboratively between Simon Fraser University and the Ministry of Forests, Lands, Natural Resource Operations and Rural Development. The study consisted of two parts; first, a targeted Phase 1 field investigation at Steele Park in Langley, B.C. aimed at determining the impacts of pumping on aquifer-stream interactions; and second, a multi-level regional stream vulnerability assessment in the Lower Fraser Valley for determining the vulnerability of other similar types of stream-aquifer systems in order to identify streams that might be similarly impacted by groundwater abstraction. This report documents the results of the Phase 1 field investigation. Middleton and Allen (2017) report on the multi-level regional stream vulnerability assessment.

Union Creek, a tributary to the Salmon River (a stream with restrictions on authorizations) was the stream of interest at Steele Park. Three wells were drilled at the site in close proximity to the creek; one was completed as a pumping well and the two others as monitoring wells. Core logging revealed three hydrostratigraphic units: 1) a layer of soil about 1 m thick, 2) a gravelly-sand aquifer approximately 10 m thick, and a lower clay unit, the full depth of which was not penetrated by the wells at Steele Park. The aquifer is considered unconfined, with flow directed to Union Creek, although the hydraulic gradient changes in magnitude and direction seasonally.

Slug and bail tests were analyzed to obtain a preliminary estimate of the hydraulic conductivity (K) of the aquifer (5.5E-05 m/s using both Hvorslev and Bower-Rice methods). A low-rate pumping test was conducted in July 2016, providing preliminary estimates of transmissivity (T), specific storage (Ss) and specific yield (Sy). A high-rate pumping test was conducted in December 2016. T varied from 2.7E-04 m²/s in the summer to 1.3E-03 m²/s during the winter, resulting in a time-averaged aquifer transmissivity of 8.1E-04 m²/s. The best estimate of S is 2.9E-04 based on the geometric mean values of the S values from monitoring wells from both pumping tests. Using the saturated thickness values during each test, the best estimate of K is 7.3E-05 m/s, and the best estimate of Ss is 3.5E-05 m⁻¹. Finally, Sy from the pumping test is 7.2E-02, which is low compared to Sy values for similar aquifer materials. This low value is attributed to the presence of the stream which altered the drawdown curve, thus influencing Sy. A more reasonable estimate of Sy (0.2) was obtained from the literature.

The degree of aquifer-stream connectivity was determined using head measurements in instream nested piezometer pairs, seepage meter measurements, and stream stage measurements coupled with streamflow measurements. Hydraulic connectivity was examined during summer and then prior to and during a high-rate pumping test in December 2016. During summer baseline conditions, hydraulic gradients between the piezometer pairs indicated predominantly downward flow, but hydraulic gradients between the individual piezometers and the stream stage showed dominantly upwards flow. These inconsistencies are thought to be due to the influence of hyporheic flow beneath the streambed, which influenced the shallow piezometer readings. Seepage measurements made using a seepage

meter during the summer showed an upward groundwater flux into the stream at a rate of $7E-7 \text{ m}^3/\text{s}/\text{m}^2$. The seepage rate measured in the winter just prior to the start of the high-rate pumping test was $3.5E-05 \text{ m}^3/\text{s}/\text{m}^2$, two orders of magnitude higher than the rate observed during the summer time. Finally, stream stage was too low to be accurately measured, but was estimated at 0.5 L/s during the summer.

During the high-rate pumping test in December 2016, drawdown was not evenly distributed along the streambed; drawdown ranged from 1 to 5 cm depending on instream piezometer location. All of the deep instream piezometers showed more drawdown than their shallow counterparts. Water levels recovered in all piezometers during recovery. Seepage decreased slightly over the pumping test, on the order of $1E-06 \text{ m}^3/\text{s}/\text{m}^2$. Stream stage dropped at all hydrometric stations following the short duration step test and recovery, and continued to drop prior to the start of the high-rate pumping test and throughout it. There was no obvious sign of recovery between the two tests. The rate of change of the decline in stream stage was generally the same for all four hydrometric stations until partway into the constant discharge test, and then the rate of decline of stream stage changed variably depending on hydrometric station. It appears that a heavy snowfall event during the step test may have influenced stream level such that it was decreasing back to its original level (pre-snow) while at the same time decreasing due to streamflow depletion due to pumping. The change in stream stage was not uniform between hydrometric stations and ranged from ~ 0.015 to 0.04 m . While discharge measurements were made for both upstream and downstream locations, the rapid fluctuations in the downstream discharge measurements and the fact that the upstream and downstream measurements were not taken at the same time rendered the discharge measurements unreliable. Moreover, an attempt to estimate streamflow from stream stage proved unsuccessful.

Streamflow depletion during the pumping test was modeled using a suite of available analytical solutions. The models converge at late time (with the exception of the Michigan screening tool which lacks physical basis) attaining 95% normalized streamflow depletion around 750 days. The Singh (2003), Hunt (1999), Hantush (1965), and Glover-Balmer (1954) models all predict a normalized streamflow depletion of around 42% by the end of the 48 hour pumping test, while the Hunt (2008) model, which includes an impedance factor, predicts 30% normalized streamflow depletion after 48 hours. Analysis of the field data highlighted the importance of accurately characterizing the hydraulic properties of the streambed sediments. Varying the streambed hydraulic conductivity and thickness showed that small changes in the streambed leakance parameter λ result in significant changes in the estimated rate of streamflow depletion in all the streamflow impedance models. Analysis of field data also highlighted the importance of properly designing and implementing the field test. This includes a more detailed examination of the seasonal variation in hydraulic connectivity, conducting the pumping test during the summer under baseflow conditions, and measuring streamflow outside the radius of influence of the pumping well to ensure the full impact of the well is captured.

CONTENTS

EXECUTIVE SUMMARY	ii
1. BACKGROUND.....	1
1.1 Evaluation of Hydraulic Connectivity in B.C.....	1
1.2 Purpose and Objectives of Study	2
1.3 Study Design	2
1.3.1 Field Site Selection	2
1.3.2 Field Investigation	5
1.3.3 Assessment of Aquifer-Stream Connectivity.....	5
2. FIELD INVESTIGATION.....	5
2.1 Regional Setting	5
2.2 Climate and Groundwater Levels.....	6
2.3 The Steele Park Field Site.....	8
2.4 Site Geology and Hydrostratigraphy.....	11
2.5 Groundwater Levels.....	13
2.6 Assessment of Aquifer Properties	14
2.6.1 Grain Size Analysis	15
2.6.2 Slug and Bail Tests	16
2.6.3 Step Test.....	18
2.6.4 High-Rate Pumping Test	19
2.6.5 Low-Rate Pumping Test.....	23
2.6.6 Summer versus Winter Site Conditions.....	24
2.6.7 Summary of Aquifer Properties and Uncertainty.....	24
3. ASSESSMENT OF AQUIFER-STREAM CONNECTIVITY	27
3.1 Instream Measurements of Aquifer-Stream Connectivity.....	27
3.1.1 Streambed Piezometers	27
3.1.2 Seepage Meters.....	34
3.1.3 Stream Stage and Discharge.....	36
3.2 Streamflow Depletion Models	40
3.2.1 Glover-Balmer Model (1954).....	40
3.2.2 Glover Model with Residual Depletion	41
3.2.3 Hantush Model (1965).....	42
3.2.4 Hunt Model (1999)	42
3.2.5 Michigan Screening Tool	43
3.2.6 Singh (2003) Model	44
3.2.7 Hunt (2008)	44
3.3 Application of the Models to the Field Site	45
3.4 Uncertainties and Difficulties in the Estimation and Calculation of Field Parameters and Recommendations for Future Studies	48
4. CONCLUSIONS AND RECOMMENDATIONS.....	50
4.1 Site Hydrogeology.....	50
4.2 Aquifer-Stream Connectivity	51
4.3 Modeling Streamflow Depletion.....	52
4.4 Recommendations	52
REFERENCES.....	53
APPENDIX A: MONITORING WELLS.....	56

APPENDIX B: WELL HYDROGRAPHS 63
APPENDIX C: GRAIN SIZE CURVES 65
APPENDIX D: SLUG AND BAIL TEST CURVES 70
APPENDIX E: PUMPING TEST ANALYSIS 73

1. BACKGROUND

Groundwater is vital for sustaining community economic development and social well-being (e.g., industrial use, agricultural use and municipal and rural uses). It is estimated that over one million British Columbians use groundwater for their drinking water supply. In many areas, groundwater is the only feasible source of water.

Groundwater abstraction, however, can have detrimental impacts on streamflow in some aquifer-stream systems. Many streams are in direct hydraulic connection with groundwater and demonstrate a direct correlation between flows and groundwater levels. Often, groundwater provides flow to surface water and surface water recharges the aquifers. However, in most studies of hydrologic systems, each system component (groundwater, surface water) is analyzed and/or modeled individually, treating the other interconnected component as a source or sink. In reality, these components are intricately linked and must be considered simultaneously. Because of the interchange of water between these two components of the hydrologic system, understanding the basic principles of the interaction of groundwater and surface water is needed for effective management of water resources (Winter, 1999). Specifically, knowledge of the hydraulic connectivity between aquifers and streams is essential for the management of both resources.

1.1 Evaluation of Hydraulic Connectivity in B.C.

Evaluation of hydraulic connectivity is required for water licensing decisions under the *Water Sustainability Act (WSA)*. The *WSA* references hydraulic connection between water in a stream and groundwater in an aquifer in distinct contexts when (British Columbia Government 2016):

1. considering environmental flow needs (EFNs) in allocating water (section 15 of the *WSA*);
2. considering precedence of rights during times of water scarcity (section 22 of the *WSA*);
3. dealing with foreign matter in a stream or an aquifer (sections 46, 47, 59, and 60 of the *WSA*),
4. considering the operation of a well (section 58 of the *WSA*),
5. determining critical environmental flow thresholds and for issuing fish population protection orders (section 87 and 88 of the *WSA*), and;
6. considering sensitive streams (section 128 of the *WSA*).

As part of the water licensing process, the decision maker must determine whether the aquifer is “reasonably likely” to be hydraulically connected to streams, and if so, whether well pumping will affect streamflow, existing water licences on these streams, and the aquatic habitat (British Columbia Government, 2016). If the test of “reasonably likely” is met for connection to a specific stream(s), the demand from well pumping can then be accounted for in relation to the connected stream(s) to assess the impact of groundwater diversion on EFNs and on holders of rights on those stream(s), or in taking of action on users during a time of water scarcity (context 2) (British Columbia Government, 2016).

Sensitive streams are particularly at risk if hydraulically connected to an aquifer from which groundwater is abstracted. A sensitive stream is defined as a stream designated by regulation as a sensitive stream in the *WSA* in order to protect fish populations that are at risk from damage to the stream’s aquatic ecosystem. While designated sensitive streams currently fall under the *WSA*, prior to 2016 sensitive streams fell under the *Fish Protection Act*. Fifteen sensitive streams were originally designated under the *Fish Protection Act* (Government of British Columbia, 1997). The *WSA* maintains the sensitive stream designation on all 15 streams. The decision maker considering an application for an authorization in respect of a sensitive stream may require that the applicant provide information on the contribution to the sensitive stream from an aquifer and the seasonal distribution of water demand from the aquifer (section 17 of the *WSA*).

1.2 Purpose and Objectives of Study

The overall purpose of this study was to build an understanding of the interaction between groundwater and sensitive streams for the purpose of identifying streams that are more vulnerable to groundwater abstraction.

The component of the study documented in this report consisted of a targeted field investigation in Langley, B.C. to determine the impacts of pumping on aquifer-stream interactions. Various analytical methods for quantifying streamflow depletion from groundwater pumping were then tested. This report provides guidance of these various approaches for science-based allocation decision-making.

1.3 Study Design

1.3.1 Field Site Selection

The original design of this project aimed to assess hydraulic connectivity for two separate field study sites in the Township of Langley; each study site representing a different type of stream-aquifer system (i.e., one site expected to be hydraulically connected and the other one not expected to be hydraulically connected). Streams expected to be hydraulic connected include those flowing through unconfined aquifers, while hydraulically unconnected streams would flow above confined aquifers. When selecting field study sites, preference was given to selecting a stream that is either (1) a designated sensitive stream or (2) a fully recorded stream.

The two streams identified included: (1) the Salmon River (specifically Union Creek, a tributary that flows through the portion of the watershed that overlaps the Hopington Aquifer and (2) West Creek (Figure 1).

The Salmon River supports at least 13 species of fish, including the endangered Salish Sucker. A Water Allocation Restriction has been placed on surface flows in the Salmon River, signifying that the river is nearing or has reached full water allocation (see Figure 1 for points of diversion). The Hopington aquifer provides summer baseflow to the Salmon River, on the order of 22,000 m³/day (Golder Associates Ltd., 2016) but there is a high degree of baseflow reduction due to groundwater extraction. Golder Associates Ltd. (2004) estimated that the Salmon River has had a 17% reduction in baseflow (relative to pre-development conditions) and a further 15% reduction is expected due to further development. Groundwater use within this area is high; approximately 500 wells are known to exist within this relatively small area (Figure 2). Long term monitoring within the Hopington aquifer has shown substantial water level declines (Figure 3). Use of both groundwater and surface water within the study area is expected to remain high for the foreseeable future. Municipal water supply pipelines are located some distance from the study area and there are no known plans to extend this service. Most of the parcels within the study area are large rural properties, making the extension of municipal water less cost-effective for local residents, who ultimately bear the costs of such extensions. Further, municipal systems are often not designed for the large water volumes required by agricultural users.

West Creek drains a neighbouring watershed, with significantly different geologic conditions. West Creek is a designated sensitive stream under the WSA. The creek flows over several known confined aquifers, indicating conditions that are not conducive to a high level of groundwater-surface water interaction. The physical conditions of the watershed are therefore in contrast with the Salmon River, and this contrast in physical conditions is a key component of the breadth of knowledge required to develop comprehensive groundwater and surface water licensing guidelines.

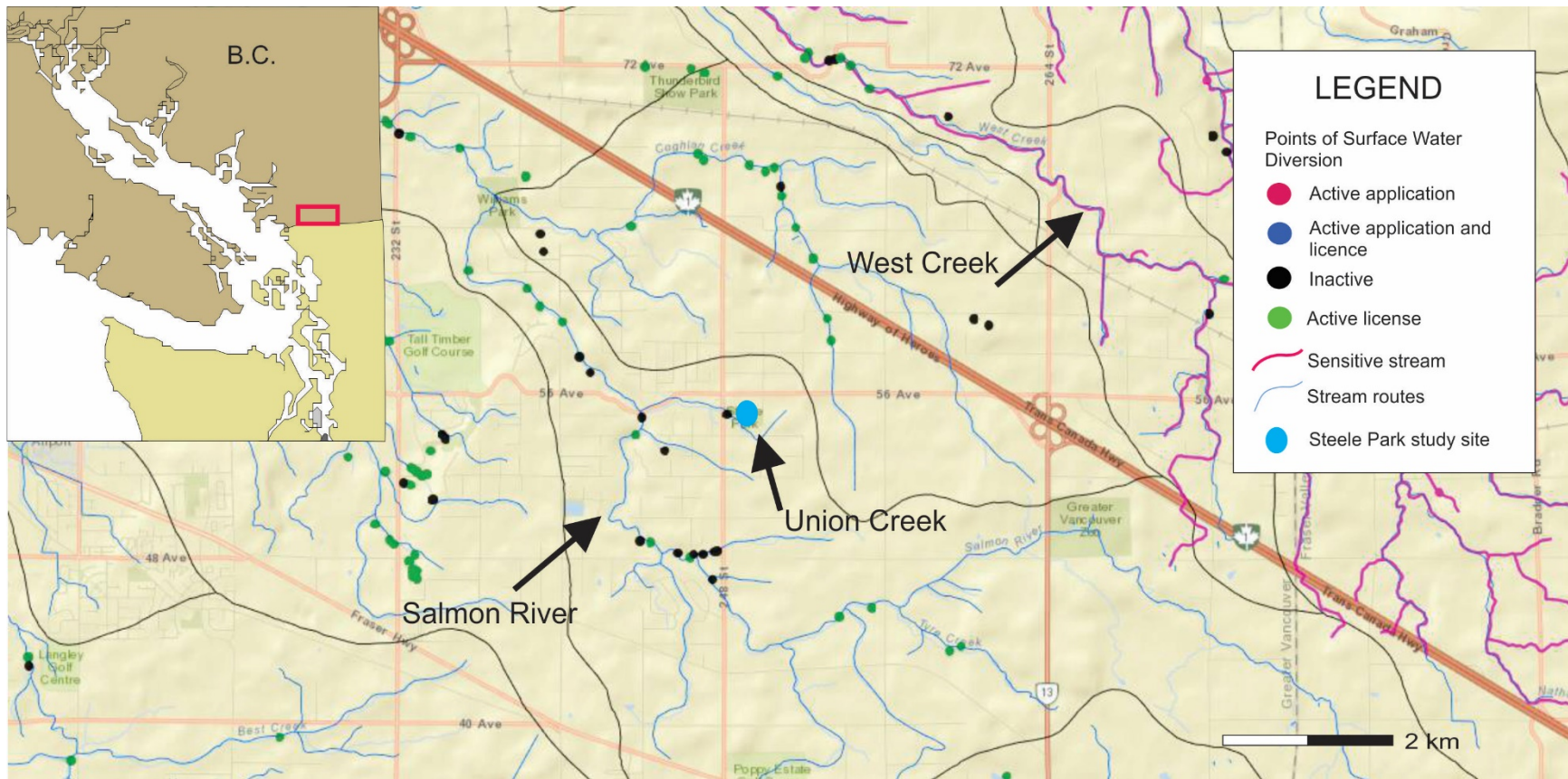


Figure 1: Location of the Salmon River (showing Union Creek) and West Creek in Langley, B.C. Also shown are points of surface water diversion. The inset map shows the approximate location of the map area in the Lower Fraser Valley of B.C.

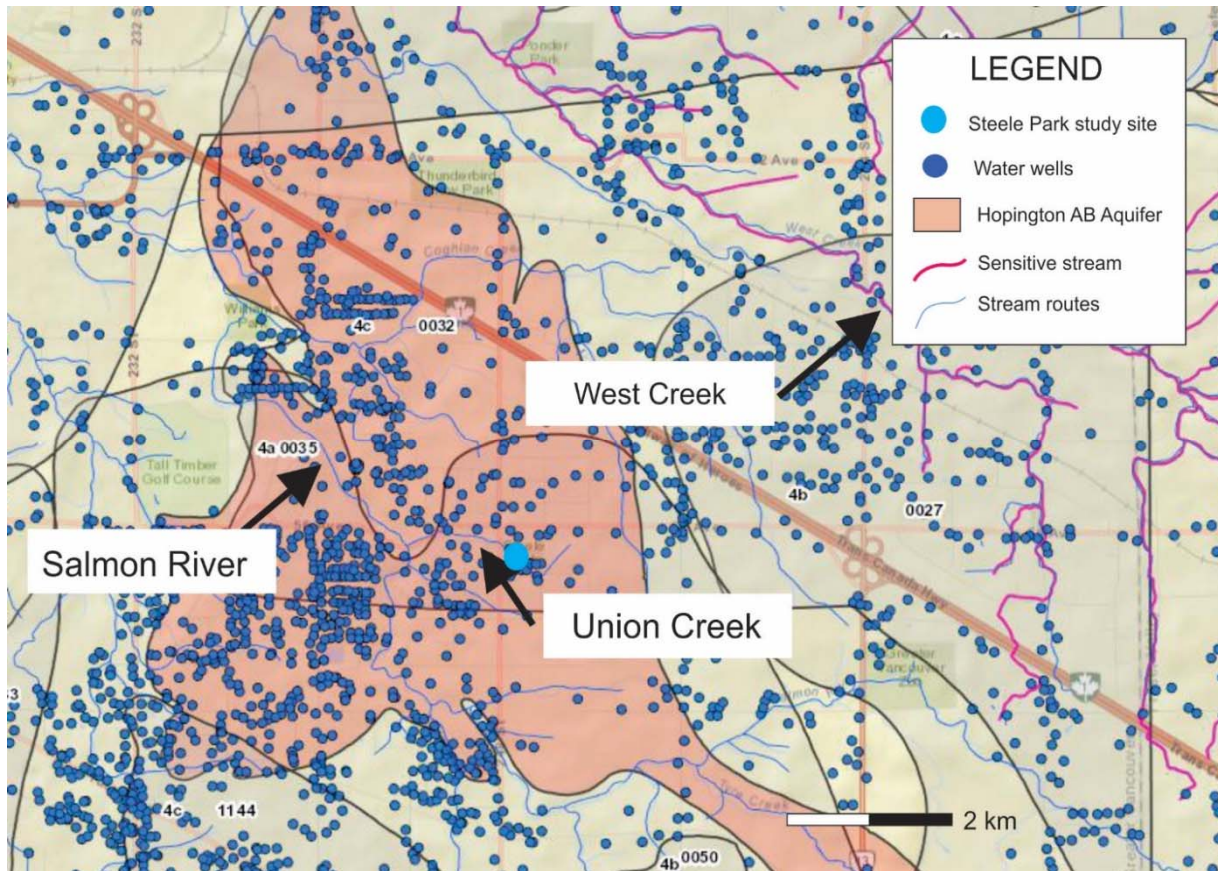


Figure 2: Location of the Salmon River (showing Union Creek) and West Creek in Langley, B.C. Also shown are water wells in the Provincial WELLS database and the Hopington AB Aquifer.

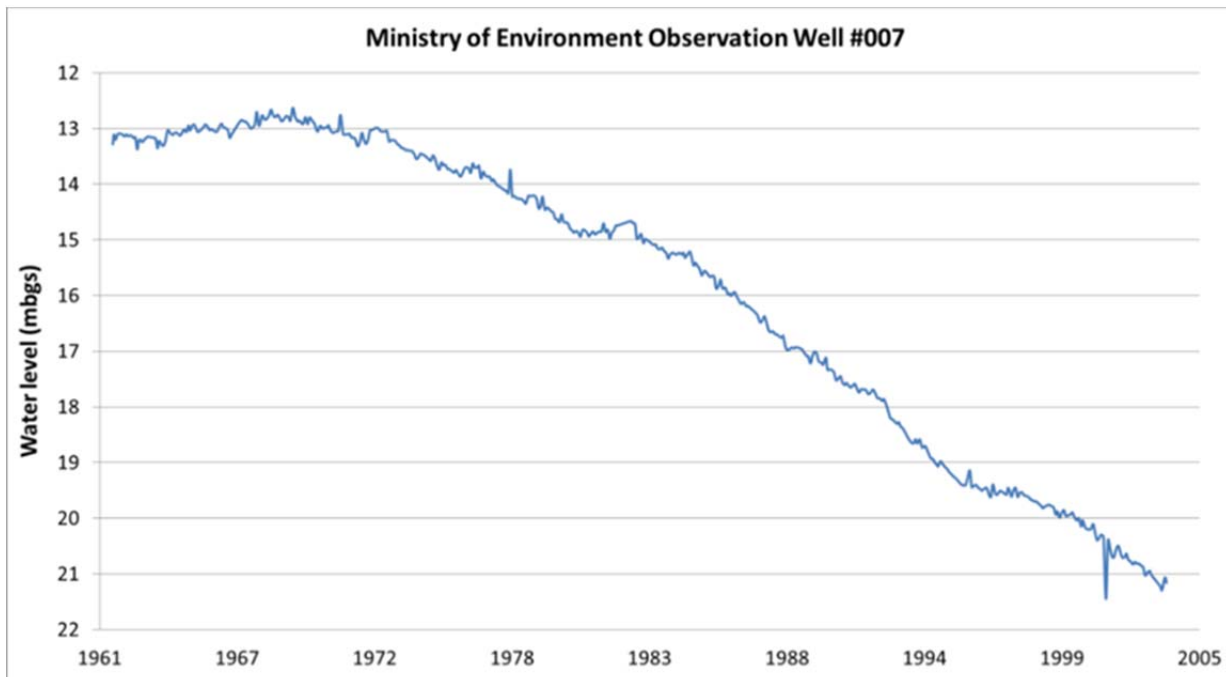


Figure 3: Provincial observation well #007 has shown substantial water level decline in the Hopington Aquifer (Langley) since the early 1970s. Note: Well #007 was decommissioned in 2004.

Field site selection along each of Salmon River and West Creek proved challenging due to access restrictions. Ultimately Steele Park at the headwaters of Union Creek was selected as the unconfined aquifer site (see Section 2). A location along West Creek at 80th Avenue west of 252nd Street was selected as the confined aquifer site. However, artesian conditions were encountered at the West Creek site and the associated costs were beyond the budgeted amount, so this site was ultimately abandoned as part of this study. The entire focus of the field investigation was on Union Creek at the Steele Park site.

1.3.2 Field Investigation

The field investigation at Union Creek involved drilling a new pumping well and two monitoring wells in relatively close proximity to Union Creek at the Steele Park site (see Section 2). The wells were completed in the spring of 2016. A baseline study was carried out in June 2016 during which slug and bail tests were completed in each of the wells to determine preliminary estimates of the hydraulic conductivity of the aquifer. The baseline study also involved making instream measurements of seepage using temporary drive point nested piezometers and seepage meters. Hydrometric stations were also installed in Union Creek in July 2016.

Two pumping tests were conducted at the site. Both tests included a preliminary step test, a constant discharge test and a recovery test. The first was a low-rate pumping test conducted in July 2016. This test was of short duration and at a low pumping rate because flows in Union Creek were very low and pumping could impact aquatic habitat. A second 48 hour high-rate pumping test was carried out in early December 2016. The data from both pumping tests were analyzed to determine the aquifer hydraulic properties and to infer the potential nature of aquifer-stream interaction.

Details concerning the field investigation can be found in Section 2.

1.3.3 Assessment of Aquifer-Stream Connectivity

Instream flow measurements in Union Creek were made during a baseline study as well as during the two aquifer tests conducted at the site. The instream measurements were analyzed to determine the nature of aquifer-stream interactions for both baseline and pumping conditions.

The responses to pumping at the Steele Park site were used to validate existing tools, specifically selected analytical methods for quantifying streamflow depletion from groundwater pumping as described by Rathfelder (2016). To date, these analytical methods implemented in MS Excel have only been applied to three locations in the Grand Forks aquifer. Through this study, these analytical tools will be more broadly verified using actual pumping test data.

Details concerning the assessment of aquifer-stream connectivity can be found in Section 3.

2. FIELD INVESTIGATION

2.1 Regional Setting

The study area is situated in the Lower Fraser Valley of British Columbia (see Figure 1). The topography of the area is relatively flat at an elevation of approximately 80 metres above sea level (masl) with the majority of topographic variation in the area due to glacial depositional and erosional features. Most of the sediments in the Fraser valley were deposited by glacial and glaciofluvial processes during the glacial and interglacial periods of the Quaternary and Holocene, and are comprised mainly of drift sequences interlayered with non-glacial deposits that correspond to the growth and subsequent decay of alpine and valley glaciers in the area (Clague and Luternauer, 1983).

All Langley soils are classified as Humic Luvic Gleysols (Luttmerding, 1981), and much of the naturally occurring vegetation in the Township of Langley (ToL) has been cleared for agriculture. There are 12,970 hectares of farmland within the ToL, totalling 1292 farms as of 2011 (HB Lanarc, 2011).

The greater Salmon River watershed, of which Union Creek is a part, is home to at least 13 species of fish including the Salish Sucker which is on the B.C. Wildlife-At-Risk list due to loss of habit from increasing urban and agricultural development (Blood, 1993).

2.2 Climate and Groundwater Levels

Climate normals from the Abbotsford International Airport¹ (Climate ID# 1100030) indicate total monthly precipitation in the area is highest between October and April with a maximum of 248.2 mm in November (Figure 4). May through to September is a period of low precipitation, with the lowest total monthly precipitation in July at 43.2 mm. The average total annual precipitation is 1538 mm. The highest average daily maximum temperature occurs in August at 24.4°C, while average daily maximum temperature is lowest in December at 5.9°C (Figure 4). The average annual daily maximum temperature is 15.1°C.

Long-term groundwater levels for the study area were obtained from B.C. provincial observation well 354 (see Figure 5 for location). The well is completed in surficial 35 (Hopington AB Aquifer). It is 26 m deep and screened from 23.5 to 26 m in sand & gravel. Overlying sediments consist variably of sand and sand & gravel.

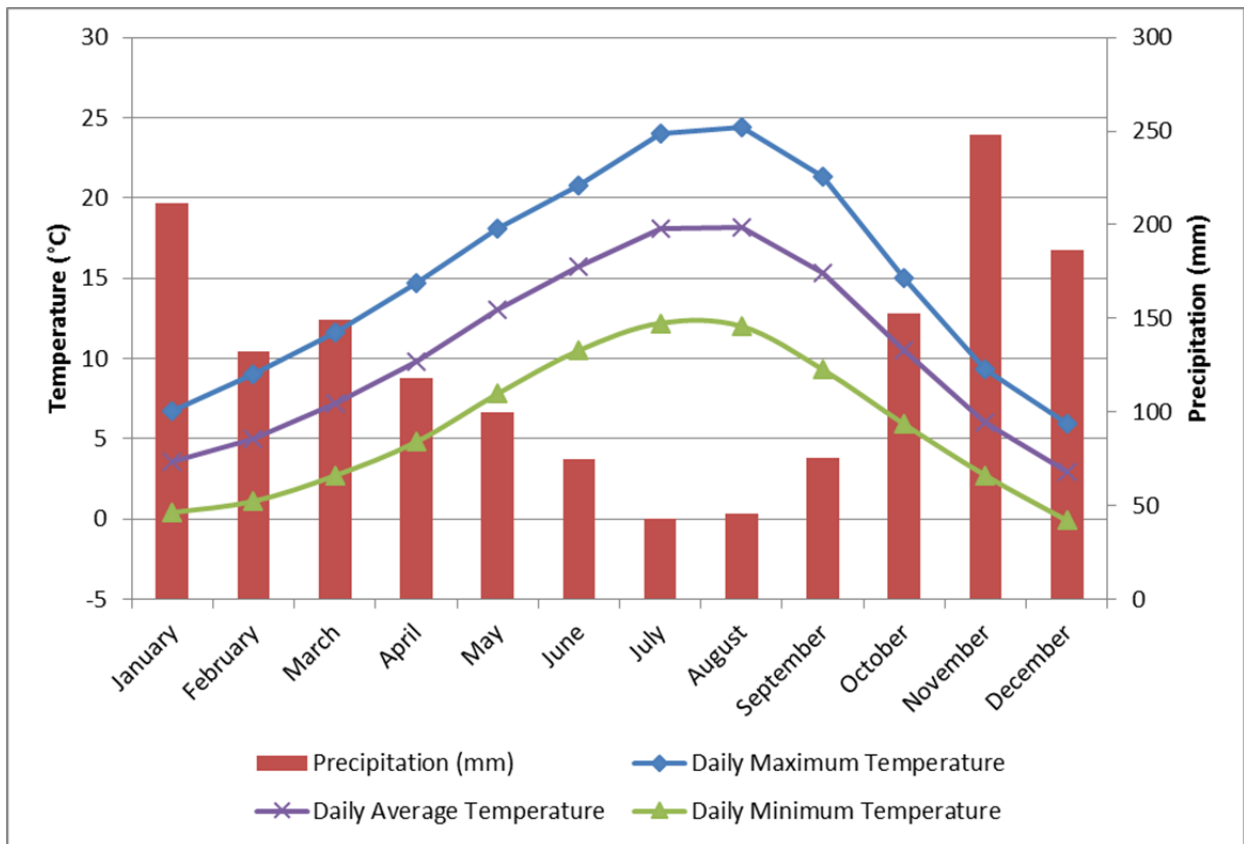


Figure 4: Temperature and precipitation normals for Abbotsford International Airport (1981-2010). Source: Environment Canada (Climate ID# 1100030).

¹ Abbotsford International Airport is the closest climate station with sufficient data to calculate climate normals.

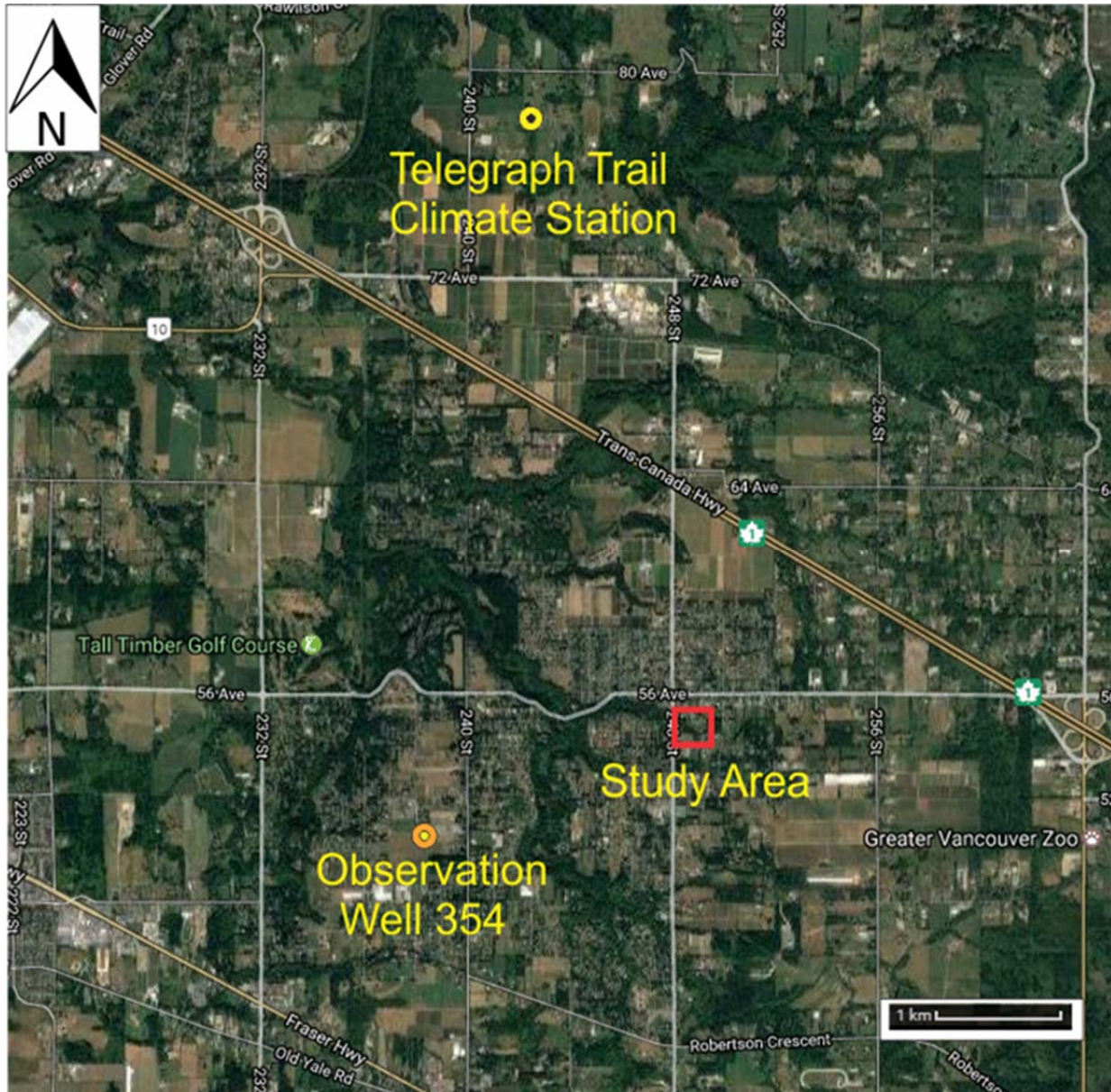


Figure 5: Location of provincial observation well 354, and the Fort Langley Telegraph Trail climate station (1102912) relative to the Steele Park study area.

Groundwater levels at well 354 are lowest in December to January at 12.2 to 12.6 m below ground surface (mbgs), and reach a maximum height in April to May at 10.6 to 10.9 mbgs (Figure 6). The data show yearly water level fluctuations of approximately 2 m.

For comparison with the groundwater levels, local climate records were obtained from the Fort Langley Telegraph Trail climate station (Station ID 1102912) situated just north of the study site (see Figure 5 for location). Groundwater levels appear to lag behind precipitation events, with the maximum groundwater levels (March) occurring approximately four months after the start of the winter rains in early November (Figure 6). The observed groundwater level response suggests that recharge to the aquifer is primarily from precipitation during the winter and spring months.

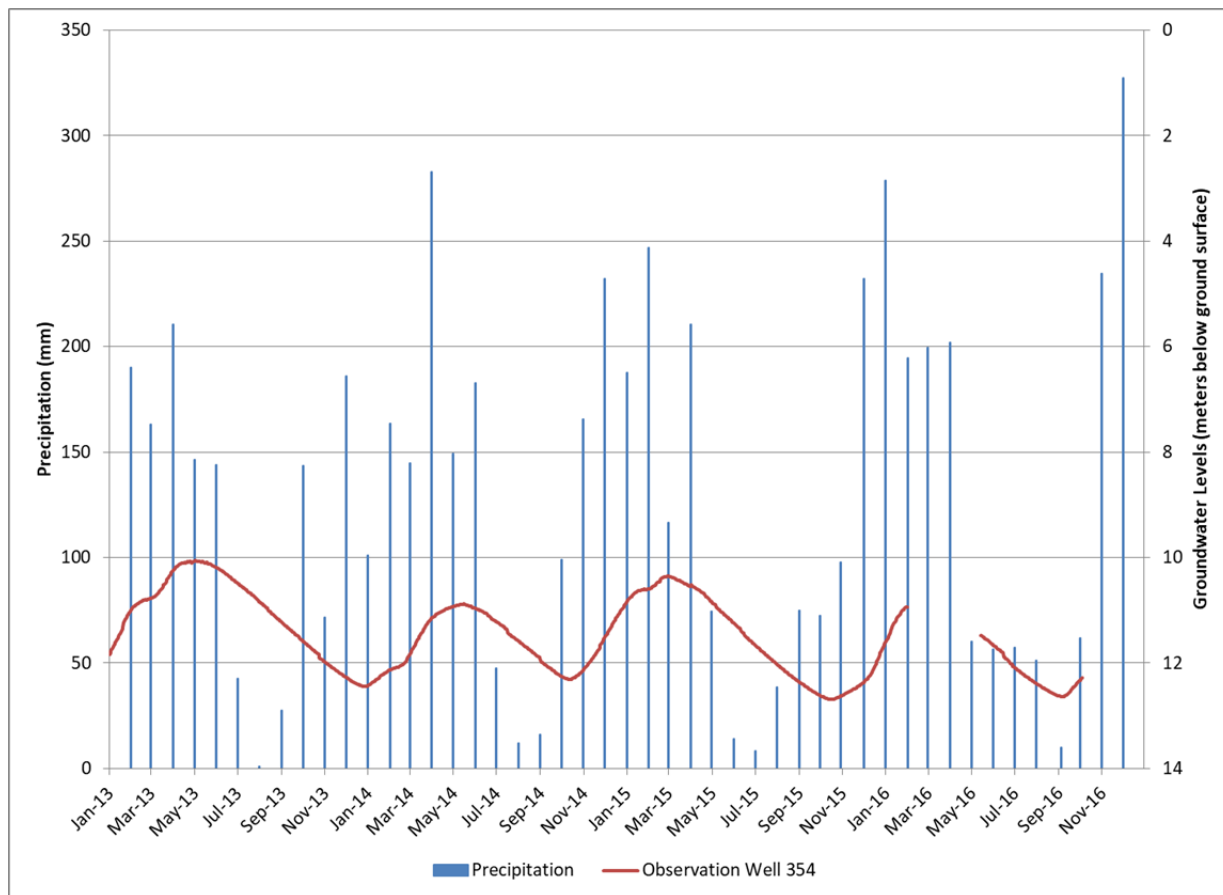


Figure 6: Monthly total precipitation (blue) and groundwater levels (red) from January 2013 to December 2016. Peak groundwater levels occur approximately four months after the initial winter rains begin in November.

2.3 The Steele Park Field Site

Steele Park is situated at the intersection of 54th Avenue and 248th Street in the ToL (study area in Figure 5). Union Creek’s headwaters are just east of the study site and it flows northwest through farmland and suburban areas for 17 km, joining other tributaries and feeding the Salmon River itself before finally discharging into the Fraser River.

In March 2016, three boreholes were drilled at Steele Park by the Ministry of Forests, Lands, Natural Resource Operations and Rural Development (FLNR) (Figure 7). The wells were drilled in a triangle, with the two monitoring wells SPMW-01 and SPMW-02 parallel to the creek and offset by roughly 13 m (Figure 8). The pumping well SPPW is located at the furthest corner of the triangle, approximately 27 m from the stream. SPPW is 13.4 m deep and screened from 9.1 m to 11.6 m, SPMW-01 is 9.8 m deep and screened from 6.7 m to 9.8 m, and SPMW-02 is 10.4 m deep and screened from 7.3 m to 10.4 m. The two monitoring wells were fitted with 3 inch PVC casing and completed slightly below grade with a well cover flush with ground level, while the pumping well was completed with an 8 inch steel casing to a height of 0.77 m above ground (Figure 9).

The wells were drilled in this triangular formation to allow for the hydraulic gradient in the horizontal plane (coincident with screened intervals of the wells) to be calculated by way of a three-point-problem. The elevations of ground surface for the three wells were surveyed and referenced to the ground elevation at the pumping well (Table 1). The original survey is provided in Appendix A (Figure A1).

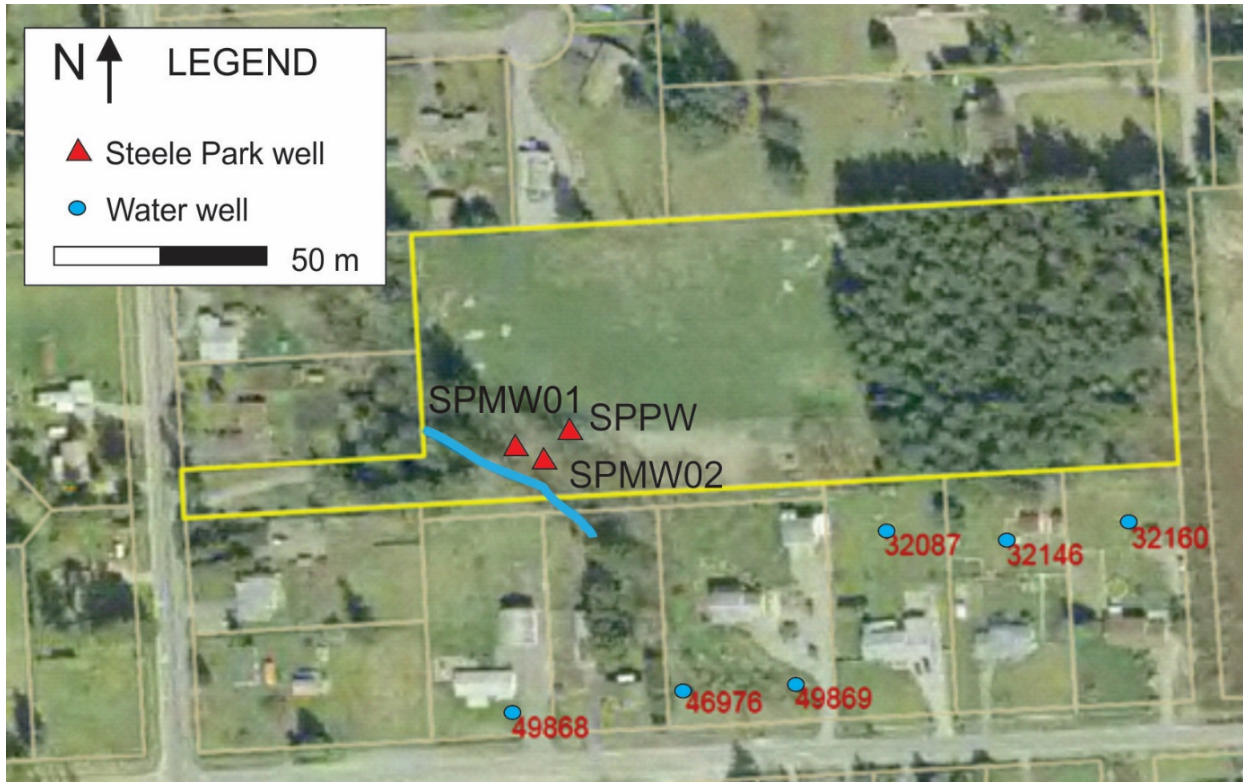


Figure 7: Map showing the location of the wells drilled at Steele Park and the surrounding domestic water wells (B.C. well tag numbers shown).

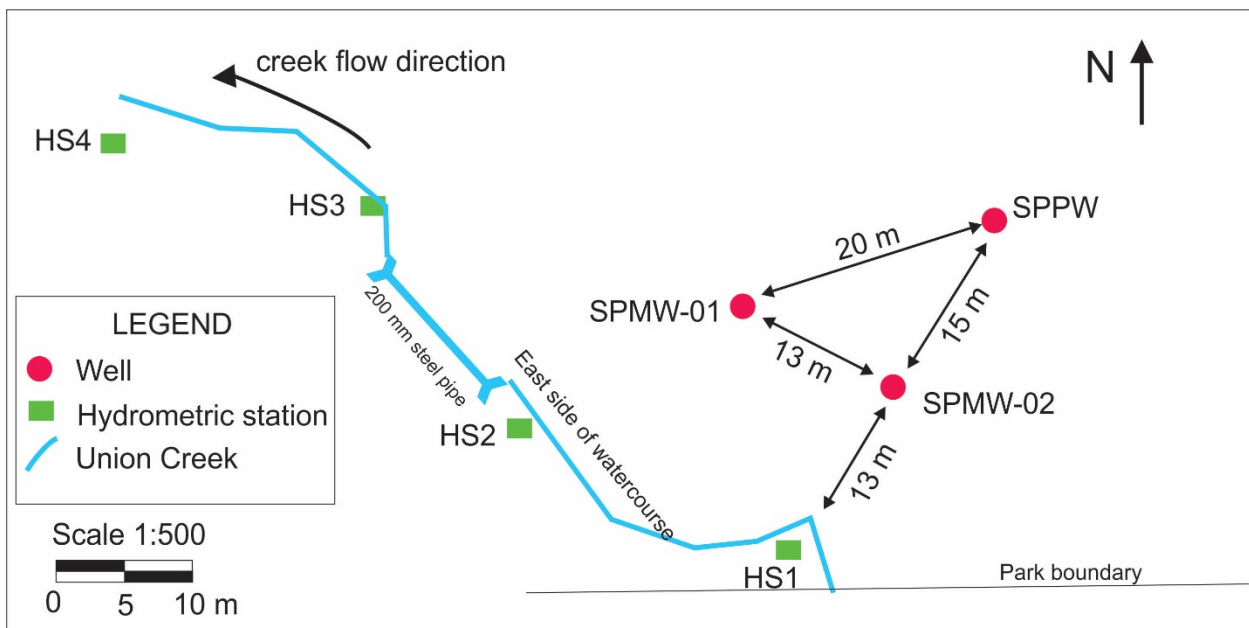


Figure 8: Site geometry showing the relative positions of the three wells, the East edge of Union Creek, and the four hydrometric stations at Steele Park.



Figure 9: Photos of the Steele Park site including: a) monitoring well SPMW-02, b) pumping well SPPW, and c) view of hydrometric station 1 (HS1) from the East bank of Union Creek.

Union creek at the study site is roughly 2 m wide and has a streambed thickness of approximately 0.1 m based on a streambed sample taken near Hydrometric Station 1 (HS1) with a clam gun. A cross section showing the geometry of the site is shown in Figure 10. The water table profiles measured on July 22nd and November 26th 2016 are also shown on Figure 10.

Table 1: Elevations of ground level at SPMW-01, SPMW-02 and Union Creek, relative to ground elevation at the pumping well (SPPW). See Figure 8 for locations.

Location	Ground elevation (m)	Elevation of top of casing (TOC) (m)	Elevation relative to ground elevation at the pumping well (m)
SPPW	87.27	88.04	0
SPMW-01	86.81	86.71	-0.46
SPMW-02	87.11	87.00	-0.16
Creek bed	83.49	-	-3.78

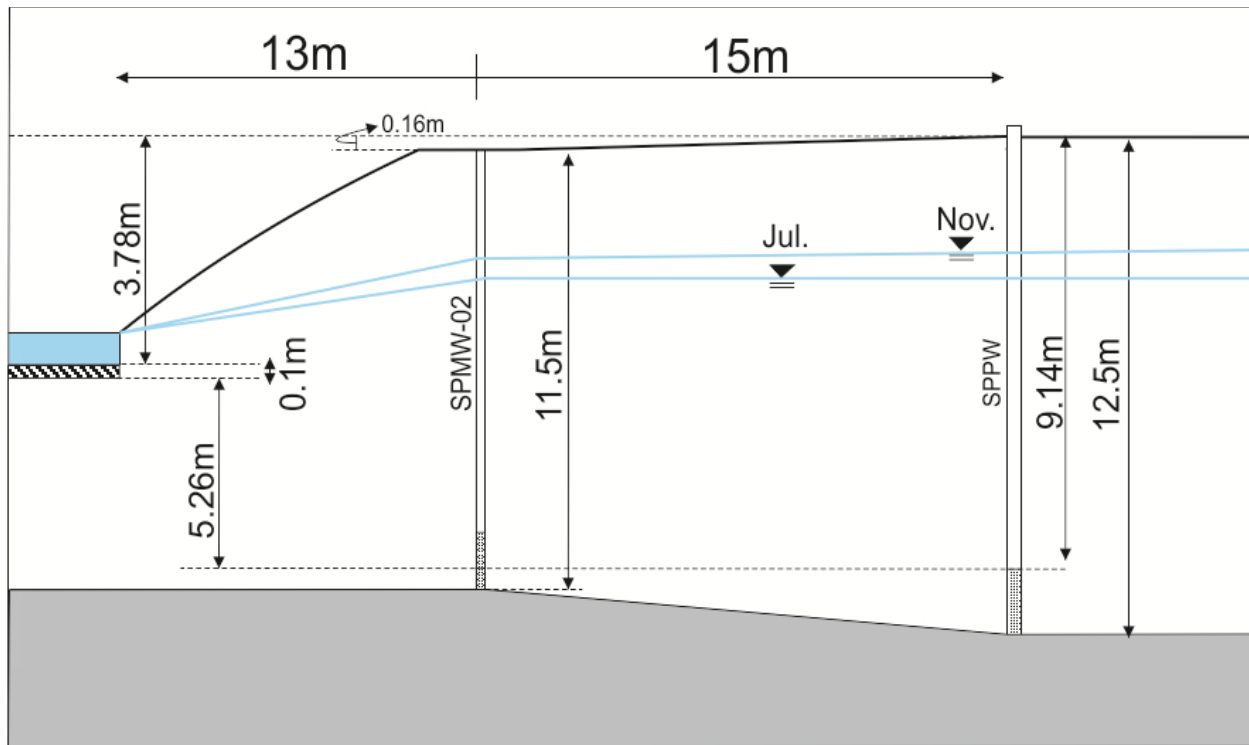


Figure 10: Cross sectional view of the study site showing both horizontal and vertical distances between SPPW, SPMW-02 and the creek (shown in blue on the left). The water table profiles on July 22nd and November 26th are shown.

2.4 Site Geology and Hydrostratigraphy

Driller's logs for the three wells drilled at Steele Park were used to determine the lithology of the site. A more detailed lithologic description of SPMW-02 was produced by logging the core in July of 2016. The driller's logs for all three wells, as well as the detailed core log for SPMW-02 are provided in Appendix A. Driller's logs for six domestic water wells along 54th Avenue (Figure 7) were also examined to determine if the site geology at Steele Park is consistent with the geology of the surrounding area. The six domestic well borehole logs are summarized in Appendix A. From these logs, the hydrostratigraphic units at the site were determined to consist of an unconfined, upper sandy gravel aquifer overlying a clay-rich confining unit, beneath which is another thin sandy aquifer unit, which is in turn underlain by a lower clay unit (Figure 11).

Three of the domestic wells only penetrated down to the upper clay layer, while the other three penetrated through the upper clay layer and down into a lower confined aquifer consisting of silty, sandy till, before ultimately terminating in a lower clay layer at approximately 70 m depth. The six domestic wells corroborate the interpretation of the hydrostratigraphy in the Steele Park wells, showing the upper unconfined aquifer to consist of layers of medium to coarse sands and gravels underlain by an extensive, undulating clay layer. The depth to the upper clay layer ranges from 4.5 m to the east of the study site, to 11.5 m south of the study site, to 12.5 m at the pumping well (Figure 12).

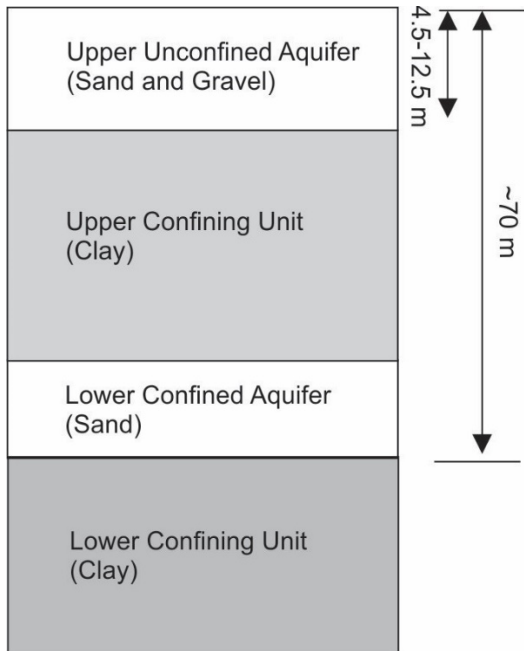


Figure 11: Schematic diagram of the hydrostratigraphic units at Steele Park. The wells at Steele Park are completed through the upper unconfined aquifer estimated to range in thickness from 4.5 to 12.5 m.

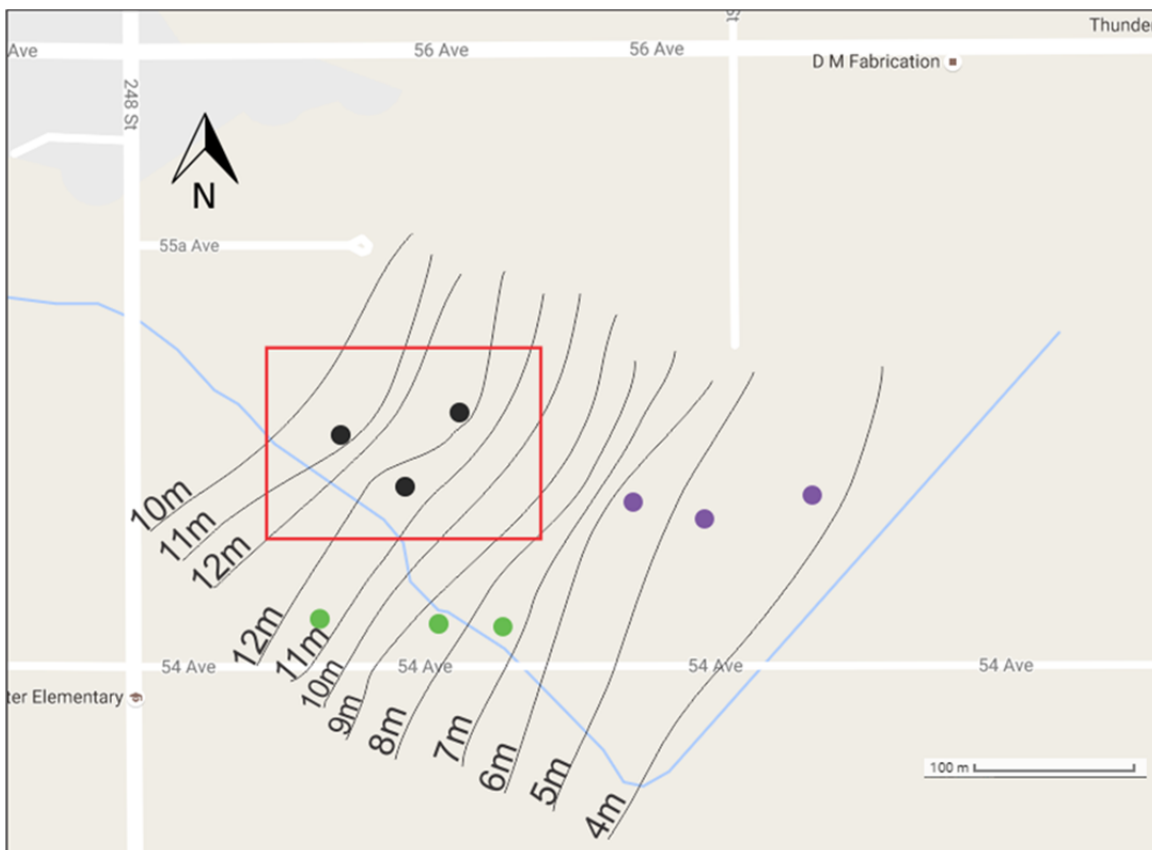


Figure 12: Interpreted depth-to-clay contours based on borehole lithology data. The Steele Park study site is outlined in red. Purple dots are domestic wells extending beyond the upper clay unit into the confined aquifer below. Green dots are domestic wells that only penetrate into the upper clay unit.

The soil at the site is dark brown to orange in colour, and is approximately 1 m thick based on the detailed core log from SPMW-02 (Appendix A). The soil has a high silt and organic content near the surface, which gradually grades to gravelly sand with depth. Plant root macro-pores and organic matter density also gradually decreased to zero at around 1 m depth. The soil at Steele Park is described as gently undulating Marble Hill deposits, which are described as eolian sediments of medium texture greater than 50 cm thick overlying gravelly glacial outwash deposits (Luttmerding, 1980). These are classified as Orthic Humo-Ferric Podzols.

Steele Park overlies a high-demand aquifer (Hopington aquifer); there are 93 other water wells within a 1 km radius of the site (Figure 13).

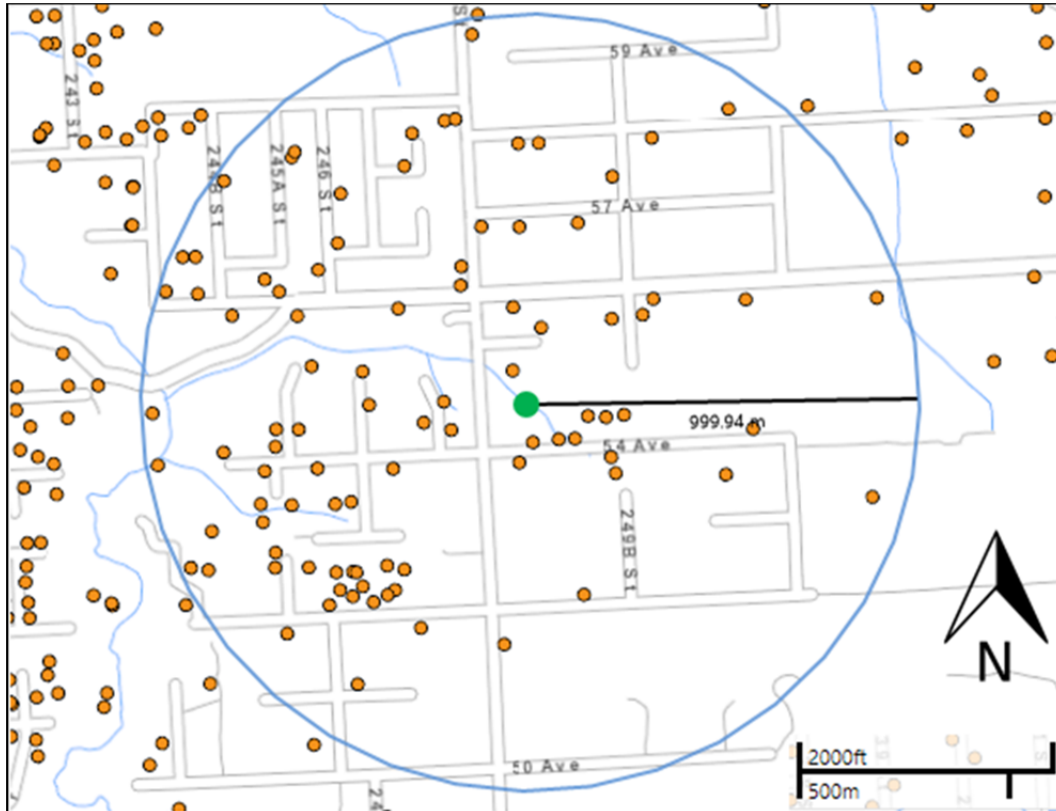


Figure 13: Zoomed view of the 1 km radius area around the study site shown in Figure 5. The green dot is the study site, the blue circle represents a 1 km radius around the site, and the orange dots are water wells supply shown in iMap BC. (Source: iMap BC).

2.5 Groundwater Levels

Due to the unconfined nature of the aquifer at the site and the variable nature of the bottom clay layer (Figure 12), the saturated thickness of the aquifer changes both spatially and temporally. The saturated thickness of the aquifer under non-pumping conditions was approximated by subtracting the depth to water level (below top of casing) from the top of the clay layer in each well. The average saturated thickness in early summer for June 15th and July 22nd ranged from 7.958 m in June 2016 to 7.892 m in July 2016, with an average of 7.925 m (Table 2). On August 11th, the saturated thickness was 7.679 m (the pumping well was inaccessible). On November 26th 2016 revealed depth to water levels of 2.434 m and 2.628 m in SPMW-01 and SPMW-02, respectively (the pumping well was inaccessible). These water levels reflect a rise in the water table of 0.682 and 0.684 m, respectively, compared to the average of the water level measurements taken in June, July, and August. Therefore, there was an average water

table rise of 0.683 m, resulting in an estimated saturated thickness of 8.419 m during the late fall. In December, prior to the high rate pumping test, the average saturated thickness was 8.654 m, slightly greater than in November.

Table 2: Water levels measured (metres below top of casing: m btoc) at the site during various field visits in 2016, depth to clay (metres below ground surface: m bgs), and estimated average saturated thickness (m) of the aquifer.

Well	Water Level (m btoc)					Depth to Clay (m bgs)	Aquifer Saturated Thickness (m)				
	Jun	Jul	Aug	Nov	Dec		Jun	Jul	Aug	Nov	Dec
SPPW	4.212	4.283	-	-	3.372	12.5	8.288	8.217	-	-	9.128
SPMW-01	3.060	3.118	3.173	2.434	2.430	10.4	7.340	7.282	7.227	7.966	7.970
SPMW-02	3.255	3.324	3.370	2.628	2.637	11.5	8.245	8.176	8.130	8.872	8.863
Average	-	-	-	-	-	11.5	7.958	7.892	7.679	8.419	8.654

The hydraulic gradient at the site under non-pumping conditions was estimated for three separate monitoring events (June, July, and December 2016) using the three point problem approach. The water table at the site was not completely horizontal; during summer the flow direction was at an angle of roughly 30 degrees to the stream in a downstream direction with gradients of 7.97E-03 (June) and 6.29E-03 (July). In winter (December) the groundwater flow direction was almost perpendicular to (in towards) the stream with a gradient of 2.05E-02.

Groundwater levels were monitored by FLNR in SPPW, SPMW-01, and SPMW-02 from 15:00 on June 15th to 11:00 on June 30th using pressure transducers sampling hourly. The groundwater level declined 3 to 4 cm over the month of June (Figure 14), which is consistent with declining water levels expected during summer months. All well hydrographs are provided in Appendix B. The groundwater level also showed a 24 hour periodic fluctuation in the water table of about 4 mm, with the maximum daily water level occurring in the early morning between 3 and 6 am, and the lowest daily water level occurring around 6 to 8 pm. These small scale fluctuations in the water table are due to transpiration by the flora at the site, which is why the maximum water levels occur early in the morning when transpiration has decreased due to lack of sunlight. These fluctuations are not related to watering of the grass playing field every morning because no watering took place. Ultimately, these daily fluctuations are very small, and were not expected to have a significant effect on the daily volumetric flux contributed to the stream through baseflow.

2.6 Assessment of Aquifer Properties

The hydraulic properties of the aquifer were evaluated through a series of different tests on the aquifer material. First, a grain size analysis on samples taken from the sonic drill core of SPMW-02 was completed in order to characterize the hydraulic conductivity (K) using Hazen's method (Hazen 1982). A series of slug and bail tests was carried out in June 2016 and the data were analyzed to estimate the in situ K in the vicinity of the well screen. The estimated K values were subsequently used to estimate, using the Theis equation (Theis 1935), the recommended pumping rate for a short term (2 hour) low-rate (0.5 L/s) pumping test conducted in late July 2016. This was followed by a longer term (48 hour) high-rate (1.51 L/s) pumping test in December 2016. Both tests were preceded by step discharge tests and were followed by recovery tests. The pumping test data were analyzed to estimate the aquifer transmissivity (T), K, specific yield (Sy), and specific storage (Ss). Due to its exploratory nature, the low-rate pumping test is discussed in this section following the high-rate pumping test, although the same methods of analysis were used for both tests.

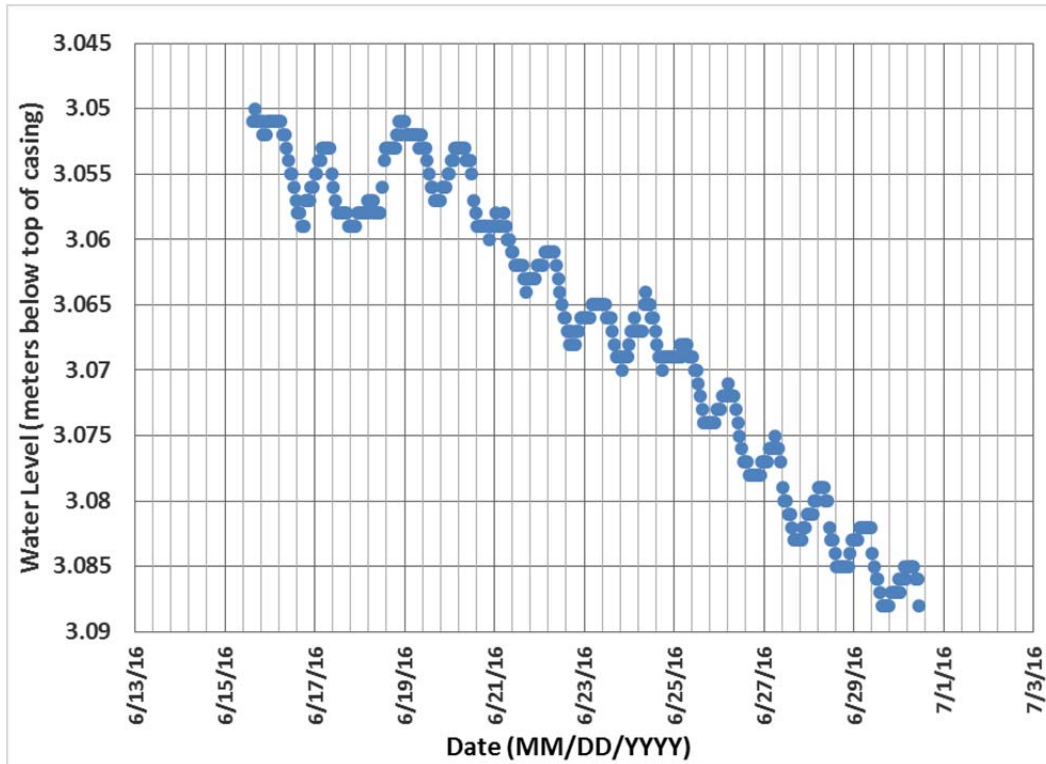


Figure 14: Groundwater levels in SPMW-01 for June 2016. Water levels are given in metres below top of casing.

2.6.1 Grain Size Analysis

Samples were taken at varying depths from the sonic core retrieved from SPMW-02 (see Appendix A for lithological descriptions of the core). Samples were taken approximately when there was an observed change in grain size.

Grain size distribution for samples 1A, 1B, 2A, 3A, and 4A were measured using a mechanical tapping sieve shaker run for 20 minutes. All samples, except sample 1B, were run through a sieve set consisting of 4 mm, 2 mm, 1 mm, 0.5 mm, 0.25 mm, 0.125 mm, and 0.063 mm sieves. Sample 1B had large clasts greater than 4 mm in diameter, and so was first hand sieved through a sieve set of 25 mm, 19 mm, 12.5 mm, and 6 mm sieves, and the remaining sample was sieved using the same mechanical tapping method as the other samples. The sample numbers, approximate depths, and corresponding visual grain size estimations are shown in Table 3.

Table 3: Samples taken from SPMW-02 sonic core for grain size analysis.

Sample #	Depth (m below ground surface)	Grain size description
1A	0.9	Very fine sand
1B	2.5	Medium to fine sand
2A	5.0	Fine sand
3A	8.5	Medium sand
4A	9.5	Medium sand
4B	11	Medium clayey sand
5A	14.5	Clay

Grain size curves for each sample were constructed in MS Excel (see Appendix C) and hydraulic conductivity was estimated for each sample according to Hazen’s method:

$$K = C(d_{10})^2 \quad (\text{Eq. 1})$$

where K is the hydraulic conductivity of the material (cm/s), d_{10} is the diameter for which 10 percent of the material passes through the sieve (cm), and C is a unitless empirical coefficient for different types of sand (Fetter, 2001) as shown in Table 4.

Hydraulic conductivity (K) values were calculated for samples 1A, 1B, and 2A using C values of 40 (fine sand), and for samples 3A and 4A for a C value of 80 (medium sand). An average K value for the aquifer was calculated as the geometric mean (Table 5). The Hazen method is not applicable for samples 4B and 5A due to their small grain size.

Table 4: Different material types and corresponding C values for use in the Hazen method (Fetter, 2001).

Material type	C
Very fine sand, poorly sorted	40-80
Fine sand with appreciable fines	40-80
Medium sand, well sorted	80-120
Coarse sand, poorly sorted	80-120
Coarse sand, well sorted, clean	120-150

Table 5: K values obtained using the Hazen method based on the grain size analysis of SPMW-02 sonic core.

Sample	d_{10} (cm)	C	K (cm/s)	K (m/s)
1A	0.009	40	3.2E-03	3.2E-05
1B	0.045	40	8.1E-02	8.1E-04
2A	0.0145	40	8.4E-03	8.4E-05
3A	0.0197	80	3.1E-02	3.1E-04
4A	0.0205	80	3.4E-02	3.4E-04
Geometric Mean	-	-	1.9E-02	1.9E-04

2.6.2 Slug and Bail Tests

Slug and bail tests were conducted for both monitoring wells (SPMW-01 and SPMW-02) and the pumping well (SPPW). In total, two tests were conducted in SPMW-01, seven tests in SPMW-02, and four tests in SPPW. Two different slugs were used. The slug used for the tests in SPMW-01 and SPPW was 0.91 m in length and 0.0484 m in diameter, equalling 0.00167 m³ total volume, or 1.67 L. The slug used for the tests in SPMW-02 was 1.5 m in length and 0.0334 m in diameter, equalling 0.00132 m³ total volume, or 1.32 L.

HOBO™ pressure transducer data loggers were suspended in the well at a depth of approximately 0.5 m below the bottom of the slug when the slug was fully submerged below the static water level. The sampling interval was one second. A preliminary slug and bail test was done in SPMW-01 to determine the time required for equilibrium. The resulting water level plot shows that it took approximately 3 minutes for the water levels to equilibrate (Figure 15). Since all three wells at the site were within 20 m of each other, it was assumed that the equilibrium time would be the same or similar for all three wells. The slug and bail tests were then performed allowing 3 minutes between insertion and removal of the slug.

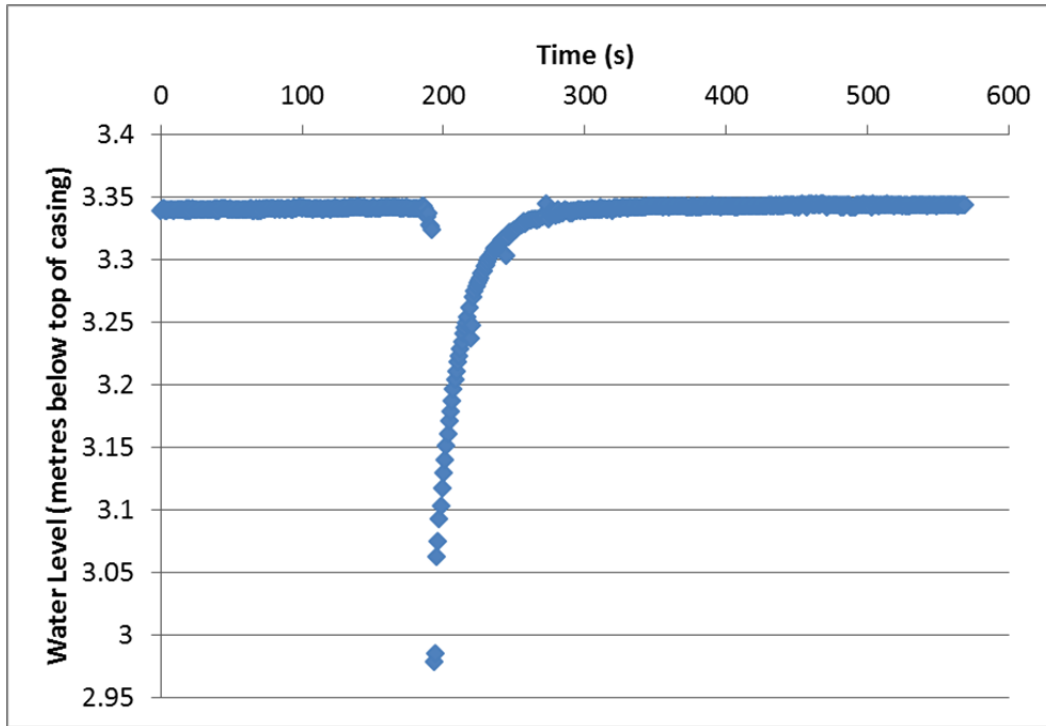


Figure 15: Initial bail test for SPMW01. Time elapsed from the moment the slug was removed from the water column to when water level returned to its pre-bail level is approximately 3 minutes.

The data were analyzed using Hvorslev’s method (Hvorslev, 1951) and the Bouwer-Rice method (Bouwer and Rice, 1976) in the analysis software AquiferTest™ (Waterloo Hydrogeologic Inc., 2016). While Hvorslev’s method is intended for confined aquifers, work by Brown et al. (1995) showed that the upper boundary condition (water level height) has a very small effect on the estimate of K , except when the water level is very close to the top of the well screen. The water table at the site was greater than 3 m above the top of the well screen in all of the wells, so the estimates of K obtained from Hvorslev’s method are likely to be fairly accurate even though the aquifer is unconfined. Hvorslev’s slug/bail test analysis method for wells with a screen length greater than eight times the screen radius is given by the equation below.

$$K = \frac{r^2 \ln\left(\frac{L}{R}\right)}{2LT_L} \quad (\text{Eq. 2})$$

where:

- K is hydraulic conductivity (m/s),
- r is the radius of the well (m),
- R is the radius of the well including the gravel pack (m),
- L is the screen length (m), and
- T_L is time required for the head displacement in the well to reach 37% of its initial magnitude (s).

Data analysis involved plotting the water level data on a semi-log plot of normalized head (h/h_0) versus time with normalized head on a log scale, and then a straight line was fit to the data over the recommended normalized head interval of 0.15 to 0.25 (Butler, 1998). The analysis results are show in Appendix D.

The K values obtained from the slug tests are shown in Table 6. The geometric mean of combined results with Hvorslev’s Method is 6.2E-05 m/s.

Table 6: Hydraulic conductivity values obtained from slug and bail testing using Hvorslev's method.

Wells	Hvorslev Method - K (m/s)						
SPMW-01	6.2E-05	5.9E-05	-	-	-	-	-
SPMW-02	5.0 E-05	3.8E-05	5.5E-05	4.1E-05	5.4E-05	4.2E-05	5.3E-05
Pumping well	1.2E-04	8.9E-05	1.2E-04	8.5E-05	-	-	-
Geometric mean (all values)	6.2E-05						

The Bouwer-Rice (1976) method for slug test analysis is intended for use in unconfined aquifers, and K is defined as:

$$K = \frac{r_c^2 \ln\left(\frac{R_e}{r_w}\right)}{2dt} \ln\left(\frac{h_0}{h_t}\right) \quad (\text{Eq. 3})$$

where:

- r_c is the radius of the unscreened part of the well in which the head is rising (m);
- r_w is the horizontal distance from the well centre to undisturbed aquifer (m);
- R_e is the effective radius, (radius over which the difference in head is dissipated within the flow system of the aquifer (m);
- d is the length of the well screen (m);
- h_0 is the initial head level in the well at time = t_0 (m); and
- h_t is the head level in the well at time t, where $t \geq t_0$ (m).

Analysis of the slug/bail test data was performed by plotting the normalized head data (h_0/h_t) on a log scale against time on a linear scale. A straight line was then fit to the data over the normalized head interval of 0.20 to 0.30 recommended by Butler (1998). The analysis results are shown in Appendix D. The K values obtained from the Bouwer-Rice analysis are shown in Table 7. The geometric mean is 4.8E-05 m/s.

Table 7: Hydraulic conductivity values obtained from slug and bail testing using the Bouwer-Rice method.

Wells	Bouwer-Rice Method - K (m/s)						
SPMW-01	4.7E-05	4.6E-05	-	-	-	-	-
SPMW-02	4.0E-05	2.9E-05	4.4E-05	3.0E-05	4.3E-05	3.3E-05	4.0E-05
Pumping Well	9.1E-05	7.0E-05	9.0E-05	6.7E-05	-	-	-
Geometric Mean (all values)	4.8E-05						

2.6.3 Step Test

A step test was carried out at the site on December 5th 2016 in order to determine the optimal pumping rate for the 48 hour constant discharge test. The test consisted of four pumping rate steps, 30 minutes in duration, each roughly 0.5 L/s higher than the previous. The pumping rates and drawdowns at the end of each step are given in Table 8. The pump was suspended in the well 7.62 m below the top of casing. The last step of the test lowered the water level to 7.2 m below top of casing, which was just above the pump. Although the specific capacity remained relatively constant over the four steps (Table 8), a pumping rate of 1.5 L/s was selected for the 48-hour test to avoid excessive drawdown at late time. This rate also accounted for the effect of additional late stage drawdown typical of an unconfined aquifer. The time-drawdown graph for the step test is shown in Figure 16. The drawdown response in steps 1 and 2 is unusual in that there are two spikes at early time. These spikes may be related to pumping rate adjustments.

Table 8: Step test pumping rates, drawdown at the end of each 30 minute step, and the calculated specific capacity for each step.

Step	Time	Pumping Rate (US gpm)	Pumping Rate (L/s)	Drawdown at the end of the Step (m)	Specific Capacity (L/s/m)
1	12:40 – 13:10	7.2	0.45	0.90	0.50
2	13:10 – 13:40	16.05	1.01	1.98	0.51
3	13:40 – 14:10	23.9	1.51	2.90	0.52
4	14:10 – 14:40	31.7	2	3.85	0.52

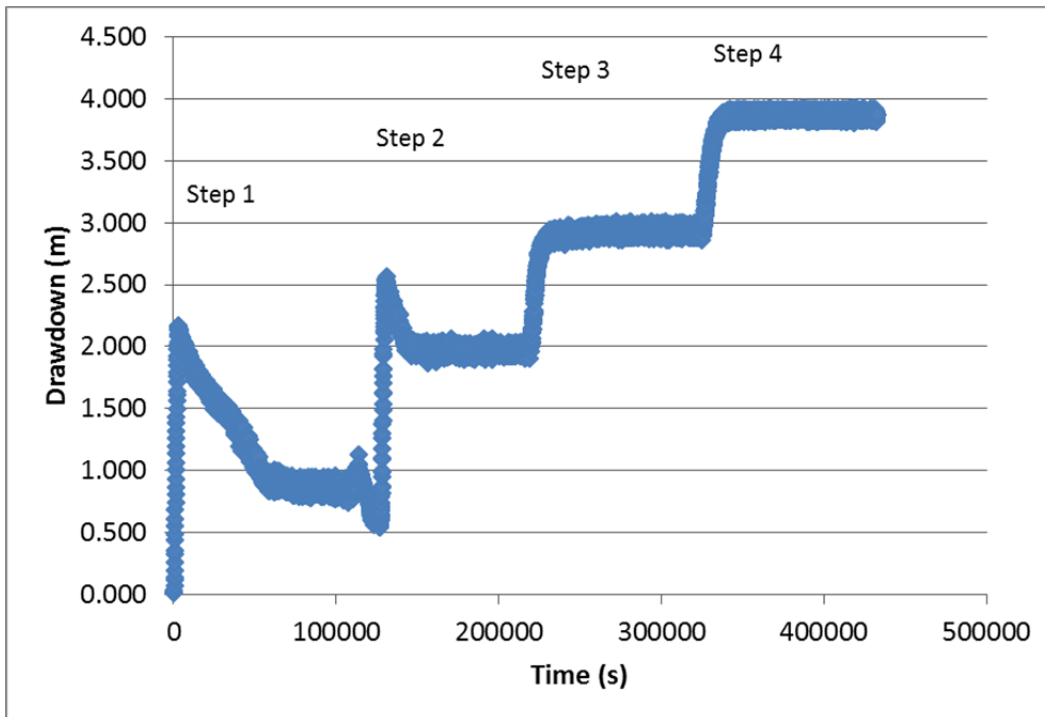


Figure 16: Step test drawdown data for the pumping well.

2.6.4 High-Rate Pumping Test

A high-rate, 48 hour constant discharge test was completed at the site in December 2016. Pumping began at 10:40 am on December 6th and the pump was shut off at 11:20 am on December 8th. The pumping rate was 1.51 L/s. Following the constant discharge test, the recovery of the water levels was monitored until 3:00 pm on December 9th; water levels had recovered 96% when the data loggers were retrieved. Water levels were recorded in both monitoring wells and the pumping well during the constant discharge test and during recovery. The logging interval was 30 seconds for the first 1 hour and 45 minutes of the test, after which the logging interval was 1 minute until the end of the constant discharge test. Recovery data were collected using a separate set of data loggers installed prior to pump shutdown to accommodate a smaller logging interval of 30 seconds.

The drawdown response for an idealized unconfined aquifer is expected to contain three main response intervals:

1. An early time interval where the drawdown follows a Theis response, whereby the flow is radial, and water is released from storage due to compaction of the grain network and the expansion of water (S_s - specific storage).

2. An intermediate time interval during which the rate of drawdown decreases and drawdown begins to level off (pseudo steady-state) due to the gravity drainage process as the water table drops. Flow remains radial from the aquifer into the well screen.
3. A late time interval where a significant source of water in the aquifer is derived from the specific yield of the aquifer rather than specific storage. Drawdown begins to increase again from the previous pseudo steady-state level until eventually leveling off again at very late time to a final steady-state value.

The presence of the lateral stream boundary at the site, however, confounds this idealized conceptual model. If the drawdown cone propagates radially and intersects the stream before a pseudo steady-state is reached, then the intermediate time response may not be observed or it may be masked. If the stream acts as an “infinite” source of water, the well will begin to source water directly from the stream, until it eventually reaches a point where the flux of water across the infinite head boundary is equal to the pumping rate at the well. As a result, the water being pumped gradually shifts from being aquifer-sourced to being boundary condition-sourced (recharge boundary).

Drawdown calculations were performed using the Theis (1935) equation in order to estimate the expected time the drawdown cone would intercept the stream. Using the distance from the pumping well to the stream of 27 metres, an estimated specific storage of $1E-04$, an approximate geometric mean hydraulic conductivity of $5E-05$ m/s from the slug tests, an aquifer thickness of 8.5 m, and a pumping rate of 1.51 L/s, the drawdown cone would be expected to intercept the stream very quickly, with 0.2 m of drawdown predicted at the stream after 15 minutes, and 0.5 m of drawdown after 1 hour.

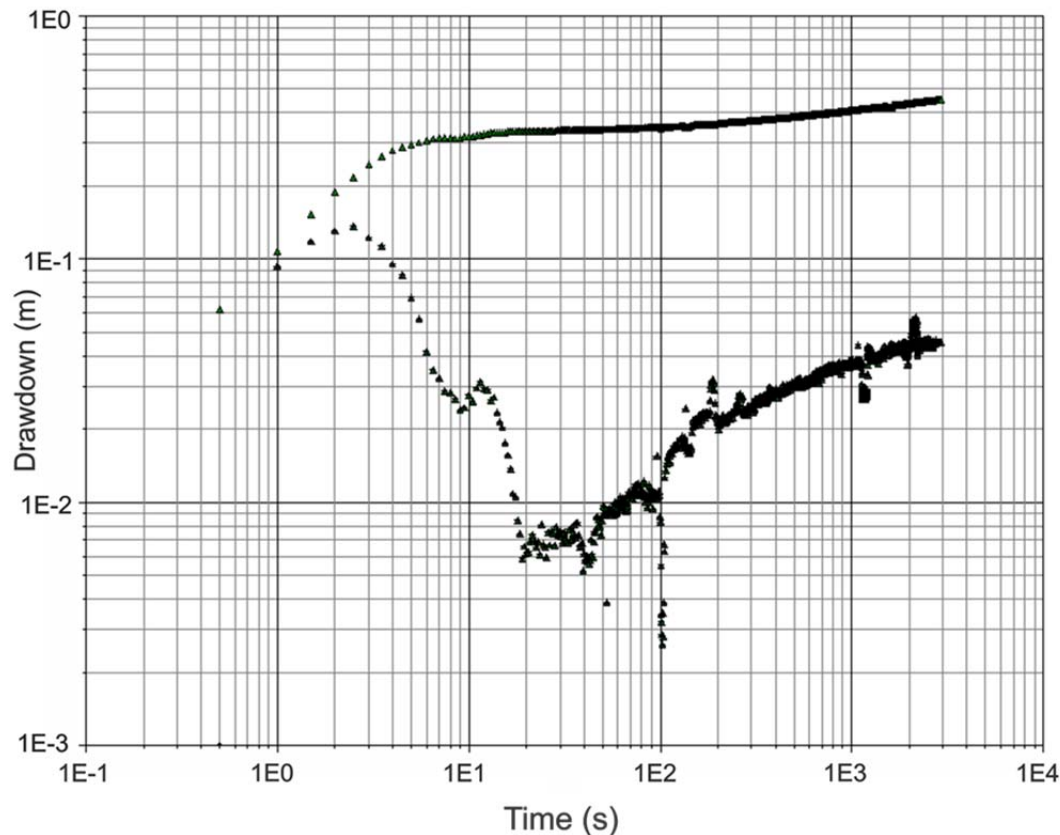


Figure 17: Drawdown response for monitoring well SPMW-02 (upper curve) and Bordeaux method derivative (lower curve).

The drawdown-time curves were first plotted and analyzed using the derivative method in AquiferTest. The first derivative of drawdown with respect to time was calculated using the Bourdet (1989) method with an L-Spacing value of 0.3; the L-spacing controls the amount of smoothing performed (see AquiferTest user manual). Figure 17 shows a drawdown response and the derivative for SPMW-02 that are generally consistent with an unconfined aquifer response. The small bump in the derivative at around 10 seconds is not interpreted to be a result of the aquifer, but more likely a pumping rate adjustment.

The pumping test data were analyzed using two different methods in AquiferTest; Neuman’s (1974) method for unconfined anisotropic aquifers, and the Cooper-Jacob time-drawdown method (Cooper and Jacob 1946). The Neuman method describes drawdown in an unconfined system as:

$$s = \frac{Q}{4\pi T} W(u_A, u_B, \beta) \quad (\text{Eq. 4})$$

where:

- s is drawdown;
- Q is the pumping rate;
- T is the transmissivity;
- $W(u_A, u_B, \beta)$ is the unconfined well function;
- $u_A = r^2 S / 4Tt$ is the type curve for the early time (identical to Theis u),
- $u_B = r^2 S_y / 4Tt$ is the type curve for later time; and
- $\beta = r^2 K_v / D^2 K_h$ where D is aquifer thickness and K_v and K_h are the vertical and horizontal conductivity of the aquifer.

The Neuman method involves matching the drawdown curve to one of a family of unconfined well function type curves. This is accomplished by first manually lining up the drawdown curve to the set of type curves in AquiferTest, and then using AquiferTest’s automatic fit function to minimize the error between the data and one of the curves. Ideally, curve matching adequately accounts for each of the early, intermediate, and late time segments of the curve. However, for this particular site, it was not possible to match the full curve for the pumping well (see Appendix E). Therefore, emphasis was placed on the early and intermediate time segments of the curve for matching, as no obvious late time rise in drawdown was observed (see Discussion in Section 2.6.7). As a result, the pumping well T and S values obtained from the Neuman method do not accurately represent the properties of the aquifer. The analysis results for all wells are shown in Appendix E.

Summary results from the Neuman analysis are presented in Table 9. Note that storage values for the pumping well are not reported in this table because they are unrealistic (calculated values are provided in Appendix E). To obtain the saturated aquifer thickness (D in Eq. 4), the distance between the water table measured prior to pumping and the clay layer in each well (Appendix A) was calculated. The results were averaged to give an average aquifer thickness of 8.654 m (see Table 2). The T values were used to calculate K using the relationship $K = T/D$ and the S values were used to calculate S_s using the relationship $S_s = S/D$.

Table 9: Aquifer properties from the high-rate pumping test using the Neuman method of analysis. S is calculated from the S_y/S ratio in AquiferTest.

Well	T (m ² /d)	K (m/s)	Kv/Kh	Sy	S	Ss
Pumping	2.09E+02	2.80E-04	9.88E-02	-	-	-
MW01	1.25E+02	1.67E-04	5.38E-03	3.80E-02	2.50E-04	2.89E-05
MW02	8.90E+01	1.19E-04	7.00E-03	4.99E-02	1.74E-04	2.01E-05
Geomean	1.32E+02	1.77E-04	1.55E-02	4.35E-02	2.08E-04	2.41E-05

The Cooper-Jacob method is a simplification of the Theis method for confined aquifers at small radial distances from the pumping well, or at large pumping times. This method was only used to analyze the early time portion of the drawdown curve. The early time drawdown response is expected to be Theis-like, because at early time in unconfined aquifers, the water is sourced from aquifer storage (Ss) rather than gravity drainage (Sy).

In the Cooper-Jacob method, the drawdown is defined as:

$$s = \left(\frac{2.3Q}{4\pi T} \right) \log \left(\frac{2.25Tt}{Sr^2} \right) \quad (\text{Eq. 5})$$

where:

- s is drawdown;
- Q is the pumping rate;
- T is the transmissivity;
- t is time;
- S is the storativity; and
- r is the radial distance from the well.

Drawdown versus time plots as a straight line on semi-log paper (time on the log scale) when the following eight assumptions are met:

1. The aquifer is confined and has infinite areal extent,
2. The aquifer is homogeneous, isotropic, and uniform in thickness,
3. The potentiometric surface of the aquifer was horizontal before pumping,
4. The pumping rate is constant,
5. The well fully penetrates the aquifer,
6. All water removed from storage is discharged instantaneously,
7. Well diameter is small; wellbore storage is negligible, and
8. Values of Theis type curve u are small, usually less than 0.01 (where $u = \frac{r^2 S}{4Tt}$).

To satisfy the last assumption (8), the u values were calculated using an approximate S_s value of $1E-04$ and the estimated geometric mean K value from the high-rate test determined from the Neuman analysis ($1.77E-04$ m/s). A minimum time to apply the Cooper-Jacob method was determined for each well by setting u to 0.01. The minimum time for SPMW-01 was 92 minutes, SPMW-02 was 51 minutes, and SPPW, essentially zero. For the two monitoring wells, the times were during the flattening period for unconfined behaviour. For the pumping well, all of the data were valid. Even though the Cooper-Jacob method technically cannot be used if the u values are greater than 0.01, a visual best fit line was drawn through the early-time portion of the time-drawdown curves for each well (see Appendix E). Table 10 shows summary results from the Cooper-Jacob analysis. The fit for the pumping well was inconsistent with the two monitoring wells and so the T and S values are not reported in Table 10 (values are reported in Appendix E). K and S_s were calculated using the same relationship stated in the Neuman method ($K = T/D$; $S_s = S/D$), and with the same aquifer saturated thickness of 8.654 m.

Table 10: Aquifer properties for the high-rate pumping test using the Cooper-Jacob method of analysis.

Well	T (m ² /d)	K (m/s)	S	Ss
Pumping	-	-	-	-
SPMW-01	1.25E+02	1.67E-04	2.96E-04	3.42E-05
SPMW-02	8.08E+01	1.08E-04	2.49E-04	2.88E-05
Geomean	1.00E+02	6.74E-05	2.71E-04	3.14E-04

2.6.5 Low-Rate Pumping Test

On July 22nd 2016 prior to the high-rate pumping test, a low-rate pumping test was conducted at the study site in an attempt to garner a greater understanding of the aquifer-stream connectivity during low-flow conditions and to provide preliminary estimates of the aquifer hydraulic properties and the aquifer response to pumping so that the high-rate pumping test could be better designed. Prior to the test, estimated drawdowns at different radial distances and for different times were calculated using the Theis equation (Theis, 1935) and the geometric mean of the K values obtained from the slug tests. These calculations were done in order to estimate how long it would take for the drawdown cone to intersect the monitoring wells and the stream at different pumping rates. In consultation with FLNR Fish and Aquatic Wildlife Division, a low pumping rate of 0.5 L/s was selected to limit the risk of significant stream flow depletion or stream dewatering. Moreover, a pumping rate of 0.5 L/s was within the operating range of the Redi-flow 2 Grundfos pump installed in the pumping well.

The goals of this low-rate test were fourfold: 1) to monitor changes in the vertical hydraulic gradient across the streambed using instream nested piezometers, 2) to monitor changes in seepage across the streambed using seepage meters, 3) to determine whether the aquifer exhibits an unconfined response, and 4) to compare the K values obtained from the low-rate pumping test with the K values obtained from the grain size and slug test analysis, and high-rate pumping test conducted later.

Water levels were monitored in all the wells with data loggers and manually using water level tapes. Water levels in the instream piezometers (see Section 4) were monitored before and during the pumping test using data loggers and water level tapes. Unfortunately, attempts to measure seepage across the streambed were unsuccessful. The low-rate constant discharge test was run for 2 hours. It was terminated when there was no further change in water levels in the instream piezometers. Moreover, there was minimal change in the water levels in the pumping well and the monitoring wells.

Drawdown data were analyzed with the same two methods (Neuman and Cooper-Jacob) described above for the high-rate pumping test. The aquifer properties obtained using the Neuman and Cooper-Jacob methods are shown in Table 11 and Table 12, respectively.

None of the drawdown curves showed obvious signs of an upswing at late time as observed in the high-rate pumping test, likely due to insufficient test duration. This made it challenging to analyze the data using the Neuman method. Moreover, both methods for the pumping well returned property values that were inconsistent with the two monitoring wells, so the pumping well results are not reported here (values are reported in Appendix E). K and Ss were calculated using the saturated thickness measured prior to the test (7.892 m).

Table 11: Aquifer properties for the low-rate pumping test using the Neuman method of analysis. S is calculated from the S_y/S ratio in AquiferTest.

Well	T (m ² /d)	K (m/s)	Kv/Kh	Sy	S	Ss
Pumping	-	-	-	-	-	-
SPMW-01	2.05E+00	3.01E-06	9.96E-01	7.55E-02	9.58E-05	1.22E-05
SPMW-02	3.60E+00	5.28E-06	1.00E+00	1.83E-01	2.01E-04	2.57E-05
Geomean	2.72E+00	3.98E-06	9.98E-01	1.18E-01	1.39E-04	1.77E-05

Table 12: Aquifer properties for the low-rate pumping test using the Cooper-Jacob method of analysis.

Well	T (m ² /d)	K (m/s)	S	Ss
Pumping	-	-	-	-
SPMW-01	1.26E+02	1.85E-04	9.26E-04	1.17E-04
SPMW-02	8.34E+01	1.22E-04	8.66E-04	1.10E-04
Geomean	1.03E+02	1.50E-04	8.95E-04	1.13E-04

2.6.6 Summer versus Winter Site Conditions

The low-rate (0.5 L/s) pumping test was conducted in late July. In the preceding 30 day period, only 95.6 mm of precipitation was recorded at the Fort Langley Telegraph Trail climate station (see Figure 5 for location). The high-rate (48 hour) pumping test was conducted in early December during and after periods of heavy snowfall. The area received 327 mm of precipitation during November 2016, which was more than any other month that year. In the 30 day period preceding the high-rate pumping test, 251 mm of precipitation was recorded (Figure 18). Therefore, the climate and hydrological conditions changed dramatically between the two testing periods. Groundwater levels in the surrounding area fluctuated between winter and summer by more than 2 m (see Figure 6) due to recharge occurring mainly through the winter and spring months from November to April. At the site, the pre-pumping water table height was roughly 0.9 m higher in the winter than during the summer, and stream stage measured at four locations upstream to downstream of the site, was also significantly higher in December, ranging from 0.24 to 0.41 m depth compared to 0.02 to 0.07 m depth during summer conditions.

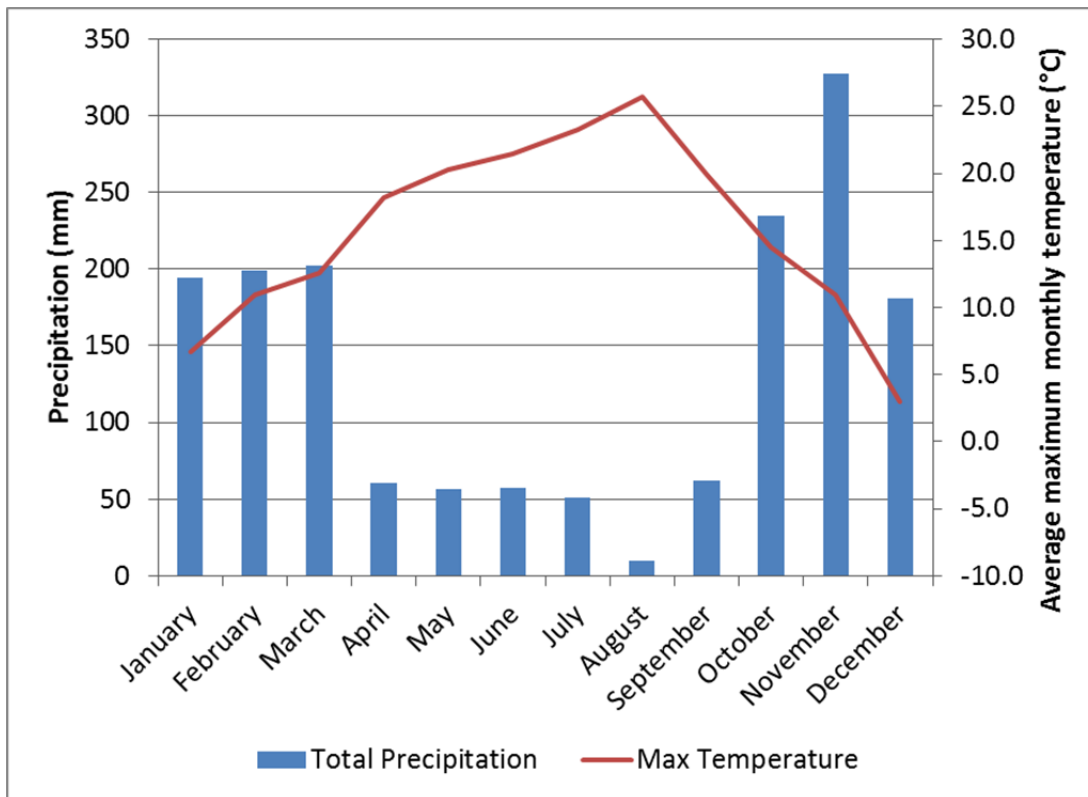


Figure 18: Total monthly precipitation and average maximum monthly temperature for the year 2016 from the Fort Langley Telegraph Trail climate station (1102912) just north of Steele Park. Note the comparatively large amount of precipitation in November.

2.6.7 Summary of Aquifer Properties and Uncertainty

A summary of all aquifer properties and analysis methods is presented in Table 13. A detailed summary is shown in Appendix E (Table E1). With the exception of the Neuman method results for the low-rate pumping test, the T and K values from the various methods are all within approximately one order of magnitude.

Table 13 Summary of aquifer properties.

Aquifer Property	Grain Size Analysis	Hvorslev	Bouwer & Rice	Neuman – High-Rate	Neuman – Low-Rate	Cooper Jacob – High-Rate	Cooper Jacob – Low-Rate
Geometric Mean of K values (m/s)	1.87E-04 ¹	6.22E-05	4.80E-05	1.77E-04	3.98E-06	6.74E-05	1.50E-04
Geometric Mean of T values (m ² /day)	-	4.24E+01	3.28E+01	1.32E+02	2.72E+00	1.00E+02	1.03E+02
Geometric Mean of S values				2.08E-04	1.39E-04	2.71E-04	8.95E-04
Geometric Mean of Ss values	-	-	-	2.41E-05	1.77E-05	3.10E-04	1.13E-04
Geometric Mean of Sy values	-	-	-	4.35E-02	1.18E-01	-	-

¹ Grain size analysis was only performed on SPMW-02.

As mentioned above, the pumping test data were not straightforward to analyze, particularly the pumping well data. The most appropriate conceptual model for the aquifer is that of an unconfined aquifer influenced by a recharge boundary (the stream). Unfortunately, no analytical model exists for this particular conceptual model. The unconfined nature of the site suggests that the Neuman method would be most appropriate to use. However, the data could not be appropriately fit to the Neuman type curve. Drawdown increased very rapidly at the beginning of the test, particularly in the pumping well, and if that portion of the data was matched to the Neuman curve, the intermediate and late time portions of the curve could not be matched because the data showed less drawdown than the model predicted, likely due to the close proximity of the recharge boundary. Moreover, for the low-rate pumping test, the absence of the late time upswing meant that the Neuman method could not be accurately applied. Thus, it is not surprising that the hydraulic property values obtained using the Neuman method for the low-rate pumping test are quite different than the values obtained from the Cooper-Jacob method, as well as both methods for the high-rate pumping test, even if the pumping well data are excluded (Table 13). In contrast, the high-rate pumping test data for both monitoring wells clearly showed the late-time upswing in the drawdown curve expected for an unconfined system. The late time upswing was less obvious for the pumping well. Thus, the aquifer properties estimated using the Neuman method for the high-rate test are considered more representative given the limitations of the Neuman method for this particular site (i.e. the presence of a recharge boundary).

As a result of the uncertainties in the Neuman method, the Cooper-Jacob method was used to analyze the early time data to obtain estimates of T and S for both the low-rate and high-rate pumping tests despite not satisfying the u value criterion for application of the Cooper-Jacob method. For the low-rate pumping test, however, there were very few data points at early time, which made fitting a straight line through the early time data subjective. The early time slope for the pumping well is also very inconsistent with the early time slopes for the monitoring wells (see Appendix E), again raising suspicion of the pumping well results.

The S parameter determined in AquiferTest by applying the Neuman method to the late time data is somewhat unclear. At late time, the total storage derives from both aquifer storage (specific storage or Ss) and gravity drainage (Sy), i.e. $S = Ss \times D + Sy$. Sy is typically much higher than Ss (by at least an order of magnitude) so it dominates late time S. The reported ratio of “Sy/S” for the Neuman method in AquiferTest is on the order of 1.0E+02, which suggests that this ratio is using the S value from the early time curve fitting. This was confirmed by observing that changing the saturated thickness in AquiferTest did not change S. Regardless of the uncertainty in the S value returned from the Neuman analysis, the

values of S_y are lower than the expected values for sand and gravel aquifers. This effect may be due to the presence of the recharge boundary condition and the nature of the source of water at late time. At late time, the drawdown cone may have intercepted the stream, and begun to draw water directly from the stream, as predicted by stream depletion theory (Hunt, 2014). This water source would lower the rate of drawdown to such a degree that the late-time upswing in the drawdown curve would be diminished. Since the late-time response is defined by the S_y value, the S_y values obtained from curve matching are likely underestimated.

Finally, the pumping test analysis methods assume that the water table prior to pumping is flat. Because the site slopes toward the stream, the water table is certainly not flat. The horizontal hydraulic gradient fluctuates throughout the site with time as discussed in Section 2. Winter pumping test results are more likely to be influenced by the strong site-wide hydraulic gradient at early time during pumping. This larger gradient in the winter suggests that the initial conditions for both the high-rate and the low-rate test were not the same, and that a relatively high gradient exists at the site in the winter that is not represented in the analytical models.

Based on these analyses and in consideration of the limitations of the available analytical models for this site, the best overall estimates for T , K , S_y , and S_s of the aquifer were made. The best estimates for T ($8.1E-04 \text{ m}^2/\text{s}$) and K ($7.3E-05 \text{ m/s}$) were determined to be the geometric means, respectively, of all four pumping test analyses, excluding the pumping well for all except the high-rate test analyzed using the Neuman method. The rationale for taking this average is that the Neuman method incorporates the late time portions of the curve and the Cooper-Jacob method best represents the early time portions, thus giving time-averaged values. The best estimates for S ($2.9E-04$) and S_s ($3.5E-05 \text{ m}^{-1}$) were the geometric mean values from all four analyses for only the monitoring wells. These values seem reasonable and provides an aquifer material compressibility estimate of $3.4E-9 \text{ Pa}^{-1}$ (assuming an aquifer porosity of 0.3), which is within the expected range for the compressibility of gravel or sand (Freeze and Cherry, 1979). Finally, S_y was estimated as the geometric mean for the monitoring wells only for both pumping tests as determined from the Neuman method, giving a value of 0.07, which, as stated earlier, is likely an underestimate. The specific yield of the aquifer materials is estimated to be approximately 0.2, which lies between the reported values for gravel (0.19) and sand (0.22) given by Heath (1983).

3. ASSESSMENT OF AQUIFER-STREAM CONNECTIVITY

The hydraulic connection between Union Creek and the underlying aquifer is arguably the most important variable in dictating how the creek responds to the stresses induced by pumping. A creek that is not in hydraulic connection with the aquifer through which it flows will see no change in its streamflow in response to pumping or other stresses to the aquifer system. In reality, most streams have some degree of hydraulic connection with their underlying aquifers, especially streams that lie atop unconfined aquifer systems (Winter et al., 1998). This connectivity can be transient in nature and vary seasonally.

This section explains the methodology used to attempt to characterize the aquifer-stream connection at Steele Park, and quantify the volumetric streamflow depletion value (ΔQ_s) that occurred as a result of the 48 hour pumping test in December 2016. The aim was to compare the measured streamflow depletion with that predicted by various analytical models for streamflow depletion.

3.1 Instream Measurements of Aquifer-Stream Connectivity

3.1.1 Streambed Piezometers

Three sets of nested piezometers were driven in the streambed on June 15th, 2016. These instream piezometers were constructed of 2.5 cm ID (3.5 cm OD) stainless steel with perforations over the bottom 20 cm of the tube. A total of six piezometers were installed at the locations indicated in Figure 19. In each nest, a long piezometer (1.5 m) was paired with a shorter one (two at 0.7 m and one 1.1 m) to enable measurement of the vertical gradient within the streambed sediments. The completion details are shown in Figure 20.

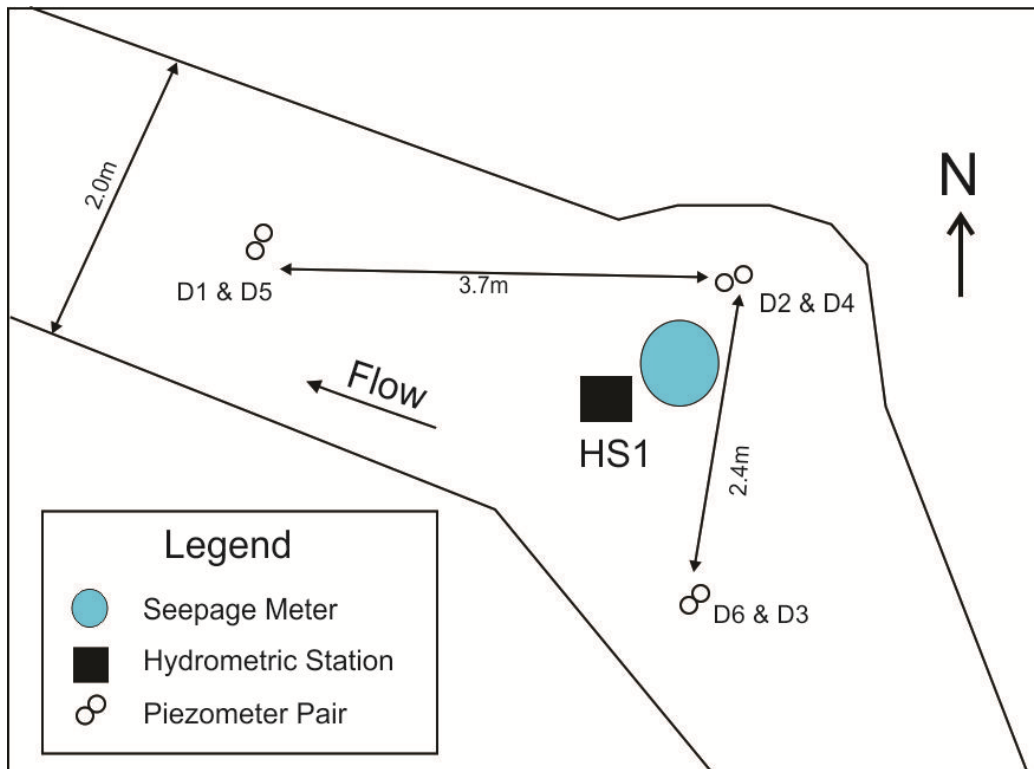


Figure 19: Piezometer and seepage meter installation locations in Union Creek. See Figure 8 for the location of the wells relative to the creek.

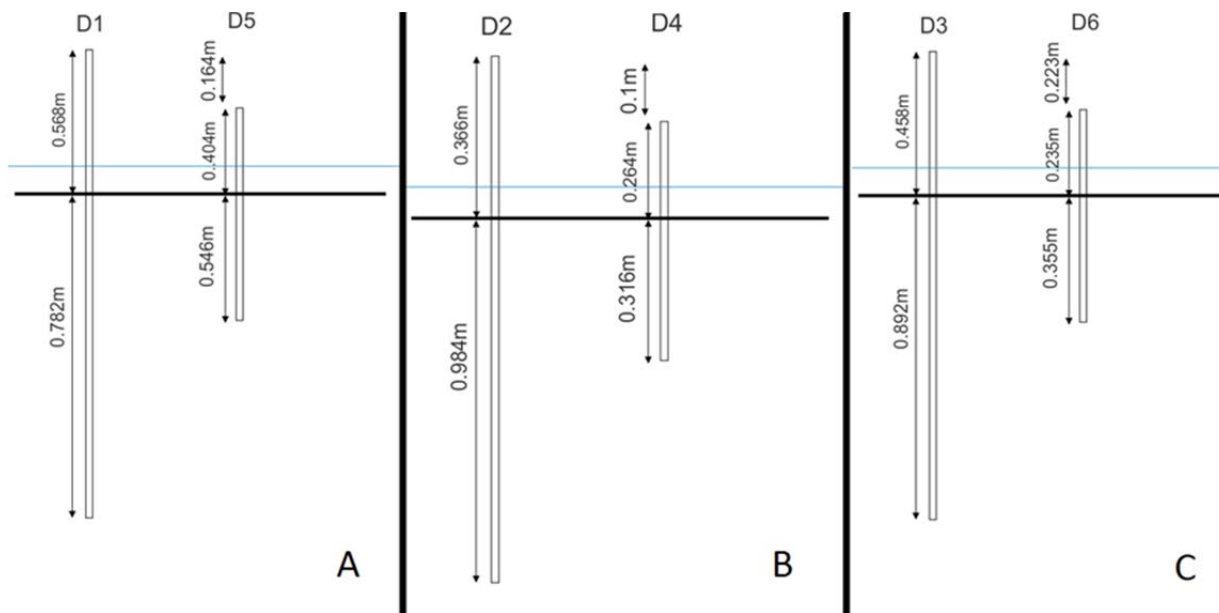


Figure 20: Piezometer geometry. A) D1-D5, B) D2-D4, C) D3-D6.

The magnitude, and possibly the direction, of the hydraulic gradient across the streambed under natural, non-pumping conditions are expected to change with time due to seasonal fluctuations in the water table. If the stream is perennially gaining, then changes in groundwater contribution to the stream act to increase or decrease the baseflow component of streamflow depending on the magnitude of the groundwater flux. Alternatively, the stream may be gaining at times when the water table is high and losing if the water table falls below creek level. Assuming Union Creek is perennially gaining, the vertical groundwater flux across the streambed would be expected to be proportional to the site-wide horizontal hydraulic gradient, and therefore would be largest during the winter and spring when the water table is high and low in the late summer and fall when the water table is low.

Water level measurements were made on June 15th, June 20th, July 22nd, and August 11th in order to characterize the baseline vertical hydraulic gradient in the streambed under non-pumping conditions. A total of three vertical gradients were calculated for each piezometer pair; one between the piezometers themselves (as they were completed at different depths), and one between the piezometer and the stream stage directly adjacent to the piezometer. Vertical hydraulic gradients were calculated between the piezometer pairs according to the geometry set out in Figure 20. Piezometer pair D3-D6 was positioned upstream from the hydrometric station (HS1) and seepage meter; D1-D5 downstream from HS1 and the seepage meter; and D2-D4 adjacent to HS1 and the seepage meter (Figure 19).

The baseline vertical hydraulic gradients between piezometer pairs are shown in Figure 21 along with daily precipitation. The majority of the error in these measurements comes from the length between the two piezometer screens due to the span of the screen holes in the piezometer casings and errors in installation depth measurements. The error associated with these measurements is estimated at 0.05 m. The hydraulic gradients were similar for all three piezometer pairs, with the exception of the initial June 15th reading for piezometer set D1-D5, which had a gradient of -0.28 (a negative gradient indicates water was flowing downward, out of the creek and into the aquifer). This value is approximately three times greater than the hydraulic gradient measured at any other time, suggesting a possible measurement error. Aside from this reading, the maximum hydraulic gradients measured between the piezometer pairs all occurred on August 22nd, with gradients of -0.11, -0.072, and -0.070 at D1-D5, D2-D4, and D3-D6 respectively. In fact, all hydraulic gradients indicated downward groundwater flow,

except the D3-D6 reading on June 15th and the D2-D4 reading on June 20th, which showed positive (upward) gradients of 0.022 and 0.01. Disregarding the Jun 15th gradient for D1-D5, the time averaged hydraulic gradients for each piezometer pair were -0.024, -0.032, and -0.090 for piezometer pairs D2-D4, D3-D6, and D1-D5, respectively (Table 14).

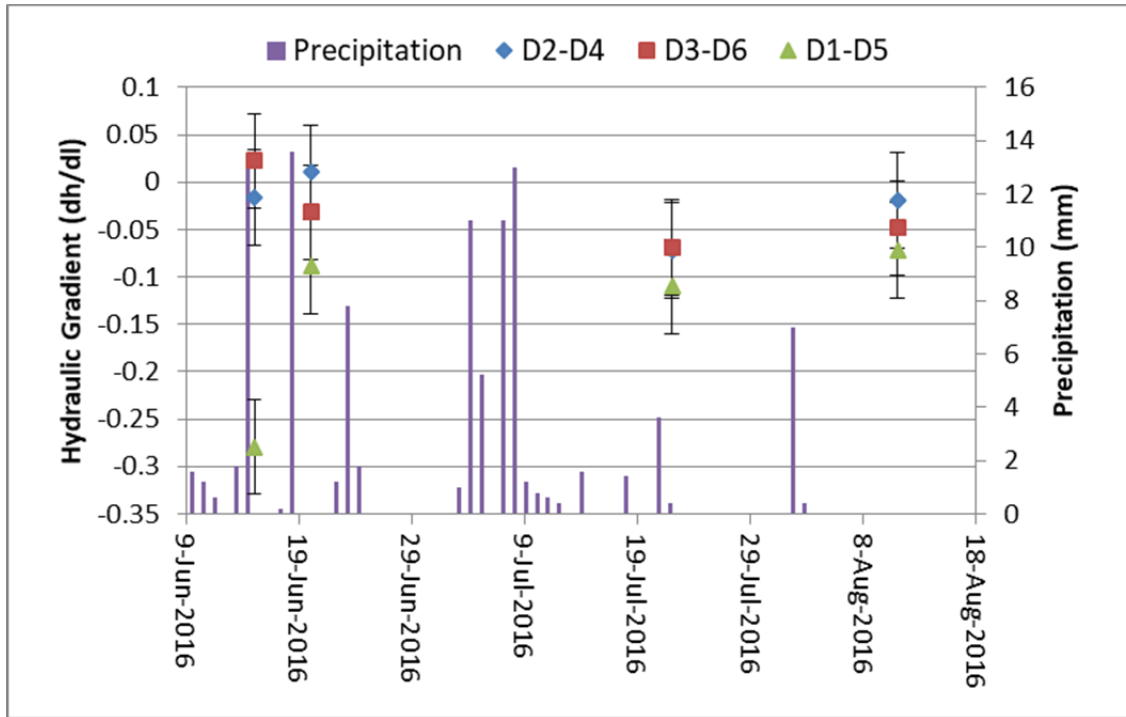


Figure 21: Baseline vertical hydraulic gradients at the piezometer pairs along with daily precipitation. The gradients at D2-D4 and D3-D6 are so similar that the points overlie each other. Note the large negative hydraulic gradient at D1-D5 on June 15th that is suspect. Gradient measurement error is ± 0.05 .

Table 14: Hydraulic gradients measured between piezometer sets for each summer field day. The time averaged hydraulic gradient for D1-D5 disregards the June 15th value in italics.

Date	D2-D4	D3-D6	D1-D5
June 15, 2016	-0.016	0.022	<i>-0.28</i>
June 20, 2016	0.010	-0.032	-0.089
July 22, 2016	-0.072	-0.069	-0.11
August 11, 2016	-0.020	-0.048	-0.072
Average	-0.024	-0.032	-0.090

Hydraulic gradients between the piezometer pairs indicated predominantly downward flow during the summer months, but hydraulic gradients between the individual piezometers and the stream stage showed dominantly positive values, indicating flow was upwards into the creek (Figure 22 and Table 15). In instances where two piezometers in the same pair showed hydraulic gradients that did not agree in direction, the deep piezometer was the one that indicated downward flow, while the shallow piezometers indicated upward flow. This was the case for all except the June 15th measurement in piezometer D6. It is theorized that the shallow piezometers may be influenced by the hyporheic zone, a zone of surface water and groundwater mixing that exists along stream banks and beneath the streambed. Water flow in the hyporheic zone can be both upwards into the stream and downwards into the aquifer (Winter et al. 1998). While the stream is shown on the site diagram as being fairly straight, it

actually winds through its cut channel. This effect is especially evident during the summer when stream stage is lower, with sharp bends enabling potential hyporheic exchange. The deep piezometer measurements in each pair could therefore be more representative of the aquifer-stream connection, as they are deep enough that they may be out of the influence of the hyporheic zone. Both piezometers D1 and D5 agreed in direction for all measurements and had overall negative hydraulic gradients, indicating that the area in which D1 and D5 were located was likely an overall losing section of Union Creek.

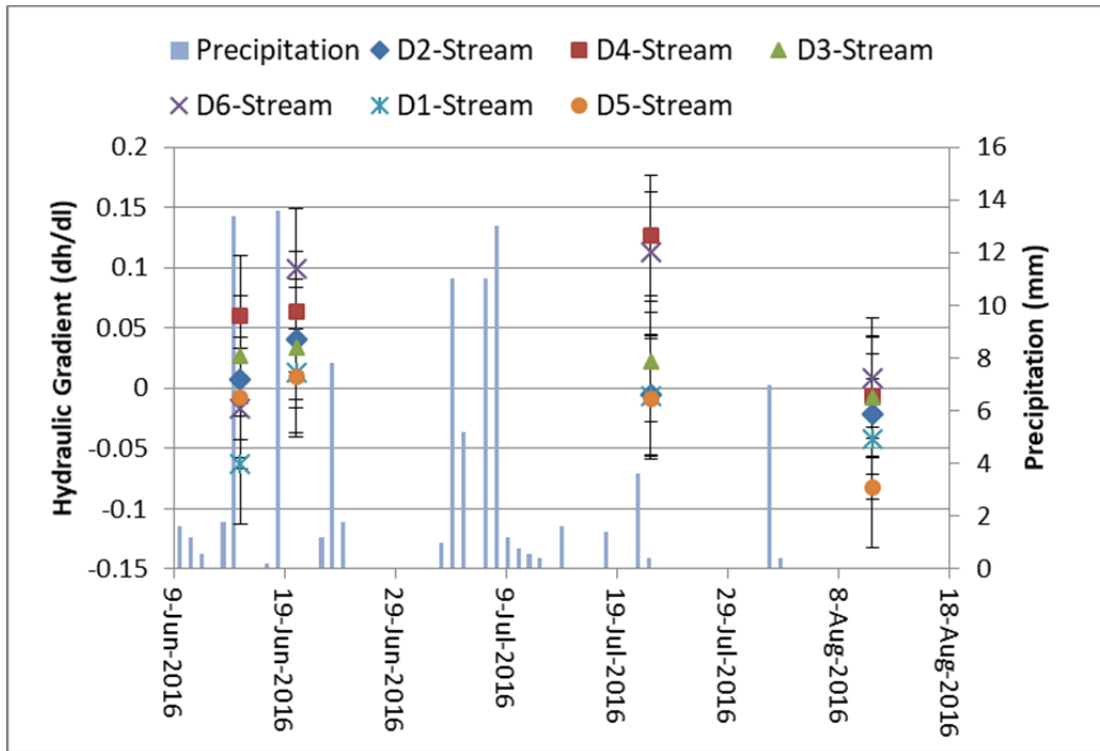


Figure 22: Baseline vertical hydraulic gradients between the piezometers and the stream along with daily precipitation. Gradient measurement error is ± 0.05 .

Table 15: Hydraulic gradients calculated between each individual piezometer and the adjacent stream stage.

Date	D2	D4	D3	D6	D1	D5
June 15 th	0.0071	0.060	0.027	-0.017	-0.063	-0.0073
June 20 th	0.041	0.063	0.034	0.099	0.013	0.0092
July 22 nd	-0.0051	0.13	0.023	0.11	-0.0064	-0.0092
August 11 th	-0.021	-0.0063	-0.0078	0.0085	-0.042	-0.082
Average	0.0053	0.061	0.019	0.051	-0.025	-0.022

During the high-rate pumping test in December 2016, piezometers were equipped with data loggers to monitor changes in water level. The installation depths for the data loggers were not measured by FLNR, but were estimated from manual depth-to-water readings taken by FLNR staff at the beginning of the test. Piezometers D4 and D6 were flowing at the beginning of the test, so logger installation depth estimates were made for these two piezometers using depth to water measurements made at 9:30 am on December 7th.

The drawdowns in the piezometers during the high-rate pumping test are shown in Figure 23. The error in these drawdown measurements is estimated to be 1 mm. Because D4 and D6 were flowing at the beginning of the test (the water level was mounded at the top of the piezometer although no flow was

observe), drawdown was calculated assuming the water level was at the top of casing. This is reasonable as the water was not visibly flowing out of the piezometers, but rather formed a meniscus at the top of casing. The calculated drawdown was not evenly distributed beneath the streambed; the greatest drawdown (5 cm) occurred in the deep piezometer furthest downstream (D1) and the least amount of drawdown (1 cm) occurred in the shallow piezometer near the seepage meter location (D4). All of the deep piezometers showed more drawdown than their shallow counterparts. Water levels fully recovered in all instream piezometers during the recovery phase of the pumping test.

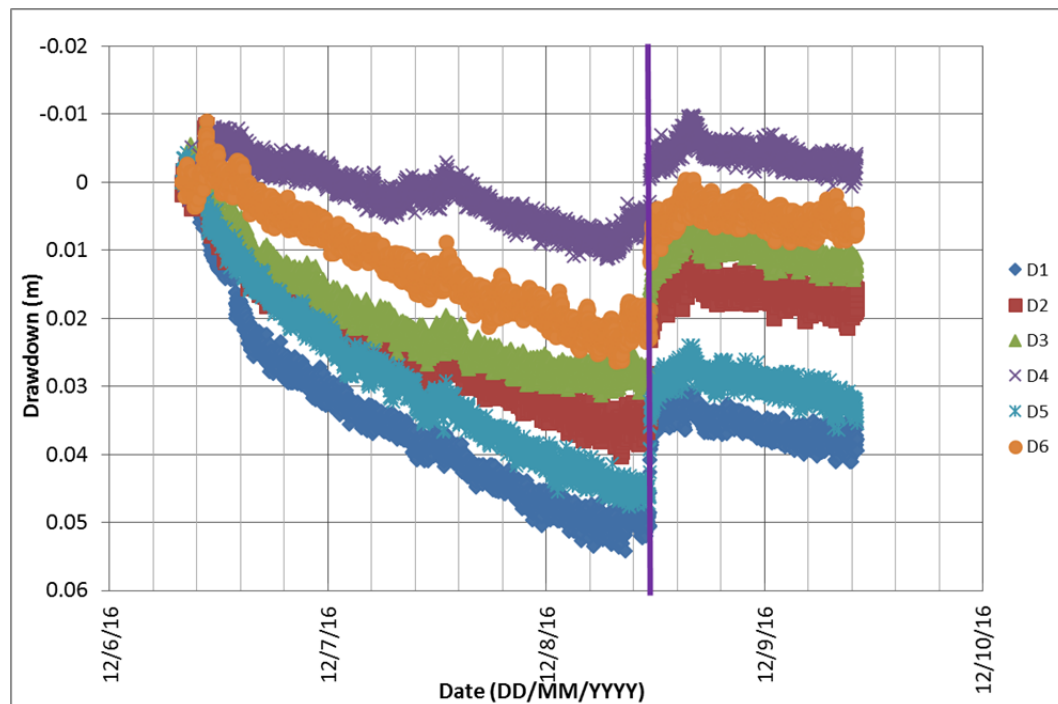


Figure 23: Drawdown in each streambed piezometer over the course of the high-rate pumping test. Recovery began on December 8th. The measurement error is ± 0.001 m.

These piezometer drawdowns contrast with the 2.25 m drawdown estimated from the Theis equation at the stream after 48 hours of pumping. This is expected due to both the delayed yield response of the unconfined aquifer, which results in a lowering of the rate of drawdown relative to that predicted by the Theis method, and due to the possible effect of hyporheic flow.

The estimated error in dh/dl during the pumping test is approximately ± 0.008 . The change in hydraulic gradient at each piezometer pair was not uniform during the high-rate pumping test. The hydraulic gradient fluctuated rapidly over time in all piezometer pairs, with the effect being most pronounced in D1-D5. Due to the rapid fluctuations, a 15 point moving average of the data was calculated to allow for the long term changes to be seen more clearly. The change in hydraulic gradient for D2-D4 is shown in Figure 24. This piezometer pair showed a response that looks very similar to the drawdown response observed in the monitoring wells, with an abrupt initial change in hydraulic gradient as soon as pumping began at 10:40 am on December 6th, and abrupt recovery in hydraulic gradient at the time the pump was shut off on December 8th at 11:20 am. The initial rapid rate of increase in the hydraulic gradient, from 0 to -0.02 occurred over the first hour of pumping. The gradient then continued to increase steadily at a slower rate, with the change leveling off around -0.038 between 9:30 pm on December 7th and 12 am on December 8th, when it then began to increase again until pump shutoff at 11:20 am on December 8th. The hydraulic gradient appeared to recover to a value 0.03 less than the pre-pumping

hydraulic gradient over the course of approximately 2.5 hours before leveling off, giving a gradient recovery rate of around 0.005 per hour. This response is very interesting in that it mirrors the shape of the kind of drawdown response seen in unconfined aquifer systems during pumping tests. If the test had run for longer, the gradient change in the piezometer pair would likely have leveled off to a steady value, similar to how the late time drawdown curve in an unconfined aquifer attains pseudo steady-state at very late time.

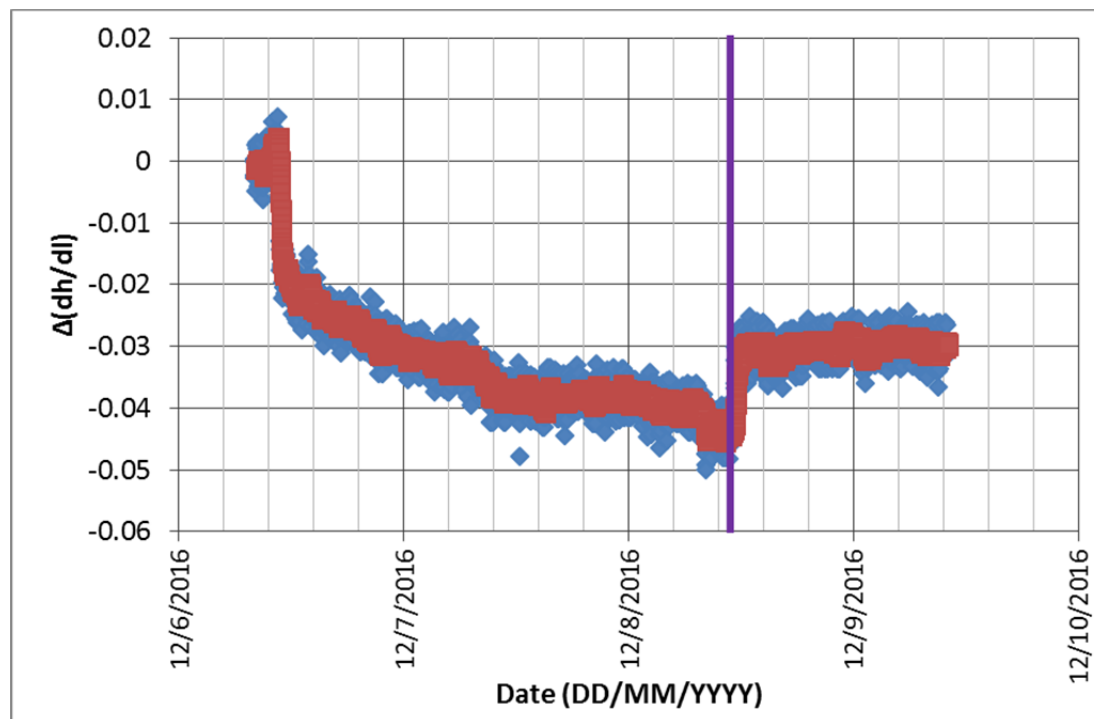


Figure 24: Change in hydraulic gradient over time during the high-rate pumping test for piezometer pair D2-D4. Blue points are the raw values; red points are the 15 point moving average. The purple line shows the time of pump shutoff. Estimated error is ± 0.008 .

The change in hydraulic gradient in the other two piezometer pairs (D1-D5 and D3-D6) is more difficult to interpret. There is an observed increase and subsequent recovery in hydraulic gradient in both piezometer pairs, but the recovery of the hydraulic gradient is not as abrupt as in piezometer pair D2-D4, possibly because D2-D4 are situated closer to the pumping well. The maximum change in hydraulic gradient was approximately -0.04 in D1-D5 and D2-D4, and -0.02 in D3-D6 (Figure 25 and Figure 26). Due to the gradual recovery in D1-D5, a gradient recovery rate could not be estimated. The recovery time in D3-D6 was approximately 4 hours, giving a gradient recovery rate around 0.001 per hour. The initial sharp increase in the hydraulic gradient occurred over the first hour of pumping in both D1-D5 and D3-D6.

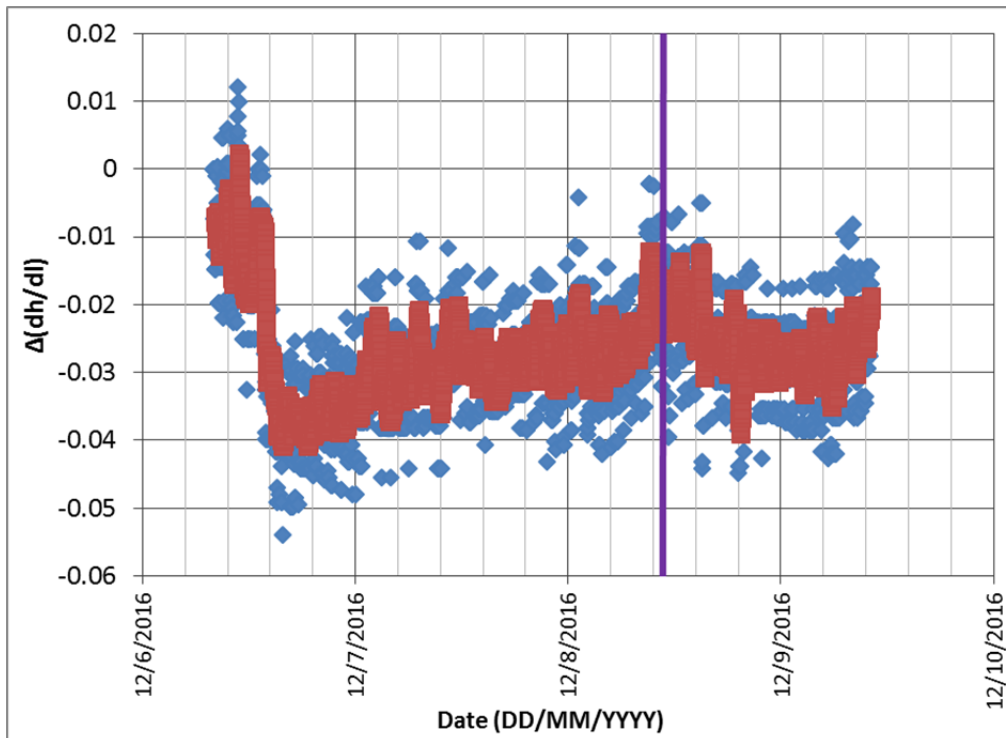


Figure 25: Change in hydraulic gradient over time during the high-rate pumping test for piezometer pair D1-D5. Blue shows the raw values; red shows the 15 point moving average. The purple line shows when the pump was shut off. Estimated error is ± 0.008 .

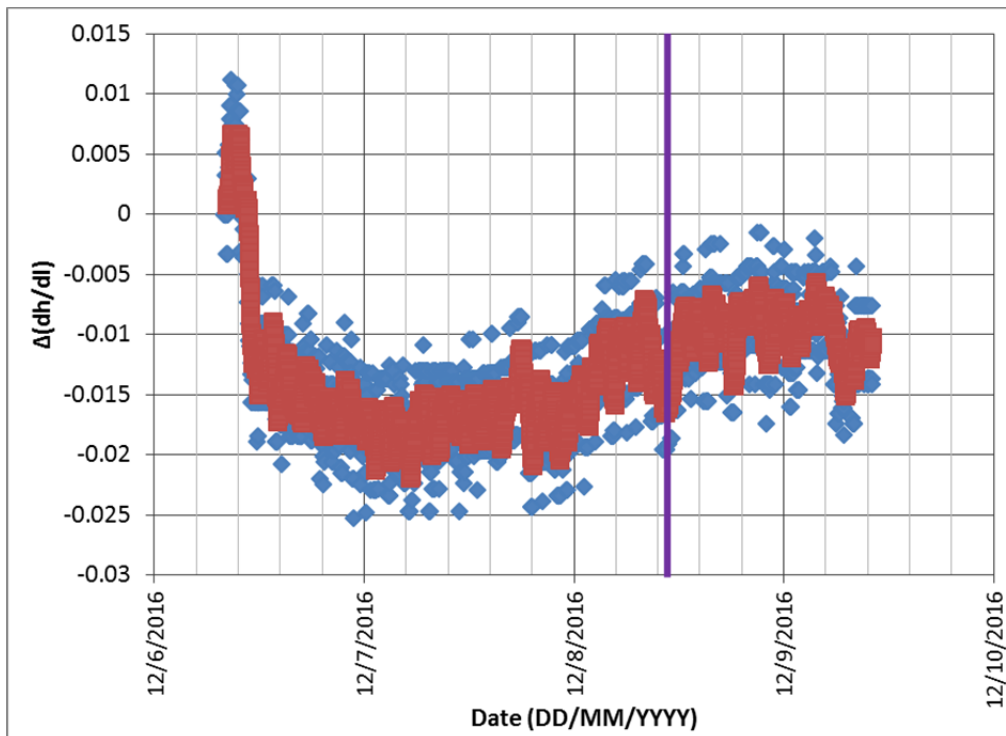


Figure 26: Change in hydraulic gradient with time during the high-rate pumping test for piezometer pair D3-D6. Blue shows the raw values; red shows the 15 point moving average. The purple line shows the time the pump was shut off. Estimated error is ± 0.008 .

All the piezometers were screened at a depth greater than 0.1 m below the streambed, and so were possibly screened within the aquifer itself, although deeper sediment samples were not collected to confirm this. Using the average K value obtained from the high-rate pumping test results (1.1E-04 m/s), the maximum and minimum Darcy fluxes were calculated for each piezometer pair. The flux at D1-D5 was negative for the entire test duration (flow downward, out of the stream), and increased in the negative direction (downwards) when pumping began. D1-D5 had a minimum flux of 3.5E-05 m/s at the start of the test, and reached its maximum of approximately 4.5E-05 m/s on December 6th after the initial drawdown due to pumping. The flux at D2-D4 remained positive throughout the test (flow upwards into the stream) but declined throughout the test; the maximum flux was 2.3E-05 m/s at the beginning of the test. D2-D4 reached its minimum value of 4.4E-06 m/s just before the pump was shut off on December 8th. The flux at D3-D6 began positive (flow upwards into the creek) at its maximum value of approximately 8.0E-06 m/s at the test start, slowly decreased and changed direction (flow downwards out of the creek) around 3 pm on December 6th, and reached its minimum value of approximately 1.9 E-05 m/s just before the pump was shut off on December 8th (Figure 27).

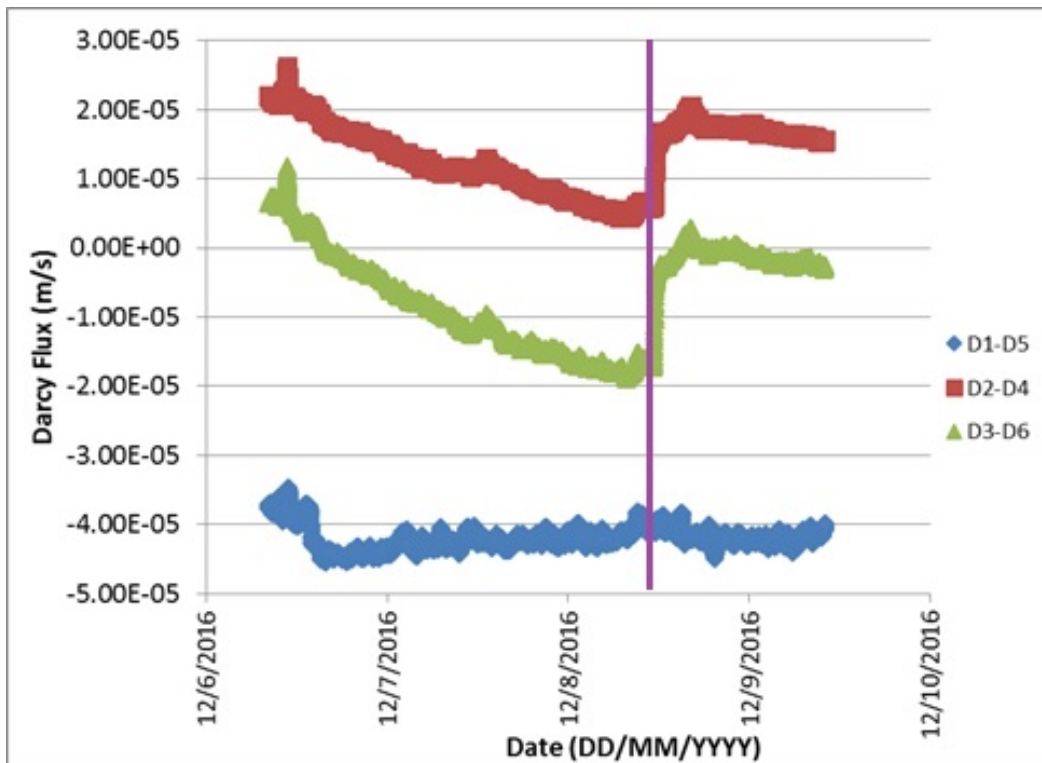


Figure 27: Darcy flux at each of the piezometer pairs over the course of the high-rate pumping test. Positive fluxes indicate upwards movement of water into the creek, negative fluxes indicate downward movement out of the creek. The purple line shows the time the pump was shut off.

3.1.2 Seepage Meters

A seepage meter was used to directly measure seepage across the streambed under both natural, non-pumping conditions as well as during pumping conditions. The seepage meter was placed in the streambed adjacent to the stream stage hydrometric station installed by FLNR (Figure 19). The seepage meter had a radius of 0.25 m, and an area of 0.2 m². Smaller diameter seepage meters were experimented with, but ultimately abandoned in favour of the larger diameter one. Ideally, more than one seepage meter would have been used.

In theory, the seepage meter provides a direct measurement of the volumetric flux in or out of the streambed over the area covered by the seepage meter. This can be used to obtain a flux for the seepage meter area. During pumping, changes in the flux can be used to directly relate decreases in baseflow contribution to volumetric streamflow (stream depletion due to pumping).

Seepage meter measurements were attempted on June 15th, June 20th, July 22nd, and August 11th. Unfortunately, the measurements on June 20th, July 22nd, and August 11th did not produce results (small seepage meters), so only seepage measurements from June 15th were used to characterize background conditions. Thus, no seepage meter data are available prior to or during the low-rate pumping test. The three seepage meter measurements from June 15th are shown in Table 16. The error associated with the seepage meter measurements is $2\text{E-}9 \text{ m}^3/\text{sec}/\text{m}^2$.

Table 16: Seepage meter measurements from June 15th.

Trial	Volume (L)	Time (minutes)	Rate ($\text{m}^3/\text{sec}/\text{m}^2$)
1	0.328	144	1.9E-07
2	0.778	70	9.3E-07
3	1.681	70	2.0E-06

The value for Trial 1 is one order of magnitude lower than for Trials 2 and 3, which may simply be human error. Nevertheless, these seepage rates are low, but are expected for the summer conditions when the water table gradient is low. It is possible that the reason seepage was not able to be measured on the other field days was due to the creek being dominantly losing, resulting in no water collecting in the seepage bag. The piezometer measurements do not support this, however, as the vertical hydraulic gradient at piezometer set D2-D4 (directly adjacent to the seepage meter) indicated downward flow on June 15th, yet seepage was still collected. The other more likely possibility is that the seepage meter was not properly sealed into the streambed during the other trials. Middleton et al. (2016) discuss uncertainty in seepage measurements and how they often disagree with instream piezometer flux measurements.

Seepage rates measured before the pumping test on December 5th are shown in Table 17. The rate of seepage was very high, and the initial two attempts may have overfilled the seepage bag, so the reported seepage rates are likely underestimates. The final background trial (Trial 3) was completed for a shorter time (2 minutes), and is likely the most reliable estimate. These seepage rates are at least one order of magnitude higher than those measured in the summer, which is expected due to the higher site-wide hydraulic gradient during the winter.

Table 17: Background seepage meter measurements from December 5th just prior to the beginning of the step test. Seepage values highlighted in bold are likely underestimates.

Trial	Volume (L)	Time (minutes)	Rate ($\text{m}^3/\text{sec}/\text{m}^2$)
1	1.623	5	2.76E-05
2	1.002	3	2.84E-05
3	0.828	2	3.51E-05

Seepage was measured during both the step test on December 5th and the high-rate pumping test between December 6th and 8th. Seepage measurements during the step test at the end of each step are shown in Table 18. The step 2 and step 4 measurements are averages of two measurements taken for each step. There was no significant decrease in seepage from step 1 through step 4. There was, however, a slight decrease in seepage rate on the order of $1\text{E-}5 \text{ m}^3/\text{s}/\text{m}^2$ from background conditions measured just before the pumping test began (Table 17).

Table 18: Seepage meter measurements made during the step test at Steele Park.

Step	Pumping Rate (L/s)	Volume (L)	Time (minutes)	Rate (m ³ /sec/m ²)
End of Step 1	0.45	1.023	3	2.89E-05
End of Step 2	1.01	0.674	2.17	2.59E-05
		0.600	2	
End of Step 3	1.51	0.775	2	3.29E-05
End of Step 4	2.0	0.597	2	2.82E-05
		0.730	2	

Seepage was measured at seven different times over the course of the pumping test. Each time seepage was measured, a series of three to five trials were done, with each trial running for two minutes. The seepage rate for each timestamp shown was calculated using the average of all seepage measurements taken at that time. The data may show a slight decrease in flux over the course of the test, on the order of 1E-06 m³/s/m² (Table 19).

Table 19: Seepage measurements taken during the high-rate pumping test at Steele Park.

Date	Cumulative Time	Volume (L)					Average Volume (L)	Rate (m ³ /s/m ²)
		Trial 1	Trial 2	Trial 3	Trial 4	Trial 5		
12/6/2016	Background	0.78	0.63	0.63	0.6	0.59	0.65	2.7E-05
12/6/2016	1 h	0.63	0.83	0.72	-	-	0.73	3.0E-05
12/7/2016	23 h 10 min	0.75	0.53	0.65	0.56	-	0.62	2.6E-05
12/7/2016	24 h 30 min	0.51	0.72	0.73	-	-	0.65	2.7E-05
12/8/2016	47 h 30 min	0.67	0.53	0.46	0.61	0.69	0.59	2.5E-05
12/8/2016	2 h recovery	0.46	0.785	0.725	0.81	0.765	0.71	3.0E-05
12/8/2016	3 h recovery	0.53	0.805	0.705	0.43	0.565	0.61	2.5E-05

3.1.3 Stream Stage and Discharge

Stream stage was recorded at 15 minute intervals during the pumping test at four staff gauges (HS1-HS4) spanning the reach both upstream and downstream of the test area (Figure 19). Stream discharge was recorded manually at an upstream location next to HS1 and at a downstream location approximately midway between HS3 and HS4 a total of 14 times over the duration of the pumping test at varying time intervals. The purpose of these measurements was to obtain discharge measurements that could be calibrated against the stream stage measurements to obtain approximate stream discharge values at any time. Unfortunately, no rating curve was available for Union Creek.

A single background measurement of stream discharge was made during fieldwork on June 15th, downstream from the reach closest to the pumping well. The background discharge was approximately 0.5 L/s, but since this value was measured during summer low flow conditions, it is not representative of conditions at the site during the pumping test in December.

During the pumping test, stream stage and volumetric streamflow would be expected to decrease downstream of the pumping site compared to non-pumping conditions as the drawdown cone intercepted the stream and the stream began to act as a water source for the pumping well. The manual stream discharge measurements made by FLNR staff during the step test and pumping test are shown in Table 20. The error for the discharge measurements is estimated to be 10%.

The discharge values in Table 20 are shown in Figure 28. Discharge at the downstream location was higher on average than at the upstream location, indicating that the stream likely gaining over this

reach. While a trend is somewhat apparent on this graph, there are no obvious shifts that coincide with the start and end of the step test, or the start and end of the constant rate pumping test (see vertical purple lines in Figure 28).

Table 20: Manual stream discharge measurements in December 2016 prior to and during the high-rate pumping test at Steele Park. The start and end times for the various stages of the test are indicated.

Date	Time	Location	Q (m ³ /s)
12/5/2016	12:30	Upstream	0.0393
12/5/2016			
12/5/2016	15:00	Downstream	0.0460
12/6/2016	8:35	Upstream	0.0322
12/6/2016	12:30	Upstream	0.0282
12/6/2016	14:15	Downstream	0.026
12/7/2016	9:45	Upstream	0.0255
12/7/2016	10:45	Downstream	0.0347
12/7/2016	11:20	Downstream	0.0315
12/7/2016	12:45	Upstream	0.0269
12/7/2016	14:45	Downstream	0.0305
12/8/2016	8:35	Upstream	0.0223
12/8/2016	9:15	Downstream	0.0197
12/8/2016	11:00	Downstream	0.0159
12/8/2016	15:15	Downstream	0.0315

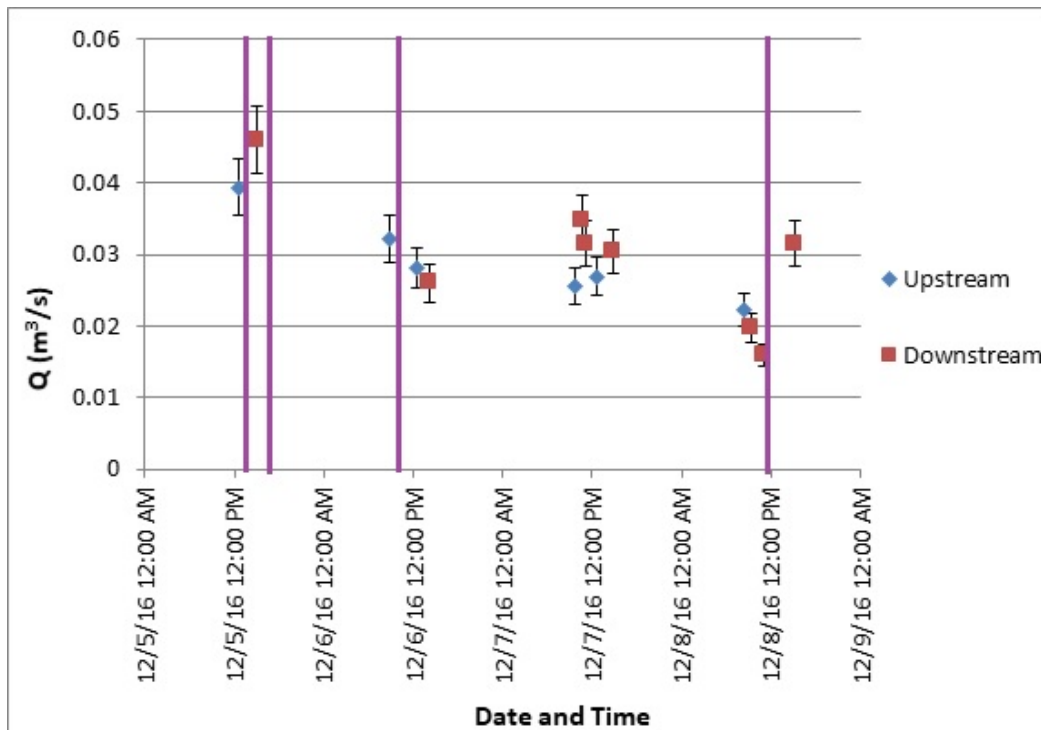


Figure 28: Manual discharge measurements from Table 20. The downstream discharge was higher on average than the upstream discharge, indicating that the stream was gaining along the reach. The purple vertical lines show the start and end of the step test on December 5th, and the start and end of the high-rate constant discharge test from December 6th to 8th.

The stream stage over the course of the step test and pumping test for each hydrometric station is shown in Figure 29. Stream stage increased slightly, reaching a maximum at approximately 5:30 pm on December 5th, following the recovery of the step test. It had been snowing heavily (wet snow) the morning of December 5th, throughout the step test; therefore it is possible that the snowmelt contributed to streamflow during the step test, masking any signal from the test itself, although the step test was of relatively short duration and so may not have intersected the stream. Thereafter, until the end of the constant discharge test, stream state continued to drop throughout the high-rate pumping test with no obvious sign of recovery between the two tests.

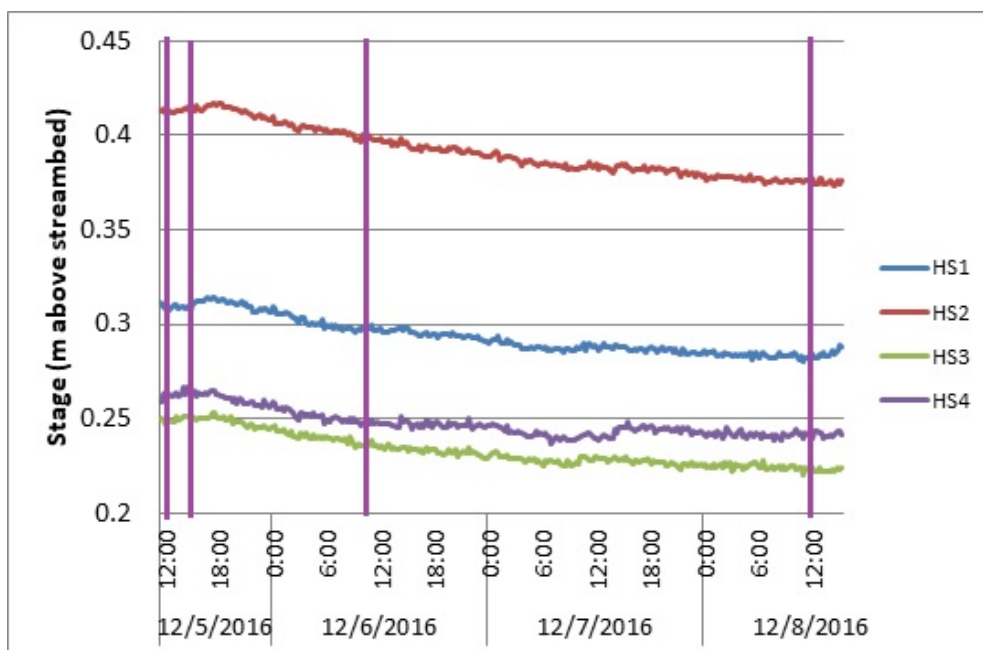


Figure 29: Stream stage at the four hydrometric stations in December. The purple vertical lines show the start and end of the step test on December 5th, and the start and end of the high-rate constant discharge test from December 6th to 8th.

The overall change in stage at each hydrometric station is shown in Figure 30. The change in stream stage at all four hydrometric stations began fairly uniformly, with all stations dropping 0.01 m over about 9.5 hours, giving a depletion rate of 0.001 m/hour. Around 6:00 pm on December 6th, roughly 7 hours after the high-rate pumping test began, the rates of stage depletion at each hydrometric station began to diverge (Figure 30). HS4 shows the sharpest decrease in stage depletion rate, while HS1 shows the least decrease. Stream stage appears to have dropped at the same rate at HS1 and HS3 for the entirety of the logging period. At around 8:00 am on December 7th, there appears to be a brief period of recovery when stream stage stopped dropping (HS2) or rebounded slightly (HS1, HS3, HS4), until 2:30 pm the same day when stream stage again began to drop for all hydrometric stations until the end of the recording period. The pumping rate remained constant and there were no significant weather changes following the heavy snowfall on December 5th. This time period roughly correlates with the time of pseudo steady-state hydraulic gradient change observed in piezometer set D2-D4. It is not known if there is a relationship between these two phenomena. Thus, it appears that the early decline in stream stage following the step test was perhaps related to a natural recovery of streamflow levels following the snowmelt input, but that part way through the constant-rate pumping test water was sourced from the stream, variably influencing the hydrometric stations. The snowfall, thus potentially significantly influenced these results.

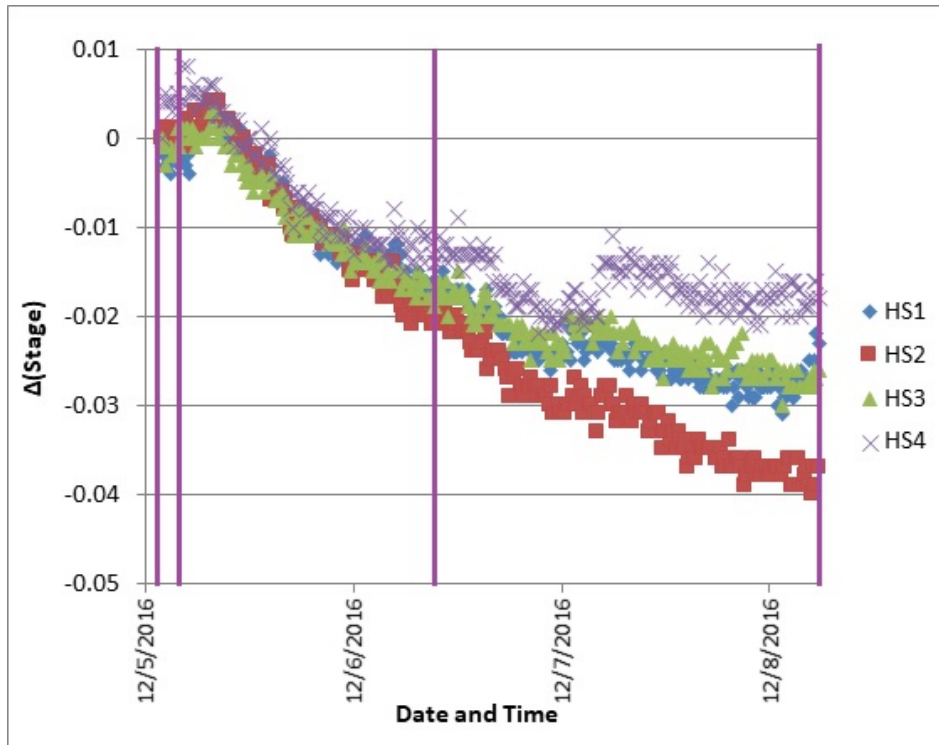


Figure 30: Change (decrease) in stream stage at each hydrometric station relative to the stage just prior to the step test. The purple vertical lines show the start and end of the step test on December 5th, and the start and end of the high-rate constant discharge test from December 6th to 8th.

An attempt was made to calculate streamflow depletion from manual measurements of discharge made upstream and downstream throughout the test period. Unfortunately, the rapid fluctuations in the downstream discharge measurements and the fact that the upstream and downstream measurements were not taken at the same time meant that streamflow depletion calculated this way contained significant oscillations and flipped between positive and negative values over the course of the test. Thus, the directly measured discharge values could not be used to calculate streamflow depletion. A second option is to calculate streamflow depletion from differences in stage if a representative rating curve is available. Unfortunately, there were insufficient background data to construct a rating curve so alternative approaches were considered. Consequently, multiple other approaches were attempted to calculate streamflow and constrain the streamflow depletion due to pumping. These included: 1) fitting a curve to the suite of manual discharge measurements at each upstream and downstream location, 2) fitting polynomial models to the changes in stage over time at each location to examine the derivatives of those best fits, 3) attempting to quantify streamflow depletion from changes in discharge at a single measurement location from changes in stage, 4) attempting to quantify stream depletion due to pumping alone at a single location using the downstream discharge best fit model with the upstream best fit model subtracted from it, and 5) using a ratio of discharge to stage (that assumes velocity and area are constant) and estimating continuous stream discharge from continuous stage measurements at each hydrometric station.

Unfortunately, none of these approaches yielded streamflow depletion values that made any physical sense. It is possible that natural changes in stream discharge related to the snowfall event was the cause for the poor results. Therefore, a direct comparison of field stream depletion to the suite of analytical streamflow depletion solutions could not be made. The results of all attempts are described in Hall (2017).

3.2 Streamflow Depletion Models

Various analytical solutions have been proposed to model streamflow depletion as a function of time, all of which are solutions to the general unsteady groundwater flow equation (Eq. 6). The streamflow depletion solutions used in this study apply the additional simplifying assumptions that the aquifer is homogeneous and isotropic, which reduces the general groundwater flow equation to a simpler form:

$$K \left[\frac{d^2 h}{\partial x^2} + \frac{d^2 h}{\partial y^2} + \frac{d^2 h}{\partial z^2} \right] = S_s \frac{\partial h}{\partial t} \quad (\text{Eq. 6})$$

While these analytical models are simplified, their advantage over numerical models is that they are relatively simple to use, require fewer parameters, and require less computing power to evaluate. This makes them particularly attractive for assessing the potential streamflow depletion from wells during the water licensing process under the WSA.

3.2.1 Glover-Balmer Model (1954)

The most commonly used analytical stream flow depletion model is known as the Glover-Balmer equation (often simply the Glover equation). Glover and Balmer (1954) redefined a previous stream depletion solution from Theis (1941) using the complementary error function rather than the original definite integral form derived by Theis. This reduced evaluation of the equation to a series approximation instead of numerical integration, making the use of the equation far more practical. The Glover-Balmer equation is given by:

$$\frac{\Delta Q_s}{Q_w} = \text{erfc} \left(\sqrt{\frac{Sd^2}{4Tt}} \right) \quad (\text{Eq. 7})$$

where:

- ΔQ_s is the stream depletion flow rate;
- Q_w is the constant pumping rate at the well;
- erfc is the complementary error function;
- S is the storativity of a confined aquifer or the specific yield of an unconfined aquifer;
- d is the distance from the well to the stream at the stream's closest point;
- T is the aquifer transmissivity; and
- t is the elapsed time since pumping began.

The assumptions made in the Glover-Blamer model are as follows:

1. The stream is infinitely long, and the stream stage is constant.
2. The streambed completely penetrates the entire thickness of the aquifer.
3. The streambed materials do not impede flow into the aquifer.
4. Aquifer materials are homogeneous with respect to T and S .
5. The aquifer extends infinitely outwards from the stream.
6. The aquifer has a constant thickness, and is bounded at the base by an aquiclude.
7. In unconfined systems, the change in thickness due to drawdown is negligible.
8. The stream is the only recharge source.
9. Pumping is from a single well screened over the entire aquifer thickness.
10. The pumping rate is constant.

The conceptualized stream geometry for the Glover model is shown in Figure 31.

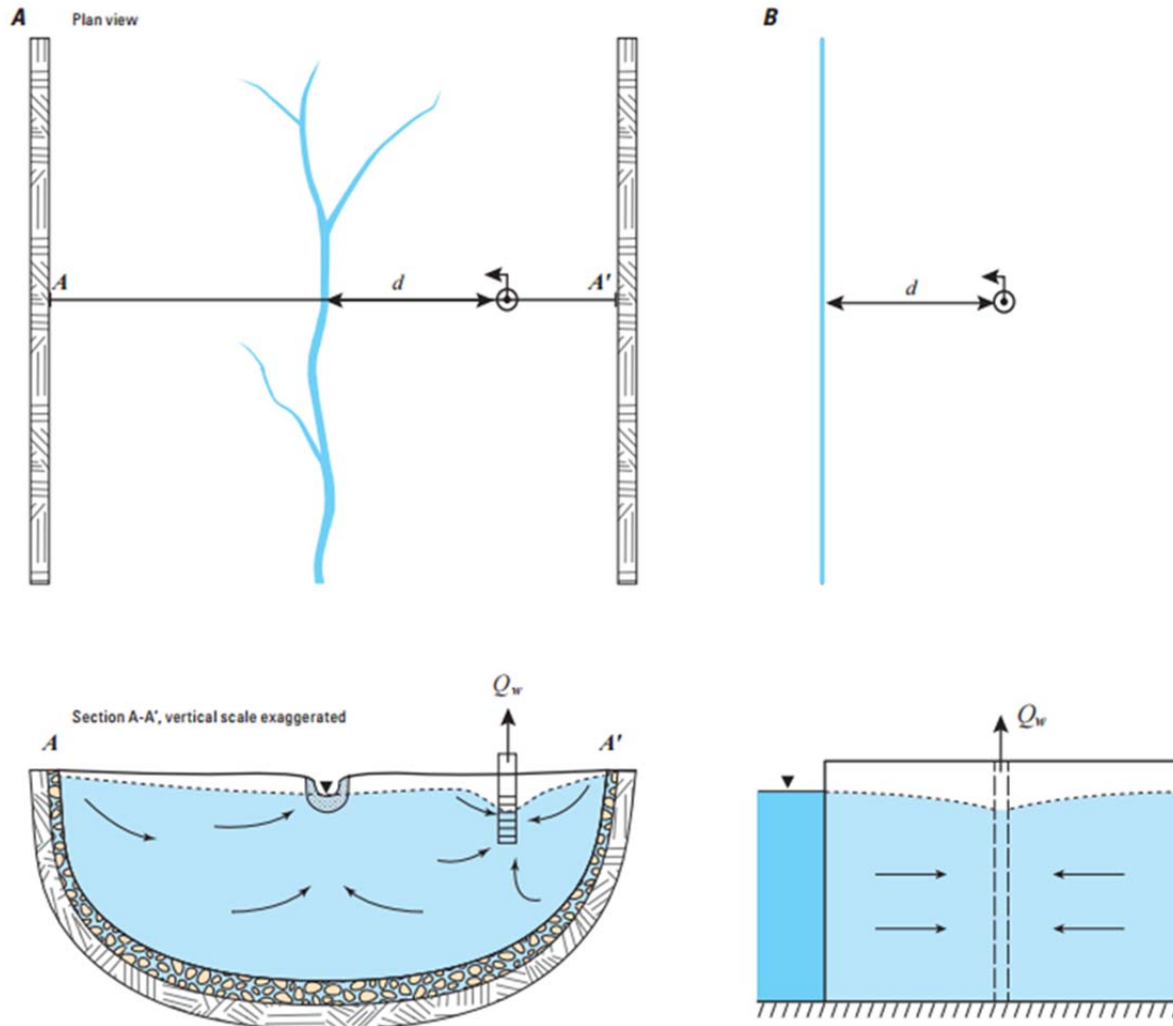


Figure 31: Plan view and cross sectional view of a real aquifer stream system (A) and the Glover model (1954) conceptualization (B). The distance between the well and the stream is denoted as d . Source: Barlow and Leake (2012).

3.2.2 Glover Model with Residual Depletion

At steady-state streamflow depletion, a significant portion of the water in the aquifer has been removed from storage (S_s and/or S_y). When the pump is shut off, streamflow depletion does not immediately stop but instead decreases slowly as water flows out of the stream and into the aquifer to return the aquifer to its pre-pumping equilibrium state. The Glover-Balmer model was altered by Jenkins (1968) to account for this continued streamflow depletion during recovery after the pump is turned off. Jenkins calculated the residual streamflow depletion as the difference between the original streamflow depletion due to the pumping well, and the streamflow depletion due to an imaginary injection well at the same point that begins injecting at the original pumping rate at the time the pump is shut off. The equation can be expressed as a piecewise function:

$$\frac{\Delta Q_s}{Q_w} = \begin{cases} \operatorname{erfc}\left(\sqrt{\frac{Sd^2}{4Tt}}\right), & 0 < t \leq t_s \\ \operatorname{erfc}\left(\sqrt{\frac{Sd^2}{4Tt}}\right) - \operatorname{erfc}\left(\sqrt{\frac{Sd^2}{4T(t-t_s)}}\right), & t > t_s \end{cases} \quad (\text{Eq. 8})$$

where t_s is the time at pump shutoff and all other variables are as defined for the Glover-Balmer model. All assumptions from the Glover-Balmer model also hold.

3.2.3 Hantush Model (1965)

The Hantush (1965) model accounts for the effects of a low conductivity streambed layer (also called a clogging layer) (Figure 32). Physically, this layer is composed of fine grained silts and sands that has a lower hydraulic conductivity than the aquifer, thereby restricting the movement of water across the streambed.

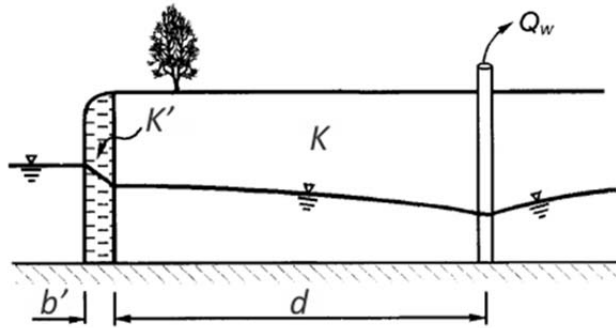


Figure 32: Aquifer-stream conceptualization used in the Hantush (1965) model. Source: Hunt (1999).

The assumptions in the Hantush (1965) model are otherwise as for the Glover model. The Hantush (1965) equation is:

$$\frac{\Delta Q_s}{Q_w} = \operatorname{erfc}\left(\sqrt{\frac{Sd^2}{4Tt}}\right) - \exp\left(\frac{Tt}{SL^2} + \frac{d}{L}\right) \operatorname{erfc}\left(\sqrt{\frac{Tt}{SL^2}} + \sqrt{\frac{Sd^2}{4Tt}}\right) \quad (\text{Eq. 9})$$

Hantush defines L as the streambed leakance, expressed as:

$$L = \frac{K}{K'} b' \quad (\text{Eq. 10})$$

where:

- K is the hydraulic conductivity of the aquifer;
- K' is the hydraulic conductivity of the streambed; and
- b' is the thickness of the streambed (Figure 32).

3.2.4 Hunt Model (1999)

The Hunt (1999) model addresses the effects of both a clogging layer along the streambed, and partial penetration of the stream into the aquifer (Figure 33). Assumptions for this model include the Glover-Balmer assumptions, as well as the following additional assumptions:

- 1) The water table drawdown is small such that horizontal flow conditions are valid.

- 2) The aquifer is of infinite areal extent and that the vertical dimensions of the stream are small when compared to the aquifer thickness, such that the stream is a line source of zero width.

The Hunt (1999) equation is:

$$\frac{\Delta Q_s}{Q_w} = \operatorname{erfc}\left(\sqrt{\frac{Sd^2}{4Tt}}\right) - \exp\left(\frac{\lambda^2 t}{4ST} + \frac{\lambda d}{2T}\right) \operatorname{erfc}\left(\sqrt{\frac{\lambda^2 t}{4ST}} + \sqrt{\frac{Sd^2}{4Tt}}\right) \quad (\text{Eq. 11})$$

where λ is the streambed conductive coefficient, defined by:

$$\lambda = \frac{w}{B''} K' \quad (\text{Eq. 12})$$

and,

- w is the streambed width;
- K' is the streambed hydraulic conductivity; and
- B'' is the streambed thickness.

This formulation of λ holds the implicit assumption that the well spacing from the stream is greater than the stream width (Rathfelder, 2016).

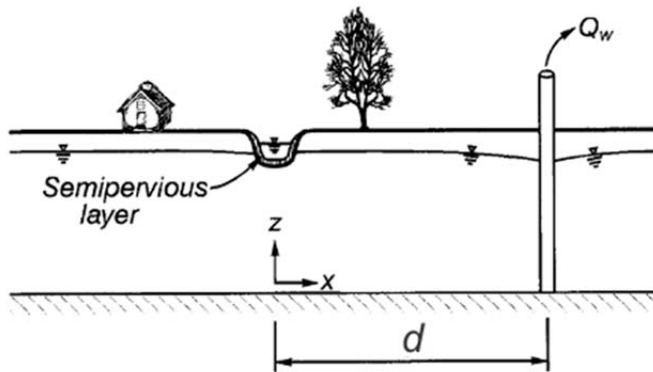


Figure 33: Aquifer-stream conceptualization for the Hunt (1999) model.

3.2.5 Michigan Screening Tool

The Michigan Screening tool is a web based tool created by the United States Geological Survey, the Michigan government, and Michigan State University. It was designed to utilize the Hunt (1999) streamflow depletion model in a more user friendly manner to aid in estimating the effects of streamflow depletion in aquifers composed of glacial deposits (Reeves et al., 2009). The Michigan Screening tool estimates the λ term in the Hunt (1999) model as:

$$\lambda = \frac{wK_v}{d_s} \quad (\text{Eq. 13})$$

where:

- w is the stream width;
- K_v is the vertical hydraulic conductivity of the aquifer; and
- d_s is the vertical distance between the bottom of the stream and the top of the pumping well screen.

The expression for streambed conductance is further simplified in terms of readily available parameters using the assumptions:

1. the transmissivity and aquifer conductivity are related by $K_h = T/b$ where b is aquifer thickness; and
2. the vertical and horizontal conductivity are related by a commonly assumed anisotropy ratio of 10; i.e., $K_h/K_v = 10$.

Eq. 13 for λ can then be re-written as:

$$\lambda = \frac{Tw}{10bd_s} \quad (\text{Eq. 14})$$

3.2.6 Singh (2003) Model

The Singh (2003) model is a modification of the Hantush leakage term. Singh appended a retardation factor, denoted R_p , to account for effects of partial penetration of the stream, thus redefining the leakage term L in the Hantush model as:

$$L = \frac{K}{K'}b' + R_p$$

$$R_p = \frac{b}{\pi} \ln \left(\frac{2e^{\frac{\pi d}{b}} - (1 + e^{-\frac{\pi w}{b}}) + \sqrt{\left(e^{\frac{\pi d}{b}} - e^{-\frac{\pi w}{b}}\right)\left(e^{\frac{\pi w}{b}} - 1\right)}}{(1 - e^{-b})} \right) - d \quad (\text{Eq. 15})$$

where b is the aquifer thickness, and all other terms are as defined before. This leakage term can be substituted into the Hantush (1965) model to account for partial stream penetration.

3.2.7 Hunt (2008)

The Hunt (2008) model takes a different approach than the previous methods in that it accounts for aquifers of finite extent. In this model, the stream has a width of γd , and is infinitely long (Figure 34). The origin of the co-ordinate system lies at the stream edge closest to the pumping well, and the aquifer extends some finite distances αd and βd on the pumping well side of the stream and the opposing side, respectively. The aquifer is overlain by an aquitard, and the stream partially penetrates that aquitard. The model holds the assumption that the free surface (water table) lies within the overlying aquitard.

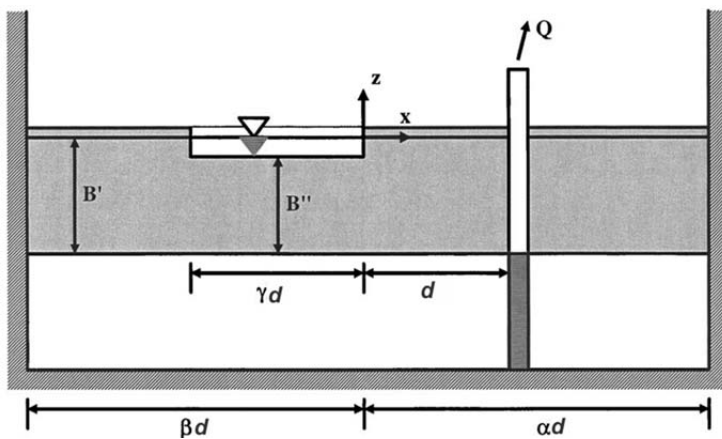


Figure 34: Aquifer-stream conceptualization for the Hunt (2008) streamflow depletion model. The shaded layer denotes the aquitard, which contains a free surface and is incised by the stream. The pumped aquifer lies beneath the aquitard. Source: Hunt (2008).

The solutions to the boundary value problem for the Hunt (2008) model are not straightforward and rely on Fourier and Laplace transforms, numerical Laplace inversions using the Stehfest (1970) algorithm. The derivations and resulting equations for streamflow depletion are presented and described in detail in Hunt (2008). Hunt implemented visual basic routines to compute the streamflow depletion in the Hunt (2008) model as part of an Excel spreadsheet available for free download on his personal webpage (<https://sites.google.com/site/brucehuntsgroundwaterwebsite/>).

3.3 Application of the Models to the Field Site

The analytical stream depletion models were tested for Union Creek at Steele Park using visual basic routines in Excel developed by Dr. Bruce Hunt at the University of Canterbury in New Zealand. These routines allow for complex mathematical functions to be computed in Excel with a higher precision than the Excel supplied functions. The parameters used in the models and the methods used to obtain them are displayed in Table 21.

Table 21: Variables used in the analytical streamflow depletion models for assessing streamflow depletion at Steele Park.

Variable	Symbol	Units	Value	Method for Determining
Distance from well to stream	d	m	27	Measured
Aquifer horizontal conductivity	K	m/hr	0.271	From pumping tests
Aquifer thickness	b	m	8.5	Saturated thickness
Transmissivity	T	m ² /hr	2.304	Calculated from Kb
Storativity or Specific yield	S or S_y	-	0.2	Estimated
Pumping rate	Q_w	m ³ /hr	5.436	Measured during pumping test
Streambed thickness	b'	m	0.1	Field measurements
Streambed hydraulic conductivity	K'	m/hr	0.0271	Assumed as $K/10$
Stream width	w	m	2	Measured
Aquifer vertical conductivity	K_v	m/hr	0.0271	Assumed as 1/10 horizontal conductivity
Vertical distance from streambed to top of pumping well screen	d_s	m	4.73	From well log
Streambed leakance (Singh Model)	L	m	2.89	Calculated
Simplified streambed conductance term (Michigan Screening Tool)	λ	m/hr	0.00361	Calculated from Eq. 15
Streambed conductance term (Hunt 1999)	λ	m/hr	0.542	Calculated from Eq. 13
Aquitard thickness (not below stream)	B'	m	1	Assumed
Aquitard conductivity (not below stream)	K''	m/hr	0	Set to zero as per Hunt (2008)
Aquitard specific yield	σ	-	1	Set to aquifer value as per Hunt (2008)
Well distance to right boundary from stream	α	-	1000	Set to large number (boundary is far away)
Well distance to left boundary from stream	β	-	1000	Set to large number (boundary is far away)
Stream width/well distance	γ	-	0.07407	Calculated

The values for σ and β were assigned to be arbitrarily large numbers to simulate an unbounded aquifer, and the aquitard conductivity (K'') was set to zero in order to simulate an unconfined system. These parameters allow for the streambed impedance models and the Hunt (2008) model to be compared for Steele Park. This is useful because the approaches for deriving the two types of models are fundamentally different. Seeing how they compare for the same site may give insight into how the conceptualization of the problem may influence the results. A graph of all models run for 1000 hours of pumping is shown in Figure 35.

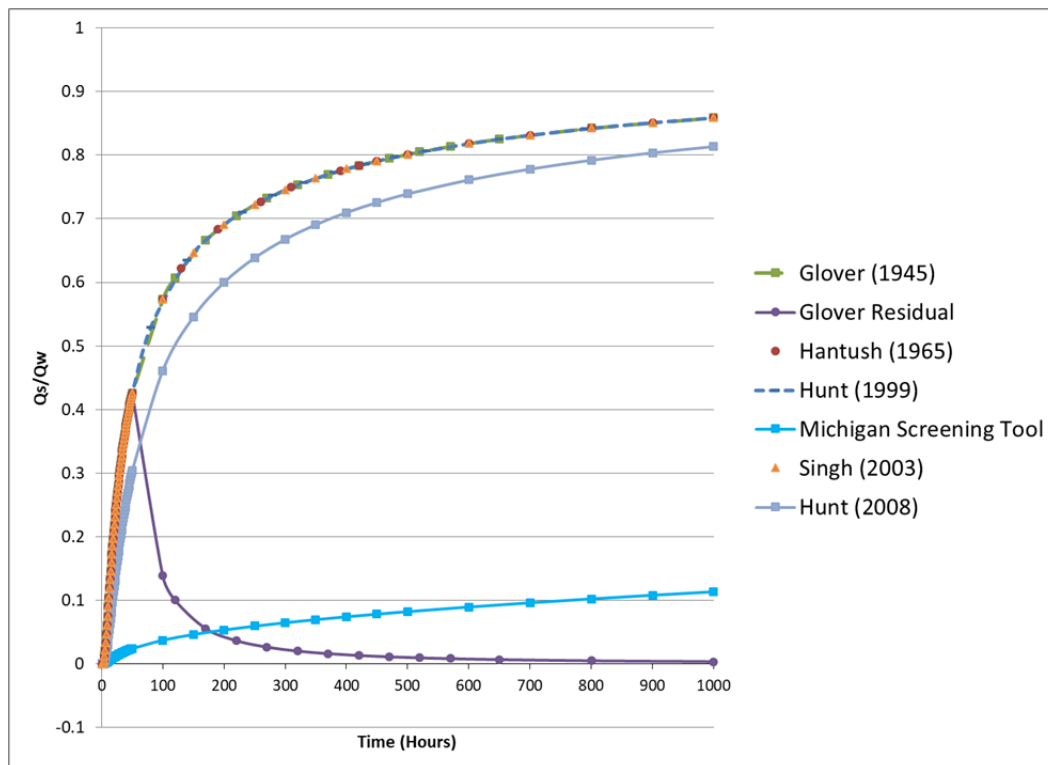


Figure 35: Modeled normalized streamflow depletion for Union Creek at Steele Park, based off of the parameters listed in Table 21. The “Glover Residual” model is the Glover Model with Residual Depletion beginning at 48 hours, to simulate the field pumping test. All other models pump continuously for the full 1000 hours.

The Michigan Screening tool drastically underestimates streamflow depletion when compared to all the other models. This likely stems from the fact that the equation used to estimate λ in the Michigan screening tool does not contain any physical streambed parameters, and so the value of λ obtained by the Michigan screening tool ($2.3E-03$ m/hr) is drastically different than the λ obtained for the Hunt (1999) model ($3.4E-01$ m/hr). Hunt (2001) describes the difficulty in characterizing the λ parameter.

After 1000 hours, all models except the Michigan screening tool show greater than 80% normalized stream depletion. Streamflow depletion was modeled for 18,000 hours (750 days) in total. The models converge at late time (with the exception of the Michigan screening tool) attaining 95% normalized streamflow depletion around 750 days. The Singh (2003), Hunt (1999), Hantush (1965), and Glover-Balmer (1954) models all predict a normalized streamflow depletion of around 42% by the end of the 48 hour pumping test, while Hunt (2008) predicts 30% normalized streamflow depletion after 48 hours.

The Glover and Balmer (1954), Hantush (1965), Hunt (1999), and Singh (2003) models all show almost identical behaviour for the entire 1000 hours of pumping. This indicates that the effects of partial penetration and streambed impedance ultimately have little to no effect on the modeling of streamflow depletion at Steele Park. This in itself is not very surprising, as the thickness of the clogging layer is fairly small (10 cm) and the hydraulic conductivity of the streambed sediments was estimated to be equivalent to the vertical conductivity of the aquifer (one-tenth the value of the aquifer horizontal conductivity). Increasing the streambed thickness in the Hunt (1999) model to a minimum of 0.3 m was required before the model could be distinguished from the Glover-Balmer (1954) model. Similarly, streambed conductivity had to be reduced to a minimum of $1/30^{\text{th}}$ of the horizontal aquifer conductivity in the Hunt (1999) model before a difference between the Hunt (1999) and Glover-Balmer (1954) models was noticeable. Changing the streambed conductivity to $1/80^{\text{th}}$ of the aquifer hydraulic

conductivity resulted in a streambed conductivity of $3.39E-03$ m/hr, which is within the accepted range of values for fine sand, and results in the model results shown in Figure 36.

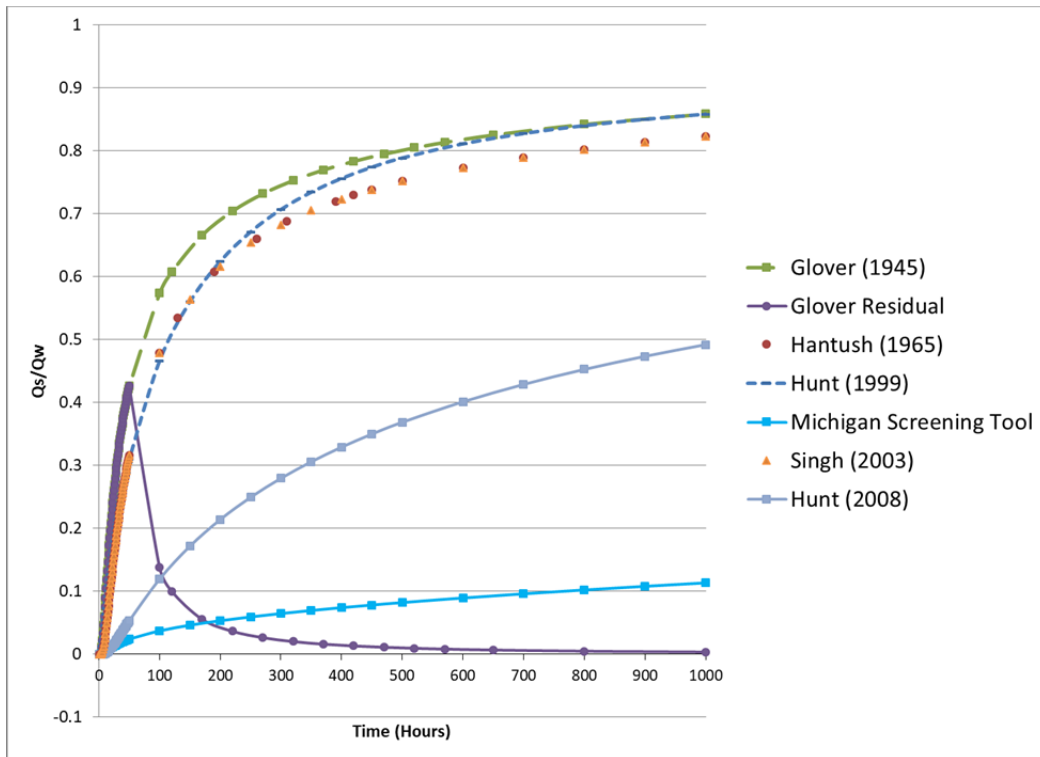


Figure 36: Streamflow depletion models for Union Creek with streambed hydraulic conductivity set to $1/80^{\text{th}}$ of the aquifer conductivity ($3.39E-03$ m/hr). The Hunt (2008) and streambed impedance models show the most change when compared to Figure 35.

The value of streambed thickness was measured based on a single sample taken with a clam gun, and while streambed thickness may vary spatially, the estimate of streambed hydraulic conductivity has a much larger error due to the order of magnitude variation inherent to K. The estimate provided in Table 21 is considered conservative, with the hydraulic conductivity of the streambed sediments equal to the vertical conductivity of the aquifer, because this provides a normalized streamflow depletion layer similar to the Glover-Balmer (1954) model, which does not account for the presence of the clogging layer.

The sensitivity analysis showed that relatively small changes in hydraulic conductivity of the streambed greatly decrease the rate of streamflow depletion in all the streambed impedance models and in particular the Hunt (2008) model. This highlights the importance of accurately characterizing the hydraulic conductivity of the clogging layer at small creek sites like Steele Park when attempting to model streamflow depletion using these more advanced models, as they are very sensitive to this particular parameter. Interestingly, the Hunt (1999) model follows the streamflow depletion of the other streambed impedance models at early time, but converges with the Glover-Balmer (1954) model around 700 hours. None of the other solutions that account for streambed impedance displays this same convergence with the Glover model within 1000 hours.

The streamflow depletion modeling of Union Creek at Steele Park showed that the suite of streamflow impedance models (Singh, 2003; Hunt, 1999; Hantush, 1965; and Glover-Balmer, 1954) had little to no variation in the rate of streamflow depletion over the first 1000 hours. The Michigan screening tool significantly underestimated streamflow depletion compared to the other models, likely due to the fact

that its leakance parameter λ does not actually contain any physical streambed parameters. The Hunt (2008) model estimated a reduced rate of streamflow depletion compared to the streambed impedance models, estimating 5% less streamflow depletion after 1000 hours. Varying the streambed hydraulic conductivity and thickness showed that small changes in the streambed leakance parameter λ result in significant changes in the estimated rate of streamflow depletion in all the streamflow impedance models.

3.4 Uncertainties and Difficulties in the Estimation and Calculation of Field Parameters and Recommendations for Future Studies

One of the goals of this study was to compare the available analytical streamflow depletion solutions with real streamflow depletion data. Due to the nature of the varying conditions at Steele Park and the type of data collected, the actual stream discharge at various reaches along the stream could not be reliably obtained. Attempts to estimate stream depletion from stream discharge and stage measurements were unsuccessful in producing values that held any degree of confidence. As a result, no comparison of field data to the analytical streamflow depletion solutions could be made.

There are four main aspects of the Steele Park study that made attempts to obtain reliable aquifer hydraulic connectivity measurements difficult. The first problem was the timing of the background site characterization with regards to the pumping test. Background characteristic measurements at the site were, for the most part, obtained in the summer during low flow conditions. In general, low flow conditions at the site resulted in streamflow, site-wide horizontal hydraulic gradient, and seepage meter measurements that were an order of magnitude smaller than the same corresponding measurements made during the winter just prior to the pumping test. The pumping test was originally scheduled for the end of the summer (in August) during low flow conditions. However, FLNR concerns of potential dewatering of sensitive riparian habitat in Union Creek necessitated the rescheduling of the pumping test to periods with higher stream flows. With a pumping rate on the order of $1\text{E-}03 \text{ m}^3/\text{s}$, this meant that the pumping rate during the winter was an order of magnitude lower than streamflow, making the impact of pumping on streamflow far more difficult to detect than if the pumping test had been completed in the summer as originally planned. The pumping rate could not be increased because of the available drawdown in the pumping well. The available drawdown was limited to 4.3 m, primarily because of the selected pumping equipment (pipe lengths). With alternative equipment, the pump could have been placed slightly deeper in the well (approx. 10 m) to maximize the available drawdown.

The second complication was the likely presence of a hyporheic zone. The exact extent of the mixing of groundwater and surface water beneath the stream is not known, and the overall effect that pumping has on the hyporheic zone is also not well understood. The presence of this zone may have influenced the shallow piezometer readings during background site characterization in the summer, and the extent of the hyporheic zone beneath the streambed likely increased in the winter proportionally to the stream discharge volume. The presence of this zone may help explain the rapid fluctuations in hydraulic gradient observed in the instream piezometers in the winter, which increases the uncertainty in vertical hydraulic gradient measurements and the corresponding estimates of groundwater discharge. The presence of the hyporheic zone may also have affected the seepage meter results, where the collected water is a mixture sourced from both seepage and hyporheic flow (Middleton 2016).

The third difficulty at this study concerned the measurement and estimation of streamflow. A total of 14 streamflow measurements were taken during the test, but these were not taken in time-synched upstream-downstream pairs. This made calculation of streamflow depletion difficult. In order to attempt to get continuous streamflow data from stream stage measurements, simplifying assumptions about the stream geometry and flow system were made, namely:

1. The stream width did not change for the entirety of its reach from HS1 to HS4 and water velocity in the stream did not change with time, so the only factor varying stream discharge was stream stage.
2. Natural additions to the stream volume from non-groundwater sources (snowmelt, bank storage flow) were negligible.

These simplifying assumptions are likely to have greatly altered the calculated streamflow values relative to the actual ones, and ultimately did not produce streamflow depletion values that made physical sense. This situation can be avoided in future studies by developing stream rating curves for each hydrometric station location, and measuring flow at the same time and at regular intervals both upstream and downstream locations. This would allow direct calculation of volumetric streamflow depletion. The use of a weir could also potentially be used to reduce uncertainty.

The fourth problem with this study was the separation of streamflow depletion induced by pumping from the natural variations in baseflow. Natural changes in streamflow, in particular due to the snowfall event, is seen to be a critical issue. But even in the absence of this snow event, the lack of acceptable background streamflow variations for the winter conditions at the site was problematic. Hunt et al. (2001) outlines a method for separating the natural streamflow variation from the streamflow depletion induced by pumping. This methodology requires that streamflow be monitored prior to the start of pumping, but also for streamflow monitoring to continue after pumping has stopped until streamflow values recover to a maximum and begin to vary naturally again. A linear relationship can then be found by connecting the streamflow values prior to the test and after full recovery, which represents the natural baseflow trend. The streamflow depletion due to pumping is then found using the raw streamflow measurements with the natural baseflow relationship subtracted.

In addition to this, Hunt et al. (2001) suggests that the location of the upstream and downstream discharge measurement sites be such that they lie outside the radius of influence of the pumping well. At Steele Park, both the upstream and the downstream measurement locations were within the radius of influence of the pumping well, meaning that streamflow depletion occurring outside the reach defined by those locations was not considered in the study. As a result, even in a perfect theoretical scenario where natural baseflow was zero, stream geometry was uniform, pumping continued for an infinite time, and discharge measurements were synched in time, the calculated streamflow depletion would never reach a value of 1 because additional unaccounted streamflow depletion would be occurring outside of the study area. Unfortunately, access to Union Creek is limited, particularly upstream, so it may not be possible to measure discharge outside the radius of influence.

An analysis of field data similar to this study was completed by Hunt et al. (2001) for data collected just outside of Christchurch, New Zealand. The purpose of that study was to determine aquifer transmissivity and storativity, as was done at the Steele Park site, but also to constrain the streambed leakage parameter λ . In order to determine λ , stream depletion measurements were made using two V-notched weirs 200 m upstream and downstream of the pumping well. As mentioned above, they also monitored streamflow rates and aquifer head levels both prior to and after the test in order to obtain correction factors to account for natural variations in these parameters. In a similar manner to the Steele Park test, they found that the 400 m spacing between the weirs was not adequate to capture all streamflow depletion, and that flow was removed from the stream outside the boundaries of their study area.

That study also identified an important factor that was not considered in the Steele Park test, but should be considered for all future studies; namely that when conducting the pumping test, water levels in the wells closest to the river must be monitored relative to the stream base and stage elevations. Drawdown cannot be allowed to grow large enough to enable the stream to become perched significantly above the surrounding water table, as this violates one of the main assumptions used in all

the analytical streamflow depletion solutions. While this was not a problem during winter conditions at Steele Park, it may have been a potential problem if pumping test had been conducted during the summer when the hydraulic factors (streamflow, site hydraulic gradient, groundwater seepage) at the site were an order of magnitude lower.

Finally, Hunt et al. (2001) describe the difficulty surrounding steady-state flow conditions in field tests for streamflow depletion. The pumping test at Christchurch was only conducted for 10 hours, with an additional 20 hours of recovery. This time period was not long enough for conditions at the site to reach pseudo steady-state, and the authors estimated that at the end of the 10 hours of pumping, the leakage from the stream was only at about 62% of its steady-state flow value. The authors state that approximately 12 days of pumping would be required at their study site for leakage from the stream to achieve 90% of its steady-state value, but that the natural variations in hydraulic head levels within the aquifer that would occur over that length of time make it nearly impossible to achieve steady-state flow conditions. This is an important point to consider when choosing areas for this type of field study; an area with background conditions that are small and as close to constant as possible would make the quality of the data collected the best it could be and would facilitate the easiest and most accurate possible comparison of field streamflow depletion and modeled streamflow depletion. Unfortunately, often it is not possible to choose an ideal site, so undertaking multiple tests may lessen the uncertainty.

4. CONCLUSIONS AND RECOMMENDATIONS

4.1 Site Hydrogeology

The site hydrogeology was characterized using a number of methods. First, an in-depth analysis of the core from well SPMW-02 was undertaken to examine any small scale heterogeneities in the aquifer with depth. The in-depth core analysis revealed three hydrostratigraphic units: 1) a layer of soil about 1 m thick, 2) a gravelly-sand aquifer approximately 10 m thick, and a lower clay unit the full depth of which was not penetrated by the wells at Steele Park. The aquifer is considered unconfined. The three borehole logs from the site (SPPW, SPMW-01, SPMW-02) were compared with driller's logs from six nearby residential wells along 54th Street to see if the general hydrostratigraphic units observed at Steele Park are consistent over a larger area. This comparison revealed a second thin sandy aquifer unit estimated to be approximately 2 m thick underlying the clay unit at about 70 m depth, which in turn is underlain by a second clay unit. The residential logs also showed that the upper clay unit has an undulating surface, resulting in the unconfined upper gravelly-sand aquifer changing in thickness from 4 m to 12 m in a southeast-northwest direction across the site. Depth-to-water measurements taken in the Steele Park wells showed that the saturated thickness of the aquifer ranged from 7.9 m in the summer to 8.7 m in the winter. Site-wide horizontal hydraulic gradients obtained by way of a three point problem ranged from 7.97E-03 in June and 6.29E-03 in July. The gradient was directed toward Union Creek at an angle of roughly 30 degrees in the downstream direction. In winter, the gradient was 2.05E-02 in December in a direction towards and normal to the stream. These gradients suggest that Union Creek is gaining in the vicinity of Steele Park throughout the year, and that the groundwater flux to the creek is higher during winter.

Grain size analyses were performed on samples taken from varying depths within the SPMW-02 core. The results were used to obtain a first order estimate of hydraulic conductivity via Hazen's method (1.9E-04 m/s). Slug and bail tests were completed for each of the three wells drilled at Steele Park to obtain an estimate of hydraulic conductivity based on Hvorslev's method (6.22E-05 m/s) and the Bouwer-Rice method (4.80E-05 m/s). The average of these values (5.5E-05 m/s) was used to design a low-rate pumping test, which was carried out in July. The pumping test provided preliminary estimates

of S_y , S_s , and T . A second high-rate pumping test was conducted in December, also yielding estimates of S_y , S_s , and T . T varied from $2.7\text{E-}04 \text{ m}^2/\text{s}$ in the summer to $1.3\text{E-}03 \text{ m}^2/\text{s}$ during the winter, resulting in a time-averaged aquifer transmissivity of $8.1\text{E-}04 \text{ m}^2/\text{s}$. The best estimate of S is $2.9\text{E-}04$ based on the geometric mean values of the S values from monitoring wells from both pumping tests. Using the saturated thickness values during each test, the best estimate of K is $7.3\text{E-}05 \text{ m/s}$, and the best estimate of S_s is $3.5\text{E-}05 \text{ m}^{-1}$. Finally, S_y determined from the high rate pumping test is $7.2\text{E-}02$, which is low compared to specific yield values for similar aquifer materials. A more reasonable estimate is 0.2, which lies between the reported values for gravel (0.19) and sand (0.22) given by Heath (1983).

4.2 Aquifer-Stream Connectivity

The degree of aquifer-stream connectivity was determined using head measurements in instream nested piezometer pairs, seepage meter measurements, and stream stage measurements coupled with streamflow measurements. Piezometer measurements were used to characterize the vertical hydraulic gradient through the streambed both during natural baseline conditions in summer and during the high-rate pumping test in the winter. The baseline conditions at the site indicated that groundwater flow was mainly downward out of the creek along the reach at Steele Park, with average summer gradients of 0.024 to 0.14 into the aquifer. However, discrepancies in the direction of water flow between the streambed and the deep and shallow piezometers in the nested pairs indicated that hyporheic flow may have been influencing the head levels in the shallow piezometers. Hydraulic gradients between the individual piezometers and the stream stage showed dominantly positive values, indicating flow was upwards into the creek. It is theorized that the shallow piezometers may be influenced by the hyporheic zone, a zone of surface water and groundwater mixing that exists along stream banks and beneath the streambed, although it is possible that aquifer heterogeneity and/or piezometer position relative to the stream bank may have influenced the results. During the high-rate pumping test in the winter, all piezometers showed drawdown in response to pumping suggesting hydraulic connectivity. Gradients that were negative (downwards out of the stream) prior to the test increased in magnitude, while gradients that were positive (showing upwards flow into the stream) decreased in magnitude and at one piezometer pair actually changed direction from upward to downward. The effect of hyporheic flow on these winter measurements is not known, but is expected to be present due to rapid fluctuations in the hydraulic gradients measured at each piezometer pair during the pumping test.

Seepage meter measurements made during the summer showed groundwater flux upwards into the stream at a rate of $7\text{E-}07 \text{ m}^3/\text{s}/\text{m}^2$. This flux disagrees with the general downward gradient direction observed in the piezometer pairs, but the effect of the hyporheic zone are again thought to potentially play a role in this discrepancy. Seepage measured in the winter just prior to the start of pumping gave a seepage rate of $3.5\text{E-}05 \text{ m}^3/\text{s}/\text{m}^2$. This value is an order of magnitude higher than the rates observed during the summer time and is expected due to the site-wide horizontal hydraulic gradient also being an order of magnitude higher during the winter compared to summer. Seepage rates measured during the step test and the pumping test varied from $2.5\text{E-}05 \text{ m}^3/\text{s}/\text{m}^2$ to $3.2\text{E-}05 \text{ m}^3/\text{s}/\text{m}^2$, respectively, but no overall trend in seepage rates was found over the course of either test.

Stream stage varied a large amount between summer and winter. At some locations during the summer stream stage was almost too low to accurately measure, while during the winter stream stage values of up to 40 cm were recorded. Stream stage dropped by about 2 and 4 cm at all four hydrometric stations over the course of the pumping test. However, stream stage was already declining when the constant discharge test started and all four hydrometric stations declined at a similar rate. Only partway through the constant discharge test did the rate of decline change between the four hydrometric stations. The snowfall on December 5th may have influenced the streamflow such that the stream level was

decreasing back to its original levels (pre-snow) while also decreasing due to streamflow depletion due to pumping, thus resulting in even greater apparent streamflow depletion.

4.3 Modeling Streamflow Depletion

One of the main goals of this project was to obtain field streamflow depletion values that could be compared against the suite of analytical models available. The aim was to determine how accurate the models are and see if any one model performed better than the others. Due to the nature of the data collected, however, this ultimately was not possible. The most critical parameter was a reliable measure of the volumetric streamflow depletion in Union Creek with time. Despite using different approaches to calculate streamflow depletion indirectly, no realistic value was obtained.

In the absence of streamflow depletion field measurements, analytical streamflow depletion models were used to estimate the rate streamflow depletion at Steele Park as well as to assess inter-model comparisons. The Singh (2003), Glover-Balmer (1954), Hantush (1965), and Hunt (1999) models showed little to no difference in streamflow depletion estimates over 1000 hours, and predicted normalized streamflow depletion would have reached 42% by the end of the 48 hour pumping test. The Hunt (2008) model had reduced streamflow depletion rates compared to the aforementioned models, and predicted 30% normalized streamflow depletion by the end of the 48 hour pumping test. The Michigan screening tool did not appear to show realistic streamflow depletion, and predicted only 2.4% normalized streamflow depletion by the end of the 48 hour pumping test.

Varying the streambed hydraulic conductivity to $1/80^{\text{th}}$ the value of the aquifer horizontal conductivity, which was still within the accepted range of values for silt and fine sand, allowed for the effects of the streambed leakance parameter to be noticeable in the modeled normalized streamflow depletion. This indicates that accurate estimation of the streambed hydraulic conductivity is paramount in estimation of the streambed leakance parameter, and that small variations in this parameter can have significant impacts on the accuracy of streamflow depletion estimates. Due to heterogeneities in the streambed sediment, a large number of samples would be needed if this parameter were to be characterized through measurement. Hunt (2001) also points out further difficulties in obtaining reliable estimates of the streambed leakance parameter λ from field data, and at the time that paper was written no satisfactory method existed for accurately characterizing the streambed leakance parameter in the field.

4.4 Recommendations

This project yielded valuable data and provided critical knowledge surrounding how to conduct a field study to assess hydraulic connectivity. In hindsight, however, things could have been done differently to achieve even better success. The main challenge for the field study was the poor timing of the pumping test. Unfortunately, the flows in Union Creek were so low in summer 2016 that a high-rate pumping test could not be conducted as it may have further compromised flows in the creek. As a result, the pumping test was carried out in December 2016 when flows in Union Creek were much higher. An added complication was the snowfall event, which appears to have strongly influenced the natural streamflow. Ideally, a field study aimed at investigating hydraulic connectivity would be carried out during baseflow conditions (i.e. during mid- to late summer) when the groundwater levels at the site are low, such that the pumping test is the most dominant stress on the aquifer system and the effects of pumping can be more easily isolated from the data. In this way, changes to the aquifer due to pumping would be most strongly manifest in the data collected. At the same time, however, the pumping test should not be conducted when snow (or rain) events are forecast in order to avoid the problem of naturally varying streamflow that may dominate the test.

Future studies in this area will also need to address the various issues with characterizing the field site, such as understanding the seasonal effects on the site-wide hydraulic conditions. Characterization of the hydraulic conductivity of the streambed sediments should be a high priority in future studies, in order to better constrain the streambed leakance parameter and ultimately improve the accuracy of the streambed depletion models. Finally, the location of streamflow measurements at the site during the pumping test must be outside the radius of influence of the pumping well to ensure the full impact of the well is captured. This may prove challenging, or indeed impossible, given access restrictions.

In closing, we recommend additional field studies be carried out at Steele Park. The following lists aspects of a field investigation that should be focused on.

1. Monitor stream stage and groundwater levels at the site for at least one full year prior to and following the pumping test. This will allow baseline conditions to be firmly understood before stressing the aquifer.
2. Measure streamflow periodically throughout the year to construct a stream rating curve.
3. Investigate the feasibility of installing weirs during low flow conditions.
4. Measure streamflow both upgradient and downgradient, outside the zone of influence of pumping, and at consistent times.
5. Measure streamflow before pumping begins and continue measuring streamflow well after the pumping test ends to re-establish baseline conditions.
6. Carry out a pumping test during mid- to late-summer, during a period of limited rainfall.
7. Pump the aquifer at a slightly higher rate, if possible. This could be accomplished by setting the pump depth lower in the well.
8. Obtain multiple samples of streambed sediments and carry out grain size analysis and/or carry out pneumatic slug testing to estimate streambed hydraulic conductivity. The streambed thickness should also be measured at different locations. Together, hydraulic conductivity and bed thickness will better constrain the leakance parameter in the streamflow depletion models that include impedance.

The original intent of this project was to undertake a comparison of hydraulic connectivity in an unconfined and a confined aquifer. However, due to budgetary constraints, only the unconfined aquifer was investigated. Therefore, we recommend conducting a similarly scoped field and modeling investigation at the West Creek site in Langley.

REFERENCES

- Barlow, P., and Leake, S. 2012. Streamflow Depletion by Wells - Understanding and Managing the Effects of Groundwater Pumping on Streamflow. USGS.
- British Columbia Government. 1997. *Fish Protection Act*. Retrieved from: http://www.env.gov.bc.ca/habitat/fish_protection_act/act/documents/act-theact.html
- British Columbia Government. 2016. *Water Sustainability Act*. Sensitivity Streams. Retrieved from: <http://www2.gov.bc.ca/gov/content/environment/air-land-water/water/water-licensing-rights/sensitive-streams>
- Blood, D.A. 1993. Salish Sucker. BC Ministry of Environment, Lands and Parks.
- Bourdet, D., Ayoub, J., and Pirard, Y. 1989. Use of pressure derivative in well-test interpretation. SPE Formation Evaluation, 4(2): 293-302.

- Bouwer, H., and Rice, R. 1976. A slug test for determining hydraulic conductivity of unconfined aquifers with completely or partially penetrating wells. *Water Resources Research*, 12(3): 423-428.
- Brown, D., Narasimahn, T., and Demir, Z. 1995. An evaluation of the Bouwer and Rice method of slug test analysis. *Water Resources Research*, 31(5): 1239-1246.
- Butler, J. J. 1998. *The Design, Performance, and Analysis of Slug Tests*. New York: Lewis Publishers.
- Butler, J., and Liu, W. 1993. Pumping tests in nonuniform aquifers: the radially asymmetric case. *Water Resources Research*, 29(2): 259-269.
- Clague, J. J., and Luternauer, J. L. 1983. *Late Quaternary Geology of Southwester British Columbia*. Victoria, BC: University of Victoria
- Cooper, H., and Jacob, C. 1946. A generalized graphical method for evaluating formation constants and summarizing well-field history. *American Geophysical Union*, 27(4): 526-534.
- Fetter, C. 2001. *Applied Hydrogeology* (4th ed.). Upper Saddle River, New Jersey: Prentice Hall.
- Freeze, R., and Cherry, J. 1979. *Groundwater*. Englewood Cliffs, New Jersey: Prentice Hall.
- Glover, R., and Balmer, G. 1954. River depletion resulting from pumping a well near a river. *Earth and Space Science News*, 35(3): 468-470.
- Golder Associates Ltd. 2004. *Final Report on Comprehensive Groundwater Modeling Assignment, Township of Langley 022-1826/5000*.
- Golder Associates Ltd. 2016. *Monthly Groundwater Budget for the Hopington Aquifer – Salmon River Area, BC*. Water Science Series, WSS2016-06, Province of British Columbia, Victoria, B.C.
- Hall, G. 2017. *Investigation of Aquifer-Stream Connectivity at Steele Park, Langley BC*. BSc Honours Thesis, Department of Earth Sciences, Simon Fraser University.
- Hantush, S. 1965. Wells near streams with semipervious beds. *Journal of Geophysical Research*, 70(12): 2829-2838.
- Hazen, A. 1892. *Some physical properties of sands and gravels*. Massachusetts State Board of Health.
- HB Lanarc. 2011. *Township of Langley Agricultural Profile*. Report prepared by HB Lanarc in association with Ground Up Rural Resource Consultants Inc.
- Heath, R. C. 1983. *Basic Ground-Water Hydrology*. Virginia: U.S. Geological Survey Water-Supply Paper.
- Hunt, B. 1999. Unsteady stream depletion from ground water pumping. *Ground Water*, 37(1): 98-102.
- Hunt, B. 2008. Stream depletion for streams and aquifers with finite widths. *Journal of Hydrologic Engineering*, 13(2): 80-89.
- Hunt, B. 2014. Review of stream depletion solutions, behaviours, and calculations. *Journal of Hydrologic Engineering*, 19(1): 167-178.
- Hunt, B., Weir, J., and Clausen, B. 2001. A stream depletion field experiment. *Ground Water*, 39(2): 283-289.
- Hvorslev, M. 1951. *Time Lag and Soil Permeability*. In: *Ground-Water Observations*. Waterways Experiment Station. Vicksburg, Mississippi: Corps of Engineers, U.S. Army.
- Luttmerding, H. 1980. *Soils of the Langley - Vancouver Map Area*. Victoria: BC Ministry of Environment.
- Luttmerding, H. 1981. *Soils of the Langley - Vancouver Map Area*. Victoria: BC Ministry of Environment.
- Middleton, M. A. 2016. *Aquifer - Stream Connectivity at Various Scales: Application of Sediment - Water Interface Temperature and Vulnerability Assessments of Groundwater Dependent Streams*. PhD Dissertation, Simon Fraser University.

- Middleton, M.A., and Allen, D.M. 2017. Assessment of Aquifer-Stream Connectivity Related to Groundwater Abstraction in the Lower Fraser Valley: Stream Vulnerability Mapping. Water Science Series, WSS2017-04. Prov. B.C., Victoria B.C.
- Middleton, M.A., Allen, D.M., and Whitfield, P.H. 2016. Comparing the groundwater contribution in two groundwater-fed streams, Lower Fraser Valley, British Columbia. Special Issue on Groundwater - Surface Water Interactions in Canada. Canadian Water Resources Journal 41(4): 554-571. doi:10.1080/07011784.2015.1068136
- Neuman, S. P. 1974. Effect of partial penetration on flow in unconfined aquifers considering delayed gravity response. Water Resources Research, 10(2): 303-312.
- Rathfelder, K. 2016. Modelling Tools for Estimating Effects of Groundwater Pumping on Surface Waters. Province of B.C., Ministry of Environment, Water Science Series WSS2016-09.
- Reeves, H. W., Hamilton, D. A., Seelbach, P. W., and Asher, A. J. 2009. Ground-Water-Withdrawal Component of the Michigan Water-Withdrawal Screening Tool. Virginia: U.S. Geological Survey.
- Singh, S. 2003. Flow depletion of semipervious streams due to pumping. Journal of Irrigation and Drainage Engineering, 129(6): 449-453.
- Stehfest, H. 1970. Numerical inversion of Laplace transforms. Communications of the ACM, 13(1): 47-49.
- Theis, C. 1935. The relation between the lowering of the piezometric surface and the rate and duration of discharge of a well using ground water storage. American Geophysical Union, 16, 519-524.
- Theis, C. 1941. The effect of a well on the flow of a nearby stream. American Geophysical Union, 22(3): 734-738.
- Waterloo Hydrogeologic Inc. 2016. AquiferTest™, version 2016.1. Waterloo Hydrogeologic Inc.
- Winter, T. 1999. Relation of streams, lakes, and wetlands to groundwater flow systems. Hydrogeology Journal 7:28-45.
- Winter, T. C., Harvey, J. W., Franke, O. L., and Alley, W. M. 1998. Ground Water and Surface Water: A Single Resource. Denver, CO.: USGS.

APPENDIX A: MONITORING WELLS

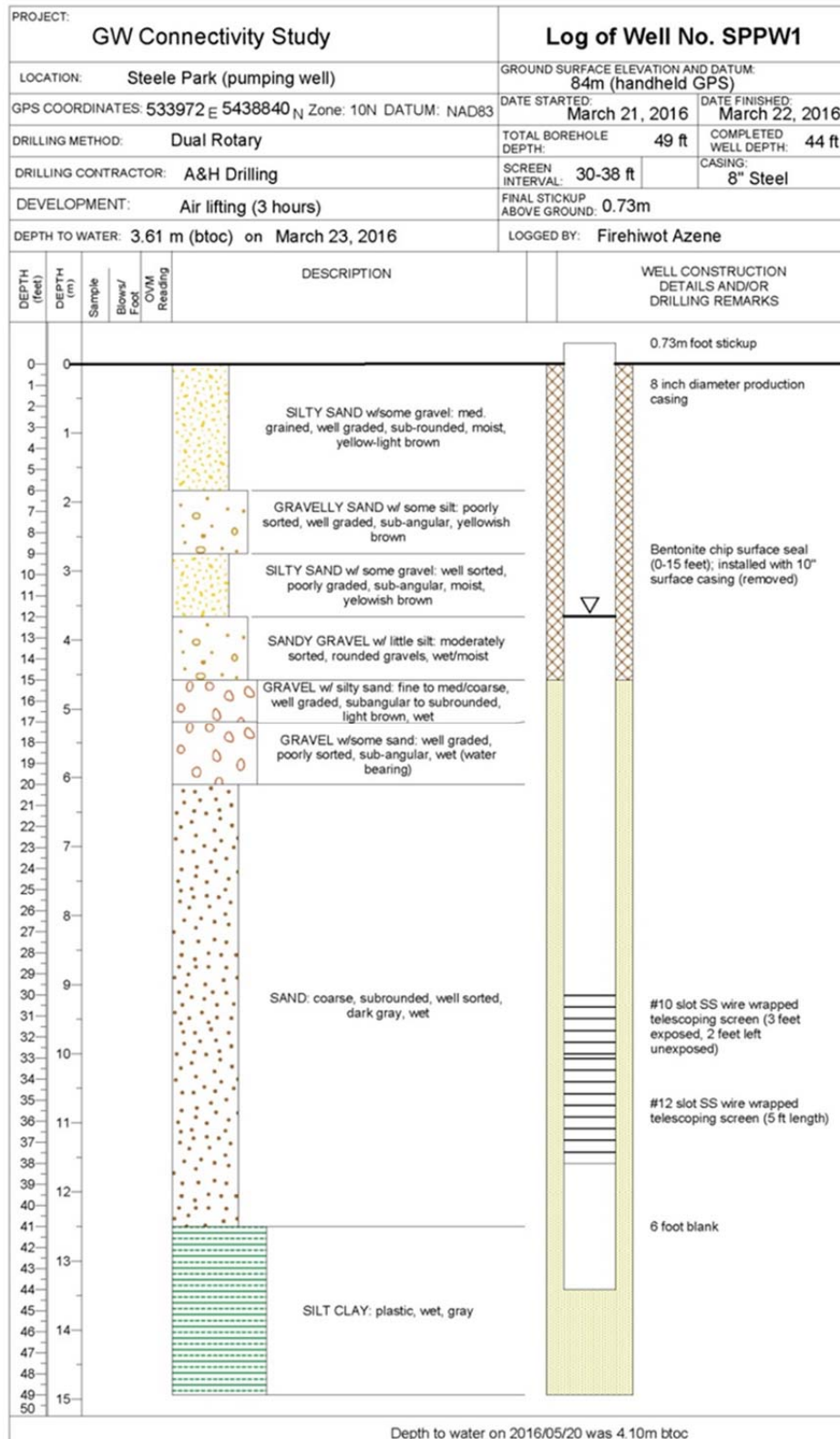


Figure A1: Lithology log of SPPW.

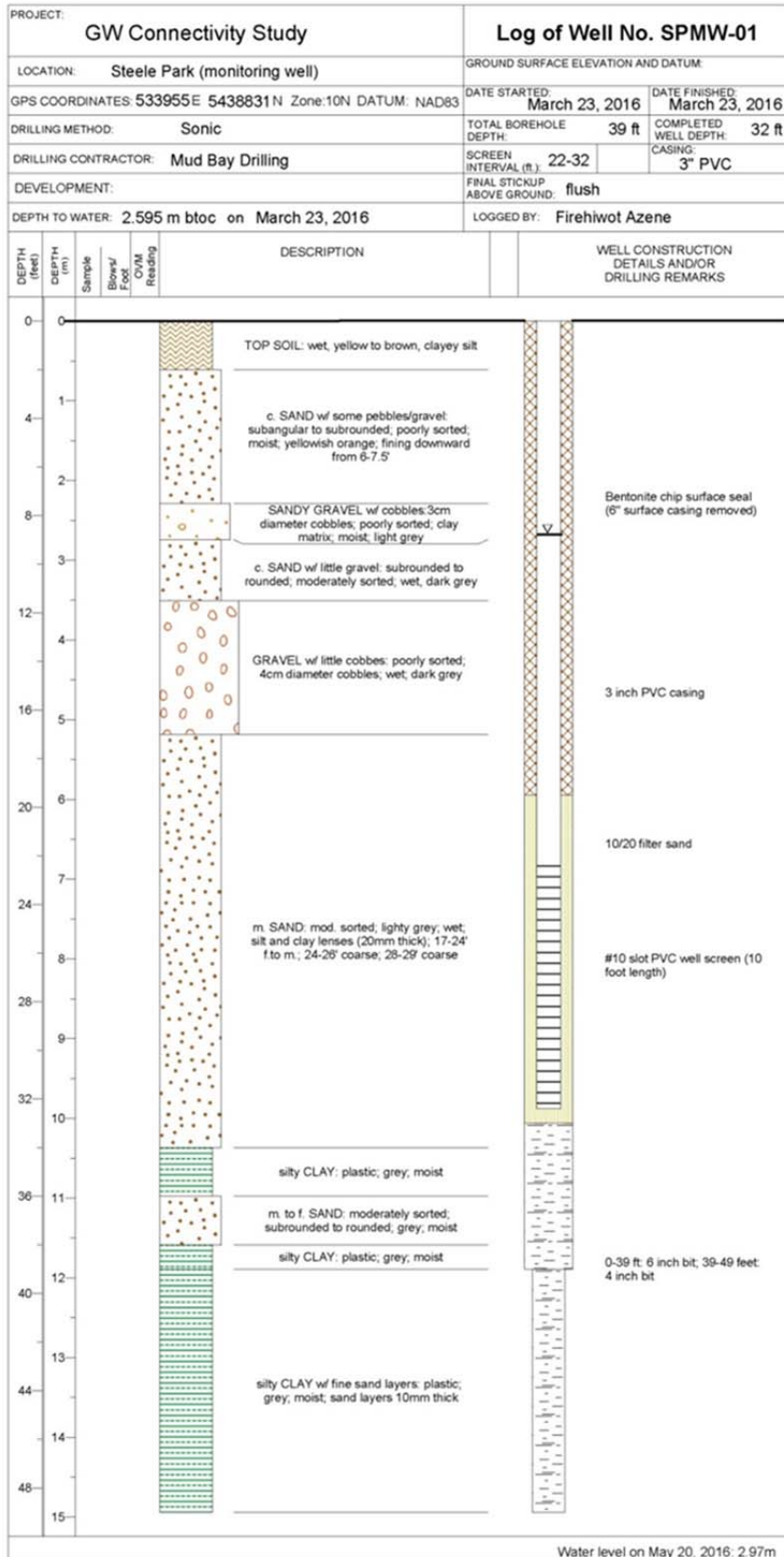


Figure A2: Lithology log of SPMW-01.

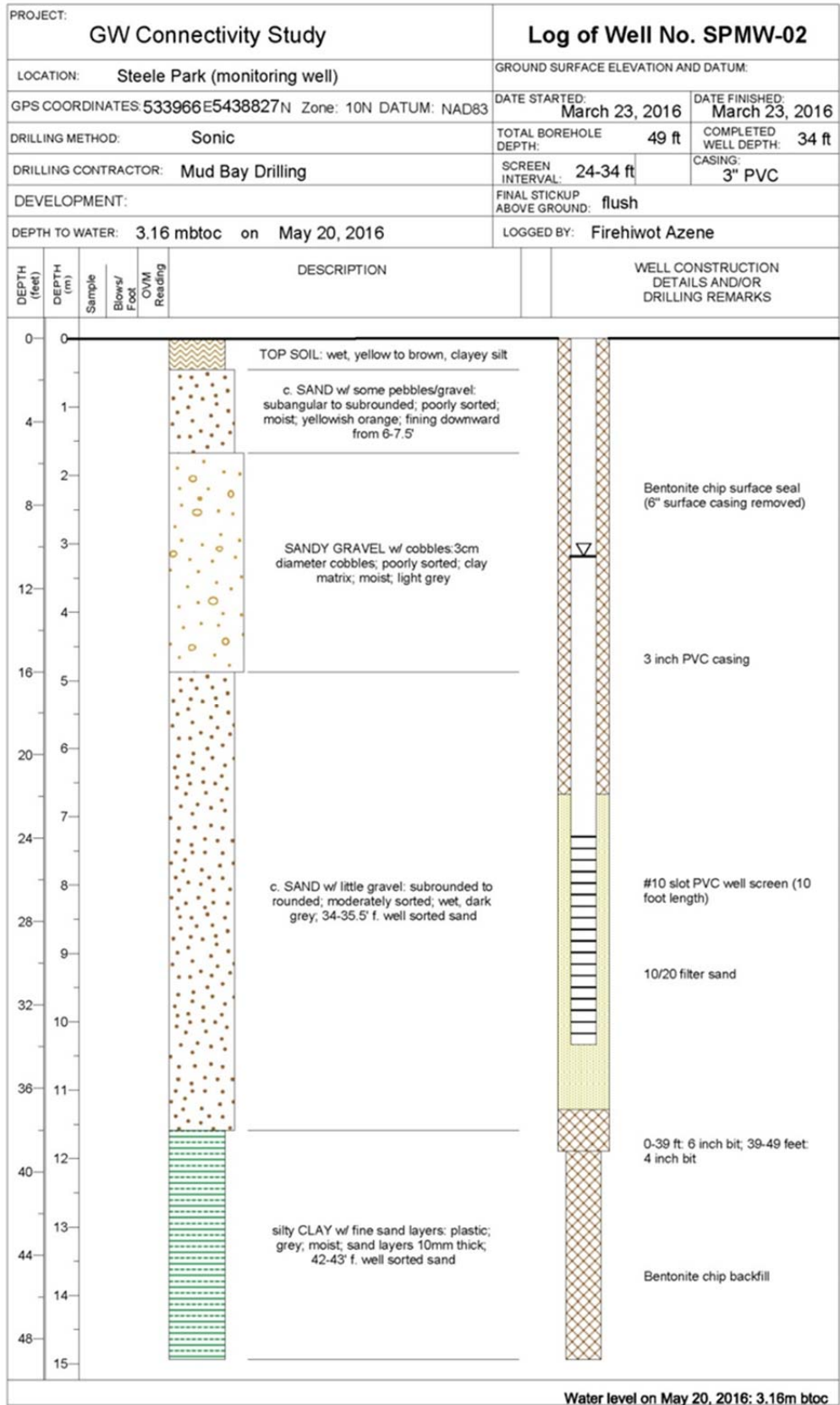


Figure A3: Lithology log of SPMW-02.

WELL: SPMW-02
 533966E 5438827N
 Date: July 15th, 2016

10N NAD83
 CORE BOXES 1-3

SCREEN INTERVAL
 7.3m - 10.4m
 Total Depth: 14.9m
 Well Depth: 10.4m

DEPTH (cm)	Rest	Clay	Sample	COMMENTS	
0.5			1A	- Dark brown-orange soil. High clay/organic content near top. Grades to more silt dominated at bottom. Tree/plant roots decrease in abundance with depth. Pebbles up to 1.5cm in diameter. Sub rounded.	0.9m
1				- Light brown/grey fine sand. No clay content. Few sub rounded pebbles up to 1.5 cm diameter.	0.3m
1.5			1B	- Light to dark grey fine sand coarsening downwards to medium-coarse sand/gravel. 15 cm clay rich section near top. Abundant pebbles. Cobble size up to 6 cm diameter. Poorly sorted, sub rounded grains. Some clay matrix below clay lens.	1.7m
2				- Light grey medium sand to gravel. Coarsens downwards. Large cobbles in sand at top of unit. (5 cm diameter) Cobble size decreases with depth. Poorly to Moderately sorted.	0.95m
2.5			2A	- Grey medium sand. Very well sorted. Contains sparse pebbles or clay lumps. One large 5cm diameter cobble at base of section. - Upper contact is not visible in core.	2.05m
3				- As above. Sand coarsens downwards. Bottom 1.5 m are coarser sand. - Well sorted	
3.5			3A		
4					
4.5					
5					
5.5					
6					
6.5					
7					
7.5					
8					
8.5					
9					

WELL: SPMW-02
 533966E 5438827N 10N NAD83
 CORE BOXES 4-5
 Date: July 15th, 2016

SCREEN INTERVAL
 7.3m - 10.4m
 Total Depth: 14.9m
 Well Depth: 10.4m

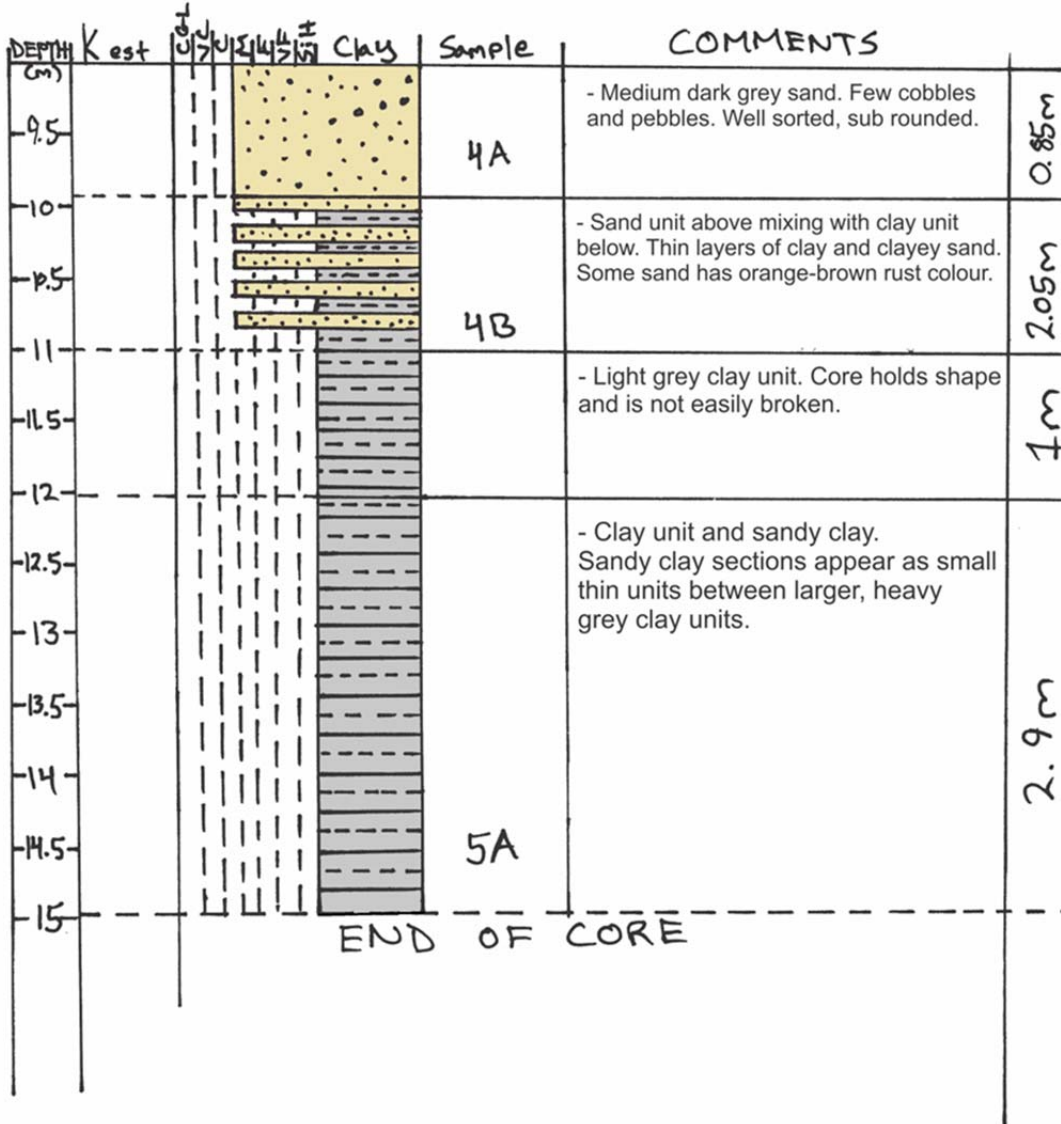


Figure A4: In-depth core log of SPMW-02

Table A1: Compiled driller's logs for the six residential wells south of Steele Park used to delineate the regional hydrostratigraphy and depth to the upper clay contour map.

Well ID	Depths (bottom of lithology)	Lithology
000000046976	2.4384 m	very dense dry gravel
	8.5344 m	sand and gravel
	15.24 m	clay
000000049868	4.2672 m	dry sand and gravel
	6.4008 m	sand and gravel
	11.2776 m	grey sand
	14.6304 m	firm grey sandy clay
	15.24 m	till
000000049869	2.4384 m	sand, gravel, and boulders
	7.3152 m	sand and gravel
	15.24 m	silty sand and clay
000000032087 (Deep Aquifer)	5.1816 m	sand and gravel
	7.62 m	blue clay
	39.624 m	till
	68.58 m	till with W.B. silt and wood and coal
	70.104 m	W.B. fine sand
	> 70.104 m	clay
000000032146 (Deep Aquifer)	2.1336 m	brown clay
	4.2672 m	sand and gravel
	35.053 m	blue clay
	45.72 m	till with layers of W.B. silt
	66.7512 m	till
	68.58 m	W.B. sand and wood
000000032160 (Deep Aquifer)	2.1336 m	brown clay
	4.572 m	sand and gravel
	35.6616 m	blue clay
	39.624 m	till
	41.4528 m	W.B. sand and gravel

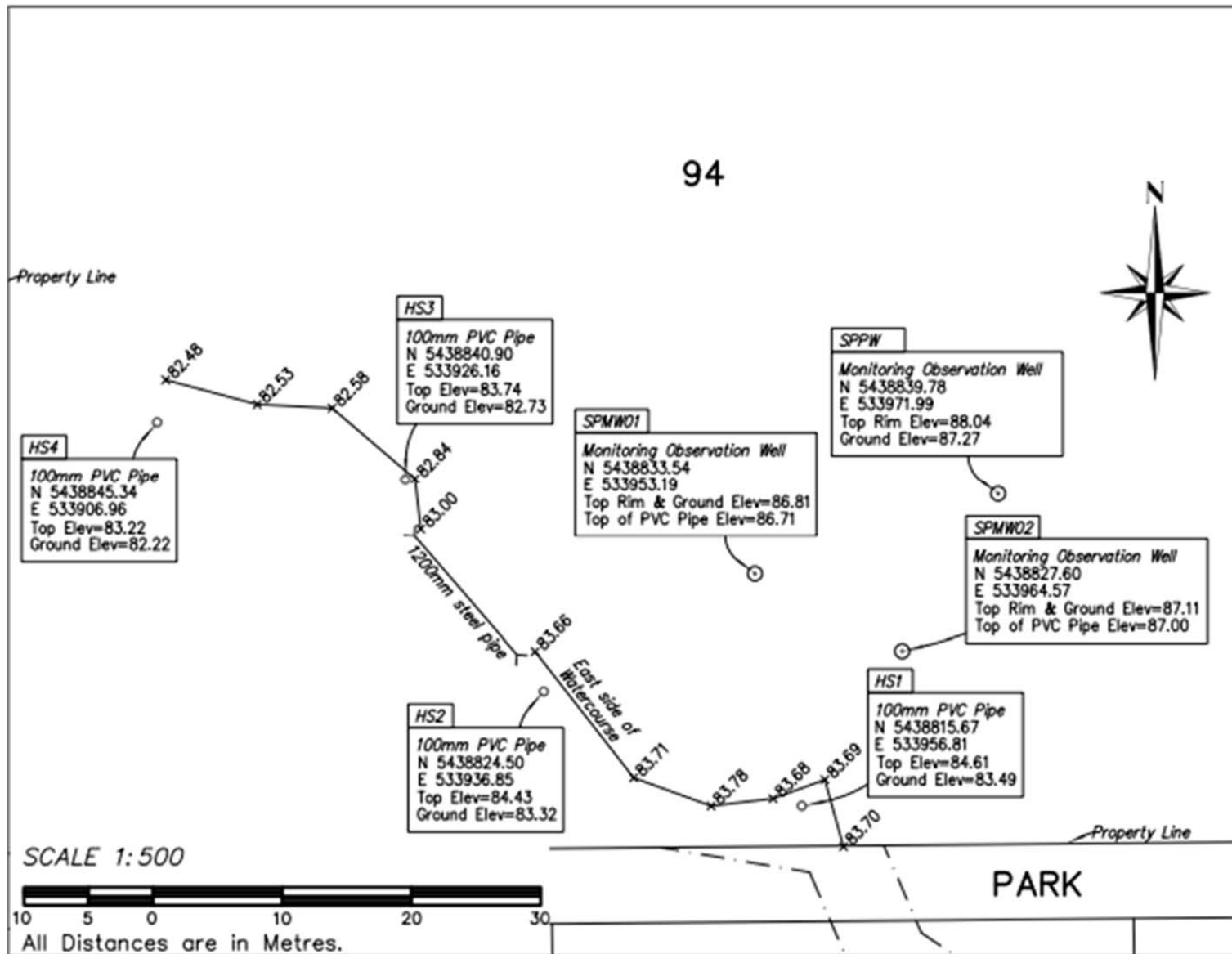


Figure A5: Surveyed locations of the stream stage measurement locations in Union creek. (Onderwater Land Surveying Ltd, 2017).

APPENDIX B: WELL HYDROGRAPHS

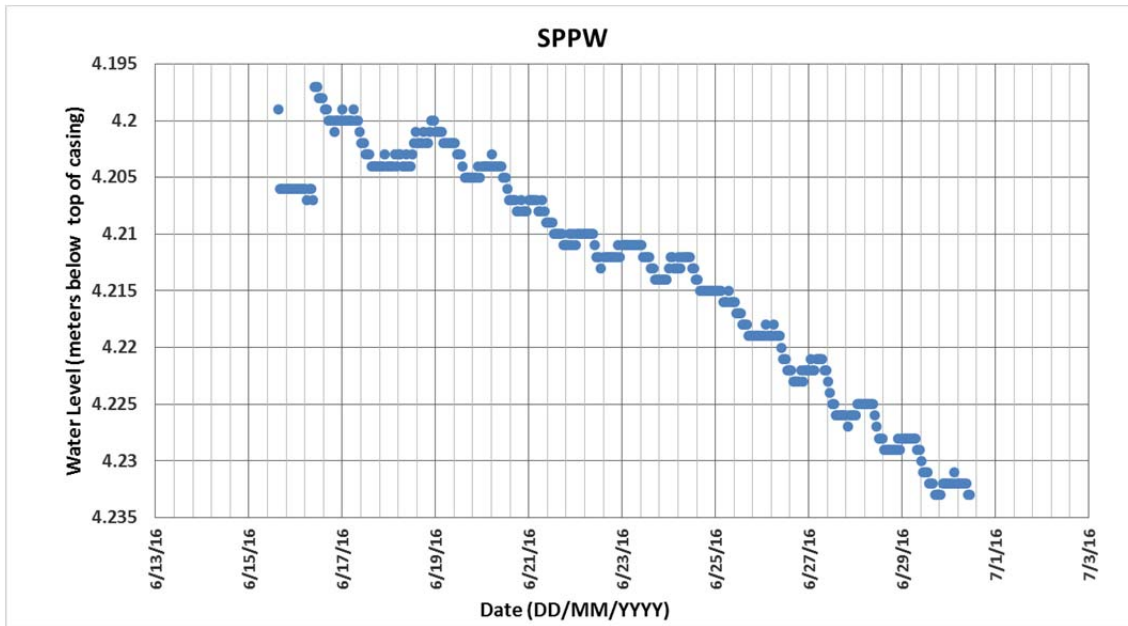


Figure B1: SPPW water levels during the summer monitoring period.

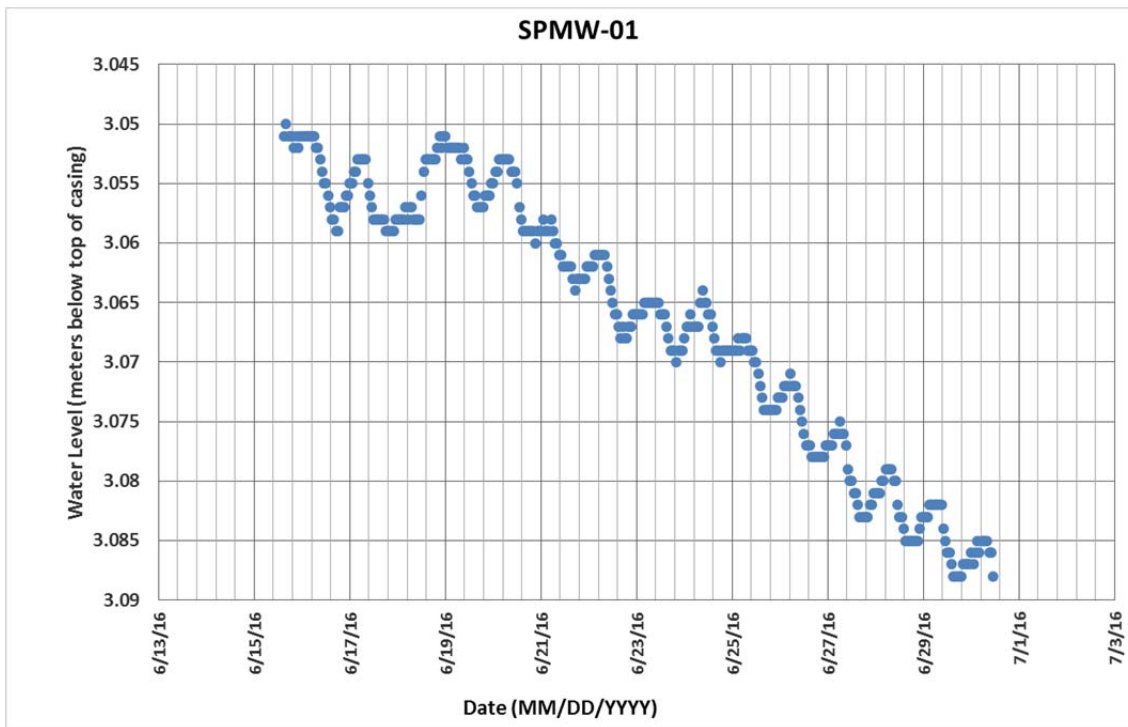


Figure B2: SPMW-01 water levels during the summer monitoring period.

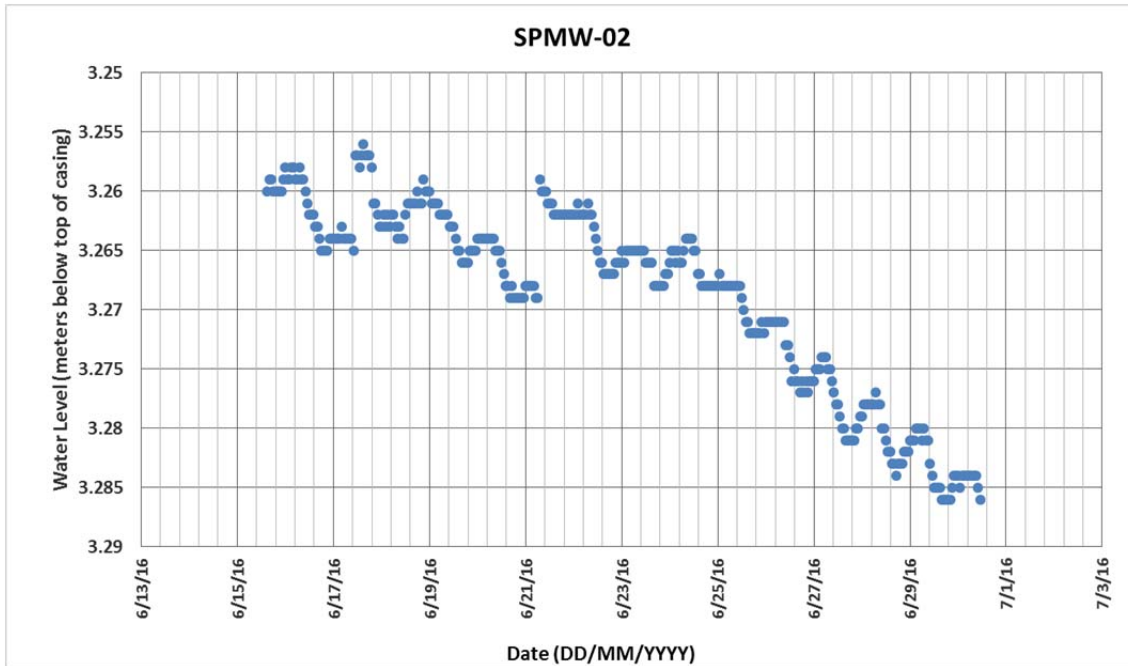
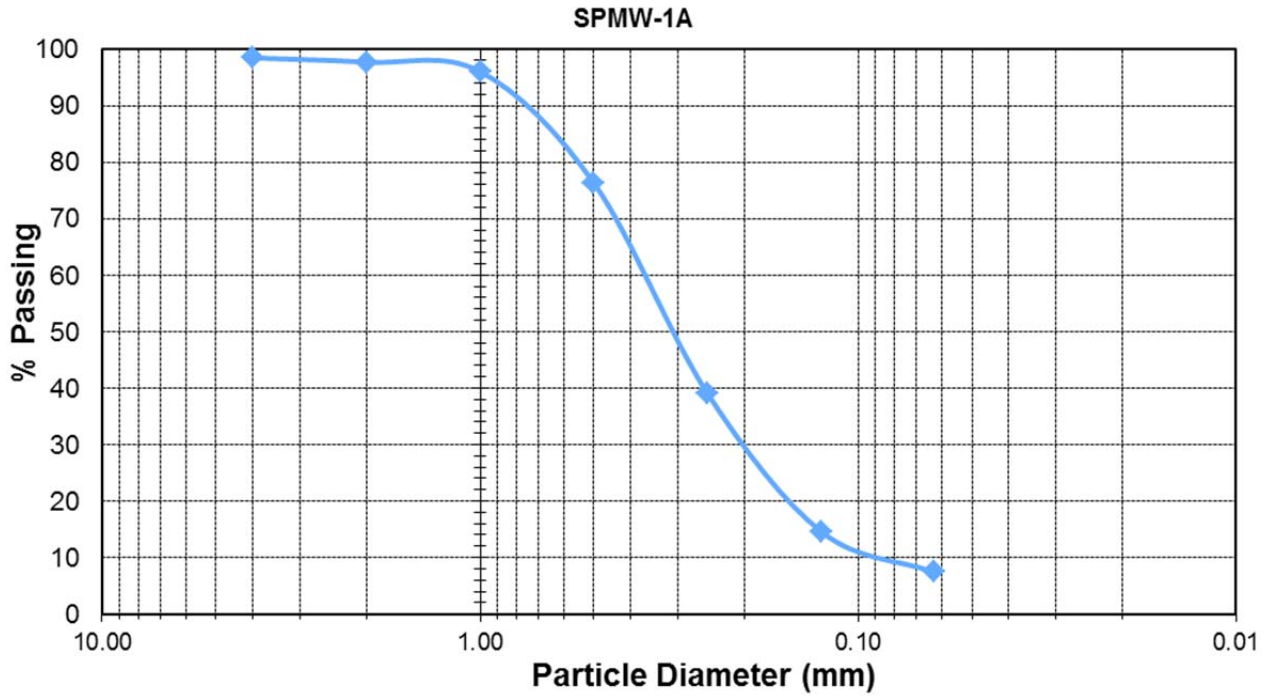


Figure B3: SPMW-02 water levels over the summer monitoring period.

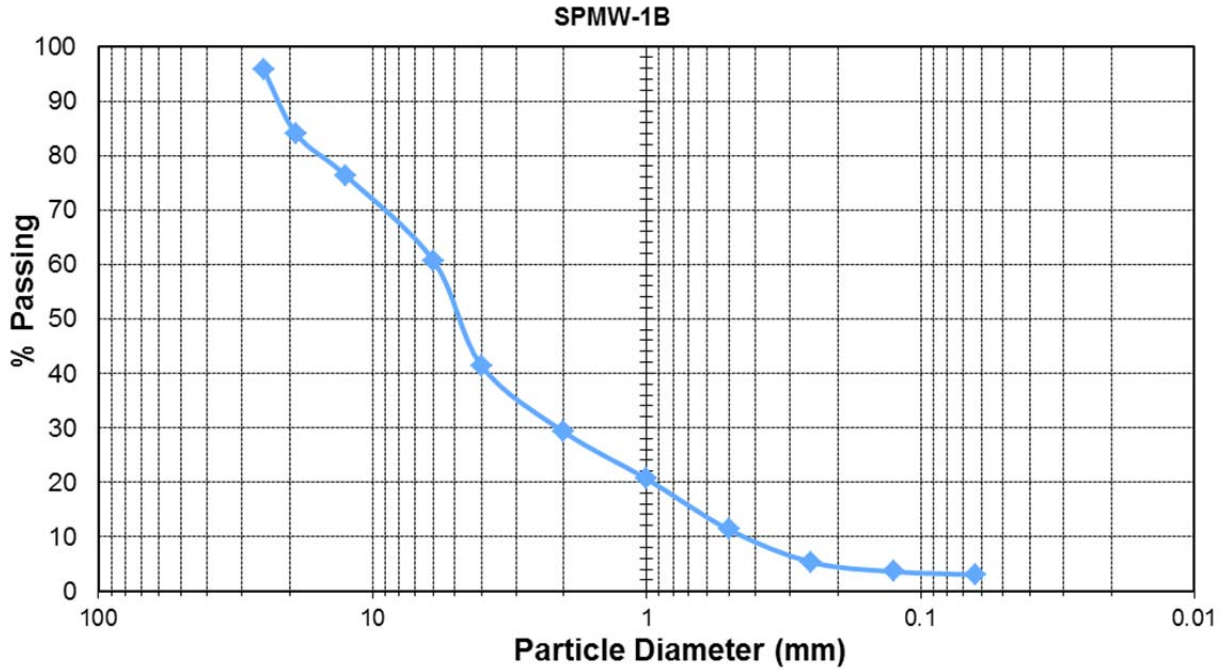
APPENDIX C: GRAIN SIZE CURVES

Weight of plate (g): 11.6
 Weight of Dry Sample (g): 109.4

Weight of plate & Sample (g): 120.9



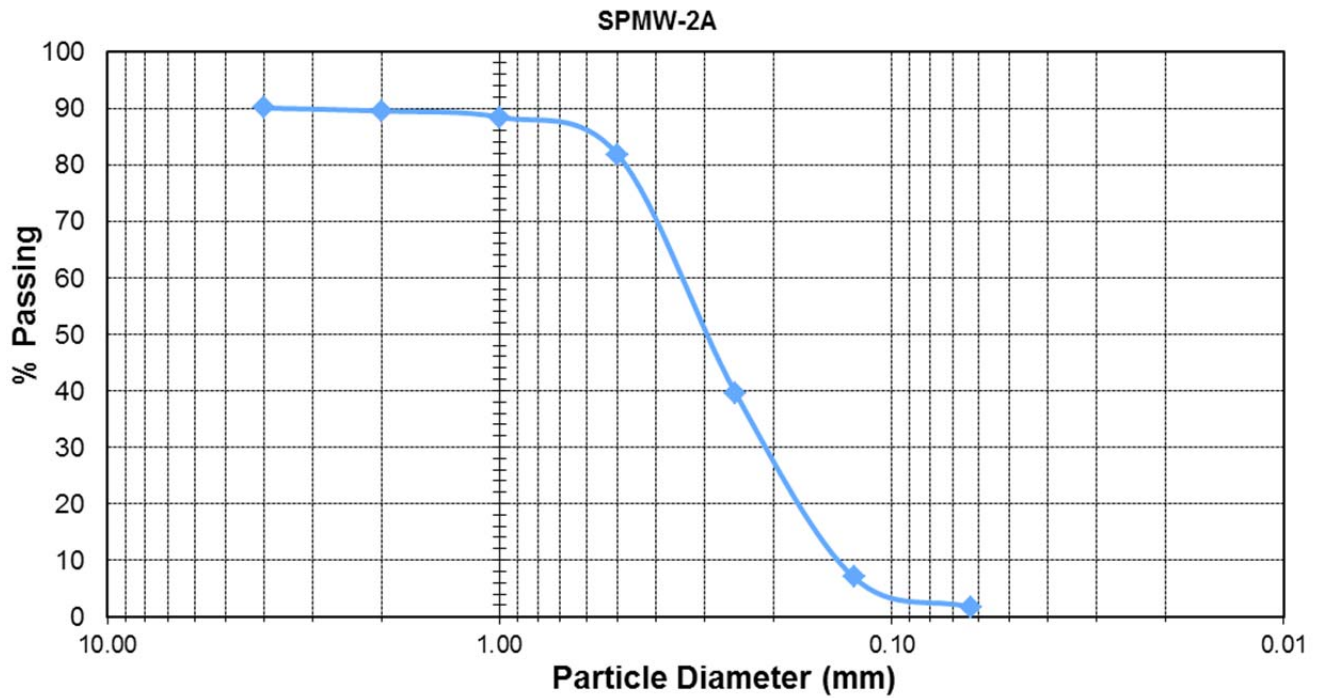
Sieve Number	Diameter (mm)	Mass of Sieve (g)	Mass of Sieve & Soil (g)	Soil Retained (g)	Soil Retained (%)	Soil Passing (%)
5	4.00	-	-	1.7	1.5	98.5
10	2.00	-	-	0.8	0.8	97.7
18	1.00	-	-	1.8	1.7	96.0
35	0.50	-	-	21.6	19.8	76.3
60	0.25	-	-	40.8	37.3	39.0
120	0.125	-	-	26.7	24.4	14.6
230	0.063	-	-	7.8	7.1	7.4
Pan		-	-	9.1	8.3	0.0
TOTAL:				110.33	100.9	



Weight of plate (g): 13.9
 Weight of Dry Sample (g): 552.1

Weight of plate & Sample (g): 565.9

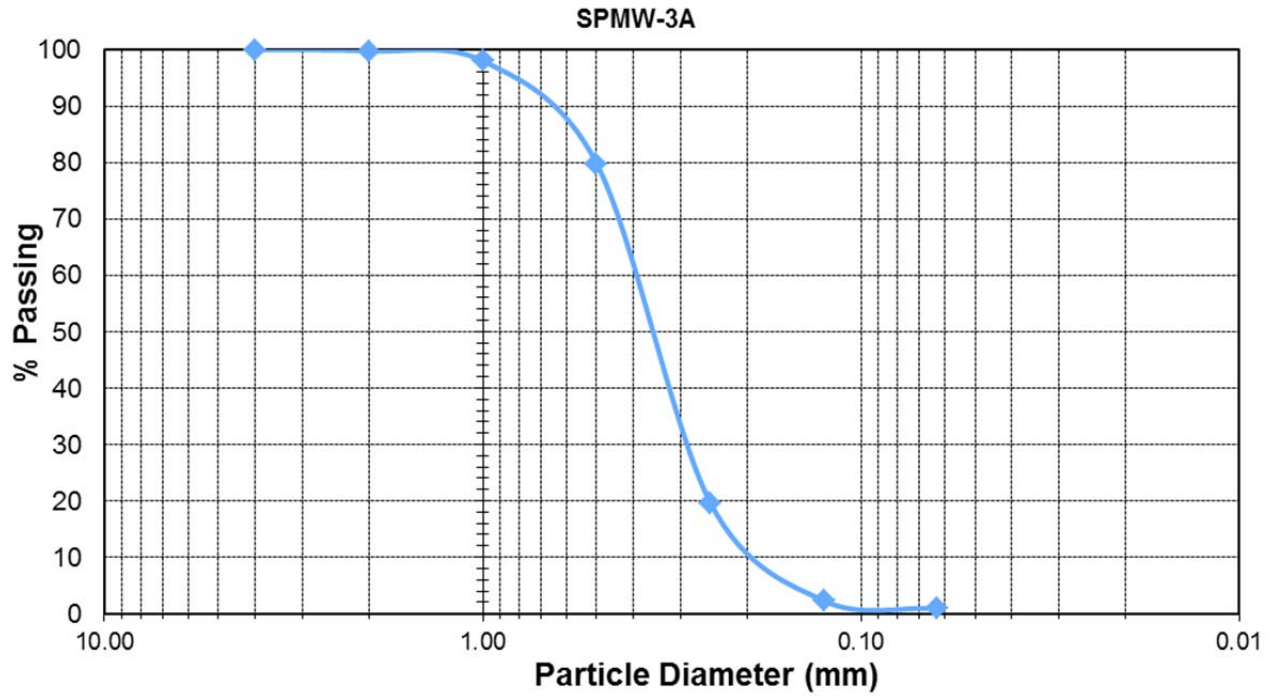
Sieve Number	Diameter (mm)	Mass of Sieve (g)	Mass of Sieve & Soil (g)	Soil Retained (g)	Soil Retained (%)	Soil Passing (%)
1in	25	-	-	23.04	4.2	95.8
3/4 in	19	-	-	65.43	11.9	84.0
1/2 in	12.5	-	-	42.46	7.7	76.3
5/16 in	6	-	-	85.97	15.6	60.7
5	4.00	-	-	106.9	19.4	41.3
10	2.00	-	-	67.0	12.1	29.2
18	1.00	-	-	47.4	8.6	20.6
35	0.50	-	-	51.6	9.3	11.3
60	0.25	-	-	33.1	6.0	5.3
120	0.125	-	-	9.5	1.7	3.6
230	0.063	-	-	3.2	0.6	3.0
Pan		-	-	4.0	0.7	0.0
TOTAL:				539.6	97.7	



Weight of plate (g): 14.0
 Weight of Dry Sample (g): 242.0

Weight of plate & Sample (g): 256.1

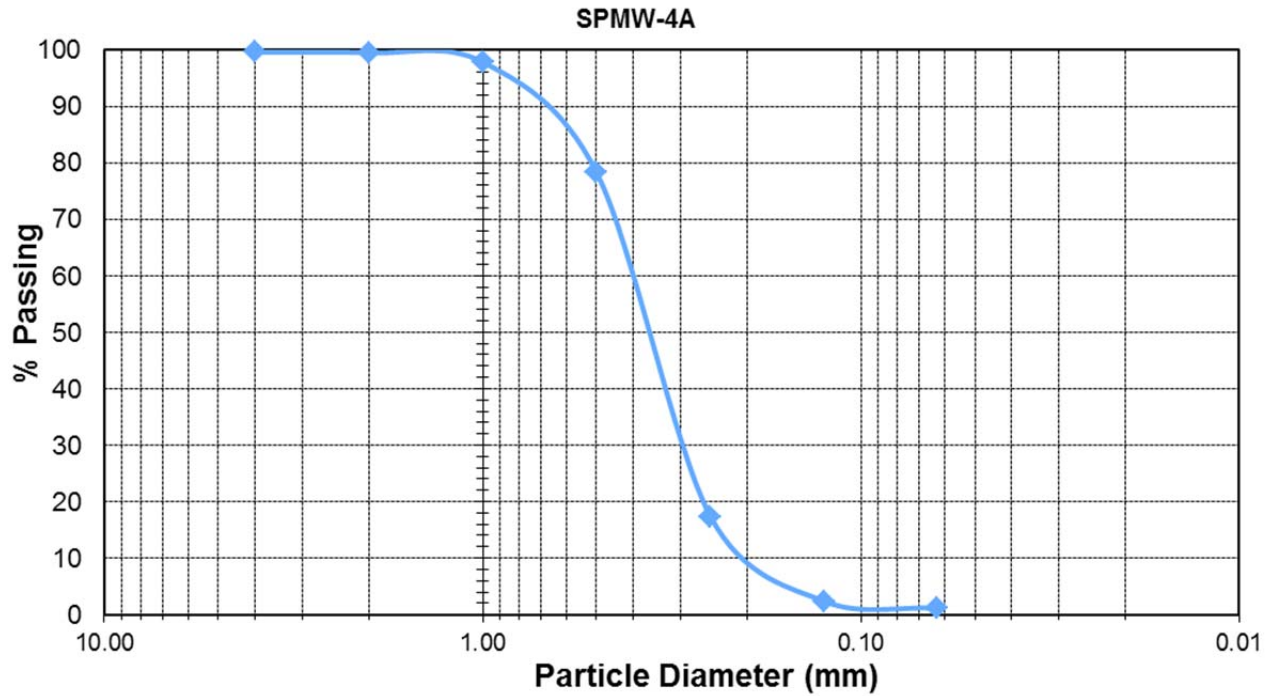
Sieve Number	Diameter (mm)	Mass of Sieve (g)	Mass of Sieve & Soil (g)	Soil Retained (g)	Soil Retained (%)	Soil Passing (%)
5	4.00	-	-	24.1	9.9	90.1
10	2.00	-	-	1.3	0.5	89.5
18	1.00	-	-	2.7	1.1	88.4
35	0.50	-	-	16.1	6.6	81.8
60	0.25	-	-	102.3	42.3	39.5
120	0.125	-	-	78.8	32.5	7.0
230	0.063	-	-	12.8	5.3	1.7
Pan		-	-	3.5	1.5	0.0
TOTAL:				241.49	99.8	



Weight of plate (g): 11.6
 Weight of Dry Sample (g): 253.2

Weight of plate & Sample (g): _____

Sieve Number	Diameter (mm)	Mass of Sieve (g)	Mass of Sieve & Soil (g)	Soil Retained (g)	Soil Retained (%)	Soil Passing (%)
5	4.00	-	-	0.0	0.0	100.0
10	2.00	-	-	0.6	0.2	99.8
18	1.00	-	-	4.5	1.8	98.0
35	0.50	-	-	46.1	18.2	79.8
60	0.25	-	-	152.5	60.2	19.6
120	0.125	-	-	43.9	17.3	2.3
230	0.063	-	-	3.4	1.4	0.9
Pan		-	-	1.6	0.6	0.0
TOTAL:				252.51	99.7	



Weight of plate (g): 13.8
 Weight of Dry Sample (g): 309.3

Weight of plate & Sample (g): 323.1

Sieve Number	Diameter (mm)	Mass of Sieve (g)	Mass of Sieve & Soil (g)	Soil Retained (g)	Soil Retained (%)	Soil Passing (%)
5	4.00	-	-	1.3	0.4	99.6
10	2.00	-	-	0.4	0.1	99.5
18	1.00	-	-	5.1	1.6	97.8
35	0.50	-	-	60.5	19.6	78.3
60	0.25	-	-	188.3	60.9	17.4
120	0.125	-	-	46.5	15.0	2.4
230	0.063	-	-	3.8	1.2	1.1
Pan		-	-	1.9	0.6	0.0
TOTAL:				307.65	99.5	

APPENDIX D: SLUG AND BAIL TEST CURVES

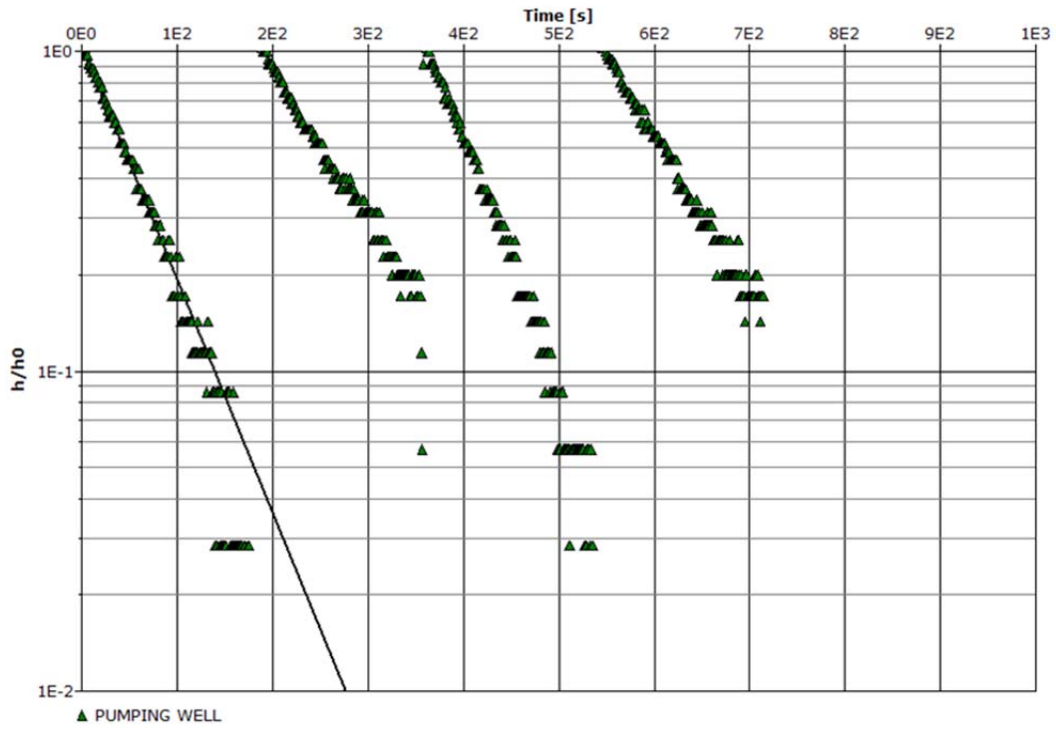


Figure D1: Bouwer-Rice analysis of SPPW data.

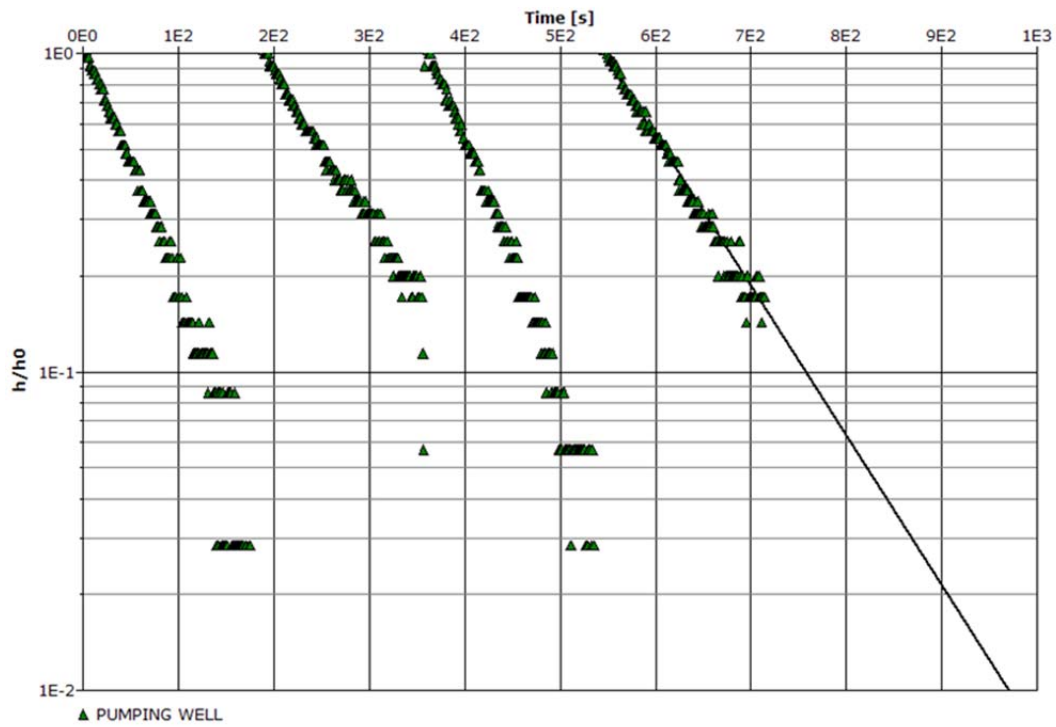


Figure D2: Hvorslev analysis of SPPW data.

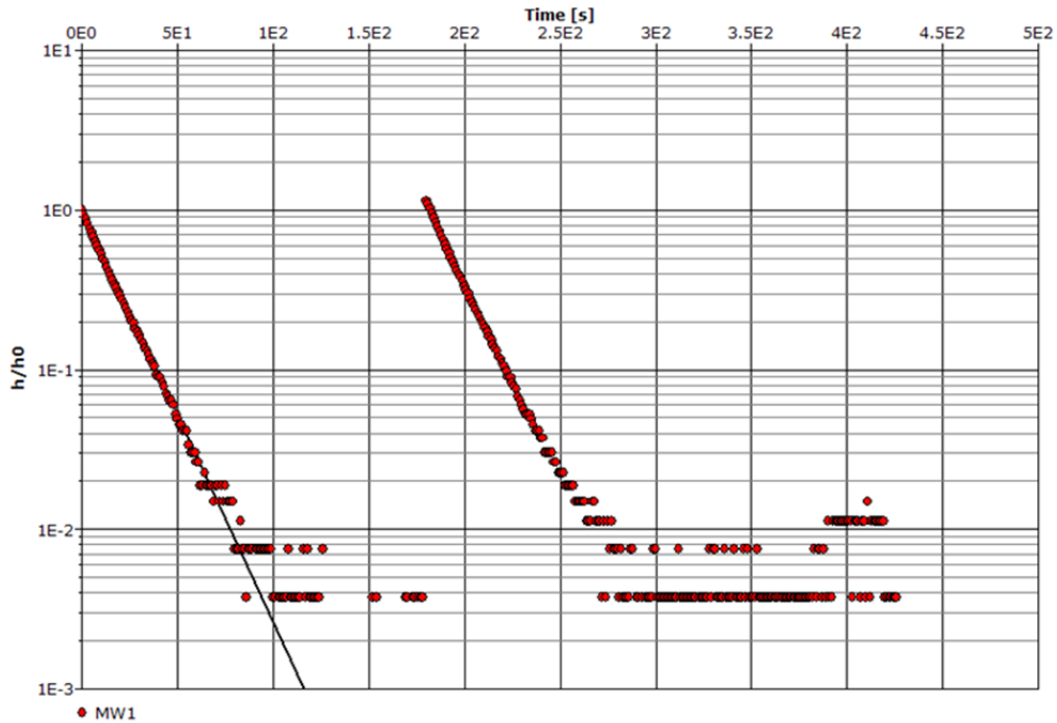


Figure D3: Bouwer-Rice analysis of SPMW-01 data.

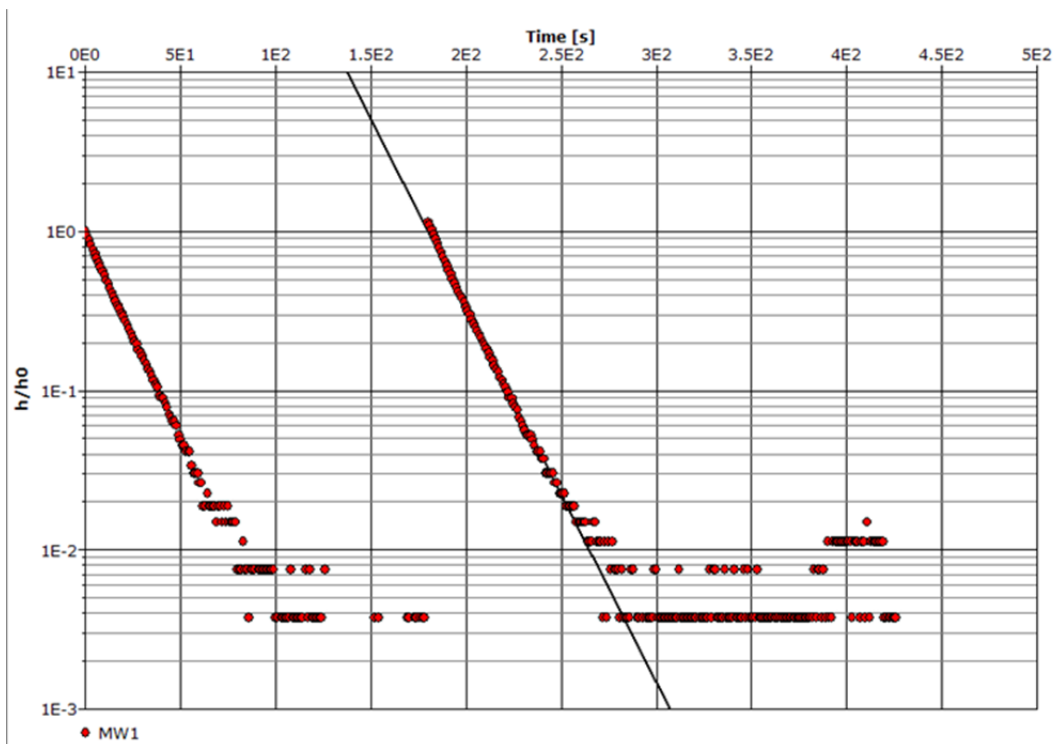


Figure D4: Hvorslev analysis of SPMW-01 data.

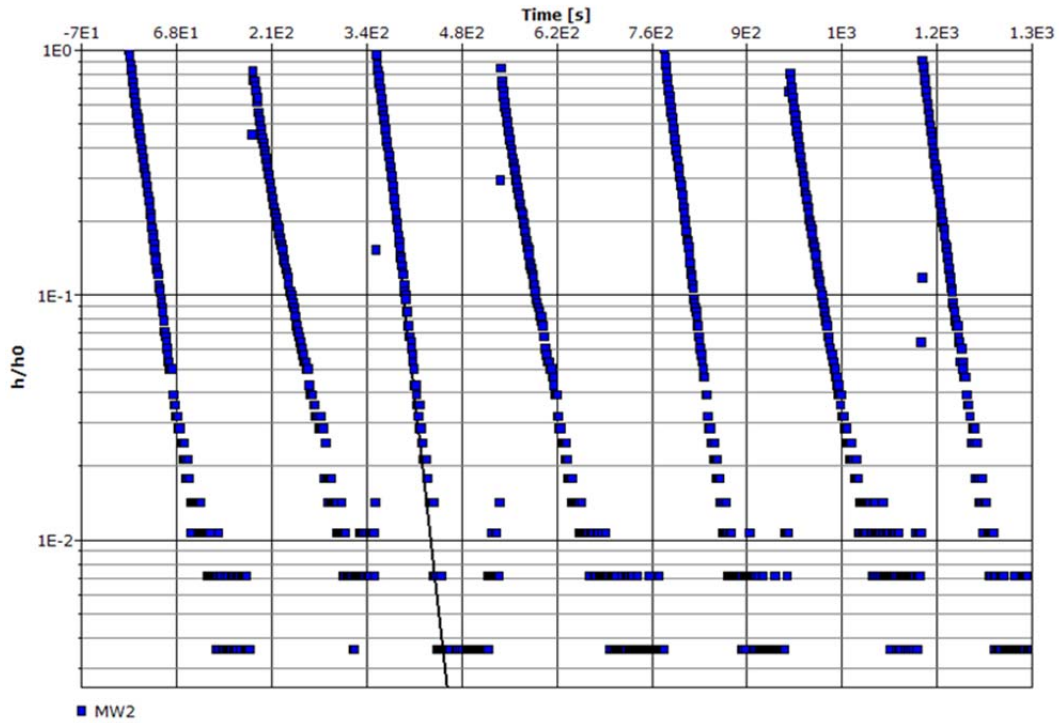


Figure D5: Bouwer-Rice analysis of SPMW-02 data.

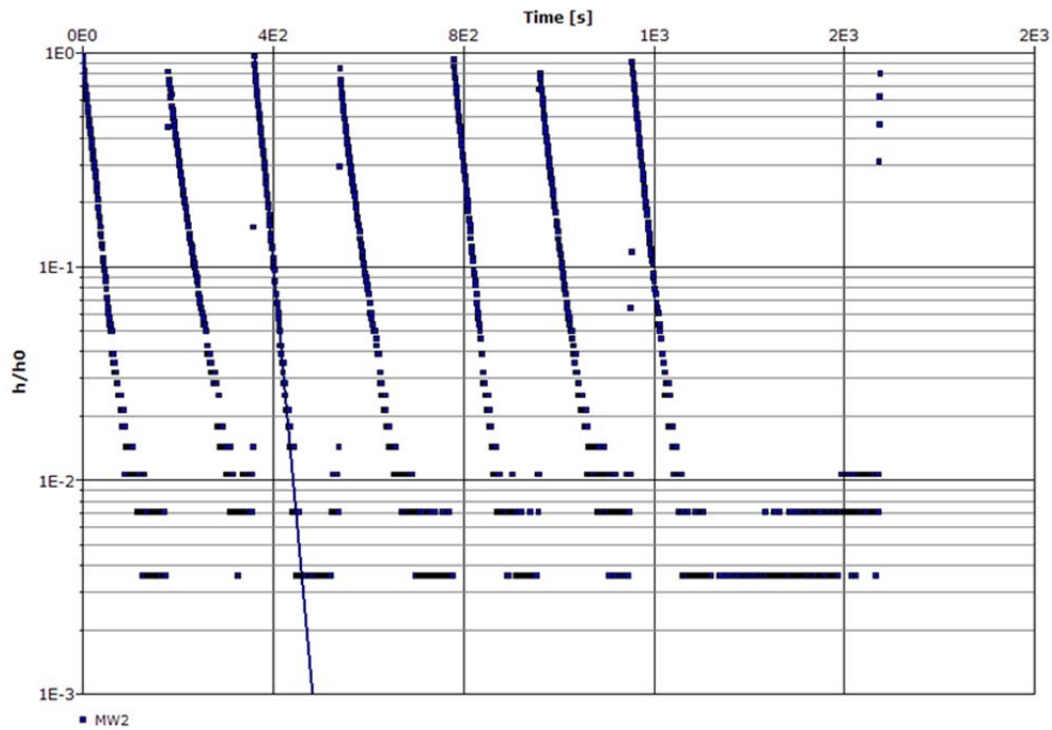


Figure D6: Hvorslev analysis of SPMW-02 data.

APPENDIX E: PUMPING TEST ANALYSIS

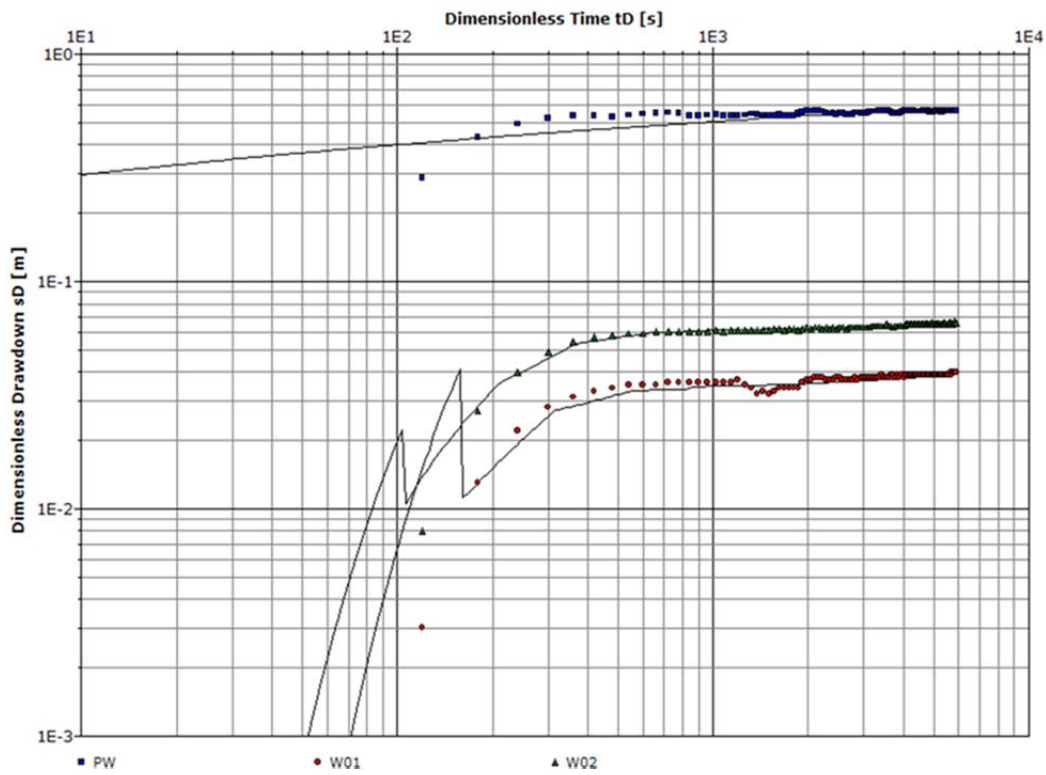


Figure E1: Neuman analysis for the low-rate pumping data.

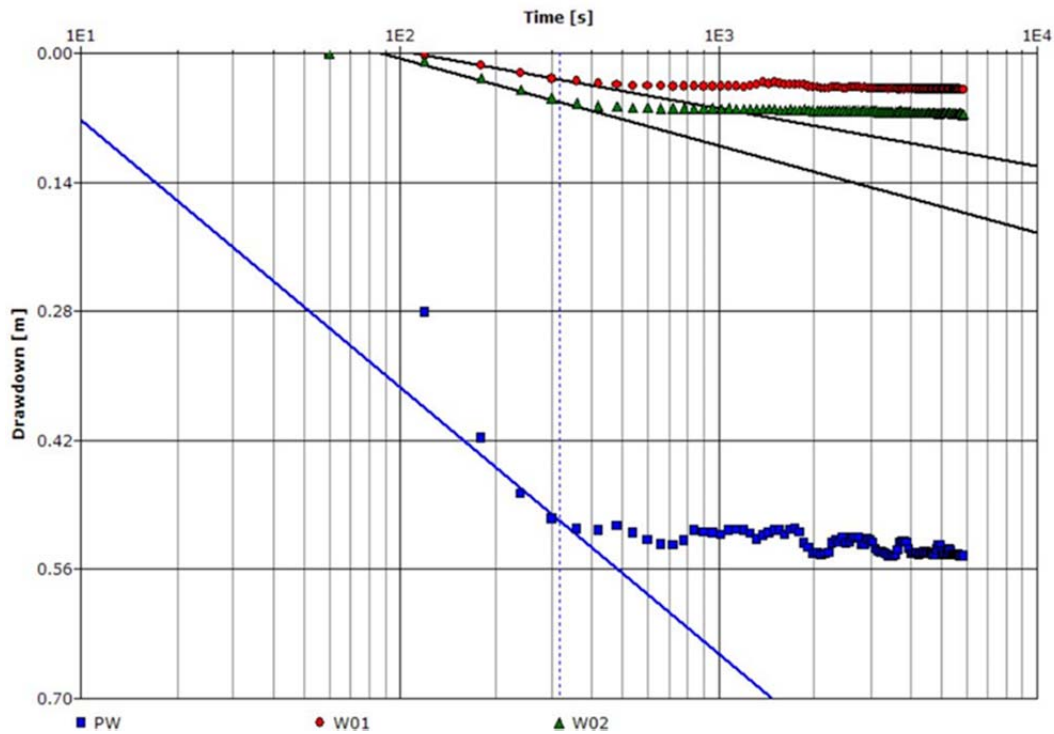


Figure E2: Cooper-Jacob analysis for the low-rate pumping data.

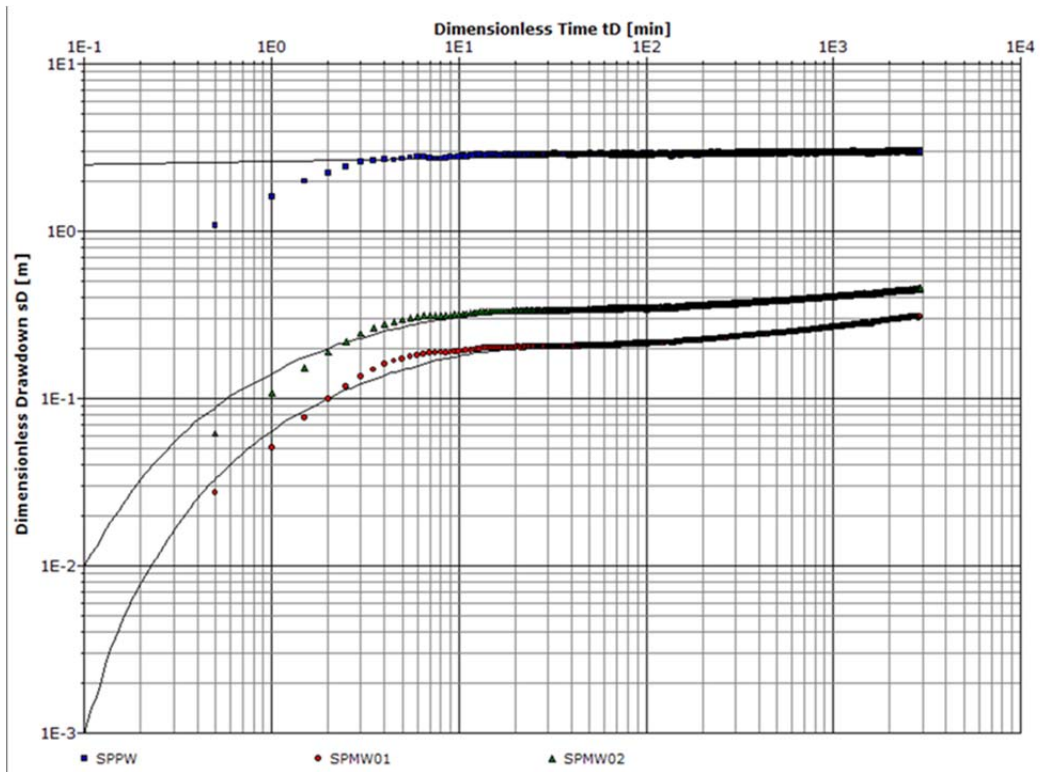


Figure E3: Neuman analysis for the high-rate pumping data.

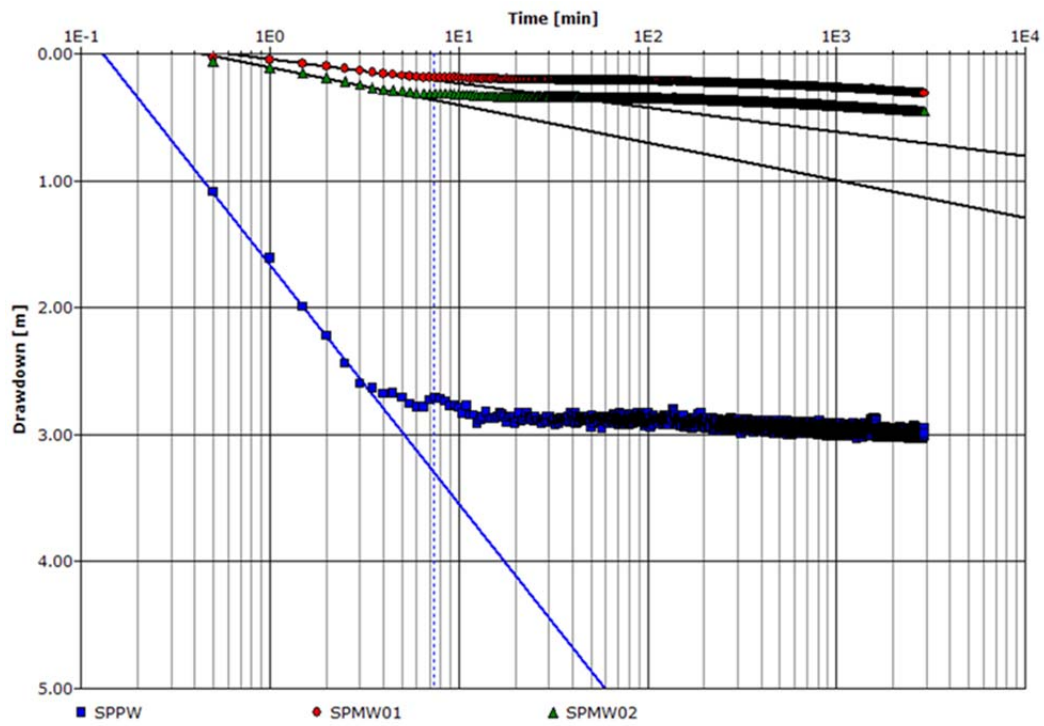


Figure E4: Cooper-Jacob analysis for the high-rate pumping data.

Table E1: Summary of aquifer properties from each analysis method. Values in italics are calculated using the average saturated thickness of the aquifer at the time of the test. Cells highlighted in orange were omitted from the geometric mean calculation for their category.

Aquifer Property	Grain Size Analysis	Hvorslev	Bouwer & Rice	Neuman – High-Rate	Neuman – Low-Rate	Cooper Jacob – High-Rate	Cooper Jacob – Low-Rate
K (m/s)	3.24E-05	6.17E-05 ^[b]	4.74E-05 ^[b]	2.80E-04 ^[a]	1.10E-04 ^[a]	1.70E-05 ^[a]	4.00E-05 ^[a]
	8.10E-04	5.91E-05 ^[b]	4.63E-05 ^[b]	1.67E-04 ^[b]	3.01E-06 ^[b]	1.67E-04 ^[b]	1.85E-04 ^[b]
	8.41E-05	5.02E-05 ^[c]	4.01E-05 ^[c]	1.19E-04 ^[c]	5.28E-06 ^[c]	1.08E-04 ^[c]	1.22E-04 ^[c]
	3.10E-04	3.80E-05 ^[c]	2.86E-05 ^[c]	-	-	-	-
	3.36E-04	5.53E-05 ^[c]	4.37E-05 ^[c]	-	-	-	-
	-	4.10E-05 ^[c]	3.03E-05 ^[c]	-	-	-	-
	-	5.36E-05 ^[c]	4.33E-05 ^[c]	-	-	-	-
	-	4.18E-05 ^[c]	3.30E-05 ^[c]	-	-	-	-
	-	5.26E-05 ^[c]	4.00E-05 ^[c]	-	-	-	-
	-	1.24E-04 ^[a]	9.09E-05 ^[a]	-	-	-	-
	-	8.89E-05 ^[a]	6.95E-05 ^[a]	-	-	-	-
	-	1.19E-04 ^[a]	9.02E-05 ^[a]	-	-	-	-
-	8.49E-05 ^[a]	6.66E-05 ^[a]	-	-	-	-	
Geometric Mean of K values (m/s)	1.87E-04	6.22E-05	4.80E-05	1.77E-04	3.98E-06	6.74E-05	1.50E-04
T (m ² /day)	-	4.21E+01 ^[b]	3.24E+01 ^[b]	2.09E+02 ^[a]	7.50E+01 ^[a]	1.27E+01 ^[a]	2.73E+01 ^[a]
	-	4.03E+01 ^[b]	3.16E+01 ^[b]	1.25E+02 ^[b]	2.05E+00 ^[b]	1.25E+02 ^[b]	1.26E+02 ^[b]
	-	3.43E+01 ^[c]	2.74E+01 ^[c]	8.90E+01 ^[c]	3.60E+00 ^[c]	8.08E+01 ^[c]	8.34E+01 ^[c]
	-	2.59E+01 ^[c]	1.95E+01 ^[c]	-	-	-	-
	-	3.77E+01 ^[c]	2.98E+01 ^[c]	-	-	-	-
	-	2.80E+01 ^[c]	2.07E+01 ^[c]	-	-	-	-
	-	3.66E+01 ^[c]	2.96E+01 ^[c]	-	-	-	-
	-	2.85E+01 ^[c]	2.25E+01 ^[c]	-	-	-	-
	-	3.59E+01 ^[c]	2.73E+01 ^[c]	-	-	-	-
	-	8.46E+01 ^[a]	6.20E+01 ^[a]	-	-	-	-
	-	6.07E+01 ^[a]	4.74E+01 ^[a]	-	-	-	-
	-	8.12E+01 ^[a]	6.16E+01 ^[a]	-	-	-	-
-	5.79E+01 ^[a]	4.55E+01 ^[a]	-	-	-	-	
Geometric Mean of T values (m²/day)	-	4.24E+01	3.28E+01	1.32E+02	2.72E+00	1.00E+02	1.03E+02
Kv/Kh	-	-	-	9.88E-02 ^[a]	9.89E-01 ^[a]	-	-
	-	-	-	5.38E-03 ^[b]	9.96E-01 ^[b]	-	-
	-	-	-	7.00E-03 ^[c]	1.00E+00 ^[c]	-	-
Geometric mean of anisotropy	-	-	-	1.55E-02	9.98E-01	-	-
S values	-	-	-	4.86E-22 ^[a]	3.06E-03	2.52E-01	3.88E-01
	-	-	-	2.50E-04 ^[b]	9.58E-05	2.96E-04	9.26E-04
	-	-	-	1.74E-04 ^[c]	2.01E-04	2.49E-04	8.66E-04
Geometric	-	-	-	2.08E-04	1.39E-04	2.71E-04	8.95E-04

Aquifer Property	Grain Size Analysis	Hvorslev	Bouwer & Rice	Neuman – High-Rate	Neuman – Low-Rate	Cooper Jacob – High-Rate	Cooper Jacob – Low-Rate
Mean of S values							
Ss	-	-	-	5.61E-23 ^[a]	3.91E-04 ^[a]	2.91E-02 ^[a]	4.92E-02 ^[a]
	-	-	-	2.89E-05 ^[b]	1.22E-05 ^[b]	3.42E-05 ^[b]	1.17E-04 ^[b]
	-	-	-	2.01E-05 ^[c]	2.57E-05 ^[c]	2.88E-05 ^[c]	1.10E-04 ^[c]
Geometric Mean of Ss values	-	-	-	2.41E-05	1.77E-05	3.14E-04	1.13E-04
Sy	-	-	-	2.85E-19 ^[a]	1.33E-01 ^[a]	-	-
	-	-	-	3.80E-02 ^[b]	7.55E-02 ^[b]	-	-
	-	-	-	4.99E-02 ^[c]	1.83E-01 ^[c]	-	-
Geometric Mean of Sy values	-	-	-	4.35E-02	1.18E-01	-	-

^[a] Values obtained with data from the pumping well (SPPW).

^[b] Values obtained with data from SPMW-01.

^[c] Values obtained with data from SPMW-02.